TRANSNEFT

Pipeline

Science and Technology

Vol. 2, No. 2, June 2018

PIPELINE
SCIENCE AND TECHNOLOGY

published by
Pipeline Transport Institute
Technical Productions (London) Ltd
ISSN 2514-541X

Founder, Pipeline Science and Technology

Yakov M. Fridlyand, General Director, Pipeline Transport Institute, Moscow, Russian Federation

Chairman of the Editorial Board and Editor-in-Chief

Dr Anatoly E. Soshchenko, Head, Department of Innovation Development and R&D, Transneft, Moscow, Russian Federation

Editorial Board Members

Vasilyeva, Zoya Andreyevna, Dr Sci. (Econ.), Professor, Director of the Institute of Business Process Management and Economics of The Siberian Federal University, Krasnoyarsk, Russian Federation.

Zholobov, Vladimir Vasilievich, Dr Sci. (Phys. and Math.), Lead Research Scientist of the Laboratory of Software Systems Maintenance of Transneft R&D, LLC, Moscow, Russian Federation.

Kontorovich, Alexey Emilyevich, Dr Sci. (Geology and Mineralogy), Academician of Russian Academy of Sciences, Science Advisor of the Trofimuk Institute of Petroleum Geology and Geophysics of Siberian Branch of the Russian Academy of Sciences, Novosibirsk, Russian Federation.

Korolyonok, Anatoly Mikhailovich, D. Sci. (Eng.), Professor, Dean of the Faculty of Design, Construction and Exploitation of Pipeline Transport Systems of Gubkin Russian State University of Oil and Gas (NRU), Moscow, Russian Federation.

Lisin, Yury Victorovich, Dr Sci. (Eng.), Moscow, Russian Federation.

Mastobaev, Boris Nikolayevich, Dr Sci. (Eng.), Professor, Pipeline Transportation Department, Oil and Gas Storage and Transportation Subdepartment, Ufa State Petroleum Technological University, Ufa, Russian Federation.

Matvienko, Yury Grigorievich, Dr Sci. (Eng.), Professor, Head of Department of Strength, Survivability and Safety of Machines, Mechanical Engineering Research Institute of the Russian Academy of Sciences, Moscow

Makhutov, Nikolay Andreevich, Dr Sci. (Eng.), Associate Member of the Russian Academy of Sciences, Professor, Chief Research Associate of the Center for Steel and Welding, Strength Analysis of Transneft R&D, LLC, Moscow, Russian Federation.

Molchanova, Olga Petrovna, Dr Sci. (Econ.), Professor, Moscow State University, Faculty of Economics, Department of Organization Management,Moscow, Russian Federation.

Nesyn, Georgy Victorovich, Dr Sci. (Chem.), Lead Research Associate of the Laboratory of Chemical Reagents of Transneft R&D, LLC, Moscow, Russian Federation.

Serikov, Pavel Yurievich, Dr Sci. (Econ.), Deputy Vice President, Head of Department of Economics, Transneft, Moscow.

Adeeb, Samer M., Ph.D. (Eng.), Associate Professor, Department of Civil & Environmental Construction, University of Alberta, Edmonton, Canada

Ariaratnam, Samuel, Ph.D. (Eng., Earth and Planetary Science), Professor, Head of Construction Engineering Program Chair, School of Sustainable Engineering & Built Environment, Arizona State University, Tempe, USA.

Green, Erik, Geotechnologist, Total E&P Russie, Paris, France.

Johnson, Cliff, President of Pipeline Research Council International, Washington, USA.

Ilieva, Galina, Ph.D. (Eng.), Associated Professor, Shipbuilding Faculty, Technical University, Varna, Bulgaria; Invited Researcher, University of Beira Interior, Covilha, Portugal.

Karuppanan, Saravanan, Ph.D. (Eng.), Deputy Dean of the Department of Mechanical Engineering, Associate Professor of the University Technology of PETRONAS, Perak Darul Ridzuan, Malaysia.

Kumar, Jyant, Ph.D. (Eng.), Professor of Civil Engineering Department, Indian Institute of Science, Bangalore, India.

Lin, Yuanhua, Ph.D. (Eng.), Professor, School of Material Science and Engineering, Southwest Petroleum University, Chengdu, Sichuan Province, China.

Makhmotov, Erbol Sakhitovich, Dr Sci. (Chem.), Academician of the Kazakhstan National Academy of Natural Sciences, Foreign Member of the Russian Academy of Natural Sciences, Chief Manager of Technical Policy Department of KazTransOil, JSC, Astana, Kazakhstan.

Mohany, Atef, Ph.D. (Eng.), Chair and Associate Professor, Head of Department of Automotive, Mechanical and Manufacturing Engineering, Faculty of Engineering and Applied Science, Institute of Technology of University of Ontario, Oshava, Canada.

Pavlou, Dimitrios G., Ph.D. (Eng.), Member of the Norwegian Academy of Technological Science, Discipline Leader for Mechanical Engineering & Materials Science, Department of Mechanical and Structural Engineering and Materials Science Stavanger University, Stavanger, Norway.

Paolacci, Fabrizio, Ph.D. (Eng.), Assistant Professor, Department of Engineering, University Rome Tre, Rome, Italy.

Pluvinage, Guy, Ph.D. (Eng.), Professor Emeritus of the Metz National School of Engineers (ENIM), Metz, France.

Rajeev, Pathmanathan, Ph.D. (Eng.), Senior Lecturer, Department of Civil Engineering, Swinburne University of Technology, Melbourne, Australia.

Reis, Luis, Ph.D., Associate Professor, Mechanical Engineering Department, University of Lisbon, Lisbon, Portugal.

Sayakhov, Berik Kartanbaevich, Cand. Sci. (Eng.), Professor at the Satpaev Kazakh National Technical University, Director of Technical Policy Department of KazTransOil, JSC, Astana, Kazakhstan.

Sigitov, Vladimir Borisovich, Dr Sci. (Chem.), Deputy Director, Institute of Polymeric Materials and Technologies, Almaty, Kazakhstan.

Sosnovsky, Leonid Adamovich, Dr Sci. (Eng.), Professor of the Belarusian State University of Transport, Scientific Director of the Interdepartmental Laboratory “Tribofatigue”, Director of Tribofatigue Ltd, Gomel, Belarus.

Xu, Shugen, Ph.D. (Chem.), Associate Professor of the Chemical Technology Institute, University of Oil Chemistry, Qingdao, Shandong Province, China.

Taleb, Lakhdar, Ph.D. (Eng.), Professor, Department of Mechanics, University of Rouen, Rouen, France.

Tiratsoo, John, Head of Tiratsoo Technical Division, Editor-in-Chief of Pipelines International and the Journal of Pipeline Engineering, Eastleigh, UK.

Hadj Meliani, Mohammed, Ph.D. (Eng., Materials Science), Associate Professor, Laboratory for Theoretical Physics and Materials Physics, University Hassiba Ben Bouali of Chlef, Algeria.

Zhang, Jie, Ph.D. (Eng.), Professor, Southwest Petroleum University, Chengdu, Sichuan Province, China.

Shcherbakov, Sergey Sergeevich, Dr Sci. (Phys. And Math.), Professor, Vice Chairman of the State Committee on Science and Technology of the Republic of Belarus, Minsk, Belarus.

Pipeline Science and Technology

PIPELINE
TRANSPORT INSTITUTE

Volume 2, No 2, June 2018

Contents

An evaluation of the factors affecting the thermal state of frozen soils at the foundations of a buried oil pipeline 83
S.B. Tataurov and V.I. Surikov

A study of the cyclic damage to buried pipelines during the passage of seismic waves 97
V.M. Varshitskiy, E.N. Figarov, and O.A. Kozyrev

Statistical analysis of mechanical test results for samples of pipes from trunk oil pipelines after long-term operation 107
D.A. Neganov, S.V. Skorodumov, and N.Yu. Nikitin

Testing of composite repairs according to ISO and ASME standards and beyond 123
J. Schoene

Assessment of a cracked pipe subject to transient flow by the Monte Carlo method 135
M. Hassani, O. Bouledroua, M. Hadj Meliani, L. Sadou, and G. Pluvinage

Forthcoming international events 146, 159, 160

Design aspects for connections, supports, and expansion loops in pipelines made from composite materials 147
D.G. Pavlou

Pipeline Science and Technology

Administrative information

1. Disclaimer: While every effort is made to check the accuracy of the contributions published in Pipeline Science and Technology, the publishers do not accept responsibility for the views expressed which, although made in good faith, are those of the authors alone.

2. 2. Copyright: © 2018 Pipeline Transport Institute, Moscow, Russian Federation, and Technical Productions (London) Ltd, Eastleigh, UK. All rights reserved. The content is licensed under a Creative Commons Attribution-Noncommercial (4.0) license (CC BY-NC 4.0).

The authors sign exclusive license agreements, whereby the authors retain copyright but license exclusive rights for their work to the publisher Pipeline Transport Institute (PTI). PTI as the copyright holder is granted the exclusive right to publish and distribute a paper, and to grant rights authorization to copying items for general distribution, for advertising and promotional purposes, for creating new collective works, and for internal and personal use by others.

This publication may be freely reproduced, stored or transmitted in any form or by any means, provided this is not done for commercial purposes and provided the user gives appropriate credit (with a link to the formal publication through the relevant DOI), and provides a link to the license, and indicates if changes were made and that the licensor is not represented as endorsing the use made of the work.

The licensor cannot revoke these freedoms as long as the user follows the license terms.

Special requests should be addressed to the Pipeline Transport Institute, Moscow, Russian Federation, or to the editor.

3. Publisher: Pipeline Science and Technology is published in Eastleigh, UK, by Pipeline Transport Institute, Moscow, Russian Federation, in association with Technical Productions (London) Ltd, Eastleigh, UK:

Pipeline Transport Institute (PTI, LLC) , 47 A Sevastopolskiy prospekt, Moscow 117186, Russian Federation
tel: +7 (495) 950-82-95 ext.2234

Technical Productions (London) Ltd, PO Box 660, Eastleigh SO50 0NT, UK. tel: +44 1494 675139.

Editor in chief (Russian Federation): Anatoly E. Soshchenko (soschenkoae@ak.transneft.ru)
Managing editor (Russian Federation: Valentin Komaritsa (komaritsavn@niitnn.transneft.ru)
Leading editorial manager (Russian Federation): Victoria Malinina (malininavn@niitnn.transneft.ru)
Production editor (UK): John Tiratsoo (jtiratsoo@gs-press.com)

4. ISSN 2514-541X

Pipeline Science and Technology (PST) is a peer-reviewed scientific journal published by Pipeline Transport Institute in affiliation with Technical Production (London) Ltd since June, 2017 (four issues per year – March, June, September, January). The Journal uses a double-blind review system. The policy on publication ethics and avoiding publication malpractice is based on Committee on Publication Ethics (COPE) Best Practice Guidelines for Journal Editors.

PST is an open-access product focusing entirely on publishing the latest original research results and related information on oil and gas pipeline transportation all over the world. The Journal covers a broad range of topics in fracture mechanics, structural integrity assessment, maintenance and life extension of pipelines to be of interest and use to both researchers and practitioners. Contributions are welcome which address to these following topics.

Full text of papers, archive issues and the guidelines for authors are placed at the home-page www.pipeline-science.com.

The Pipeline Transport Institute is interested in receiving ideas for co-operation with international pipeline-industry partners. Ideas for this could include joint industry research project, dedicate research projects, and submission of scientific papers for publication in Pipeline Science.

For further details, please contact: Victoria Malinina (MalininaVN@niitnn.transneft.ru)

Vol. 2, No 2, June, 2018

An evaluation of the factors affecting the thermal state of frozen soils at the foundations of a buried oil pipeline

by S.B. Tataurov* and V.I. Surikov

Pipeline Transport Institute, LLC, Moscow, Russian Federation

ARTICLE INFO

Received: 31 January, 2018
Revised: 16 February, 2018
Accepted: 30 March, 2018

ABSTRACT

THIS ARTICLE IS A STUDY of the temperature conditions of frozen soils at the foundation bed of the VSTO-1 underground pipeline. It establishes the primary and secondary factors which affect these soils' thermal state. In particular, this work demonstrates that there is no link between average annual air temperatures and a change to the temperature of frozen soils depth of yearly zero amplitudes close to underground sections of the oil pipeline route. As a first approximation, relationships were found for stabilizing the soil temperatures at the foundations of pipe hanging supports in underground sections over time with a combination of heat-insulating coatings and soil-temperature stabilizers. Primary and secondary factors were established which affect the thermal state of soils at the foundations of pipe hangers in the underground sections.

Key words: oil pipeline, frozen soils, temperature, soil temperature stabilizers, climate, supports, pipeline system.

1. Introduction

Developing and improving trunk pipeline transport is one of the most important global trends in the area of economic, political, and social stability. Countries leading the way in oil transport in conditions where frozen soils are prevalent include Russia, the USA, Canada, and Norway. Oil transport in Russia is complicated not only by harsh natural and climatic conditions; it is further affected by the significant length of trunk pipelines in operation and under construction which run through areas that are difficult to access, such as the Eastern Siberia - Pacific Ocean pipeline, the Zapolyarye – Purpe pipeline, the Kuyumba – Taishet pipeline, and the Skovorodino – Mohe pipeline.

At present, the longest oil pipeline in Russia is the VSTO Eastern Siberia - Pacific Ocean pipeline system at 4,740 km. This oil pipeline runs through the Taishet in the Irkutsk Oblast to the oil-loading port of Kozmino in Nakhodka Bay. The considerable length of the pipeline system's route, both from West to East and from North to South, is characterized by difficult natural, climatic, engineering, and geological conditions, which are determined by its geographical location.

A high level of difficulty for construction and operation is characteristic for the territory through which the VSTO-1 route runs. This can be explained by the lack of infrastructure in many

---

*Corresponding author: Sergey B. Tataurov, email: tataurovsb@gmail.com

http://doi.org/10.28999/2514-541X-2018-2-2-83-95

© 2018 Pipeline Science and Technology. Published by Pipeline Transport Institute (PTI)
in association with Technical Productions Ltd. All rights reserved.

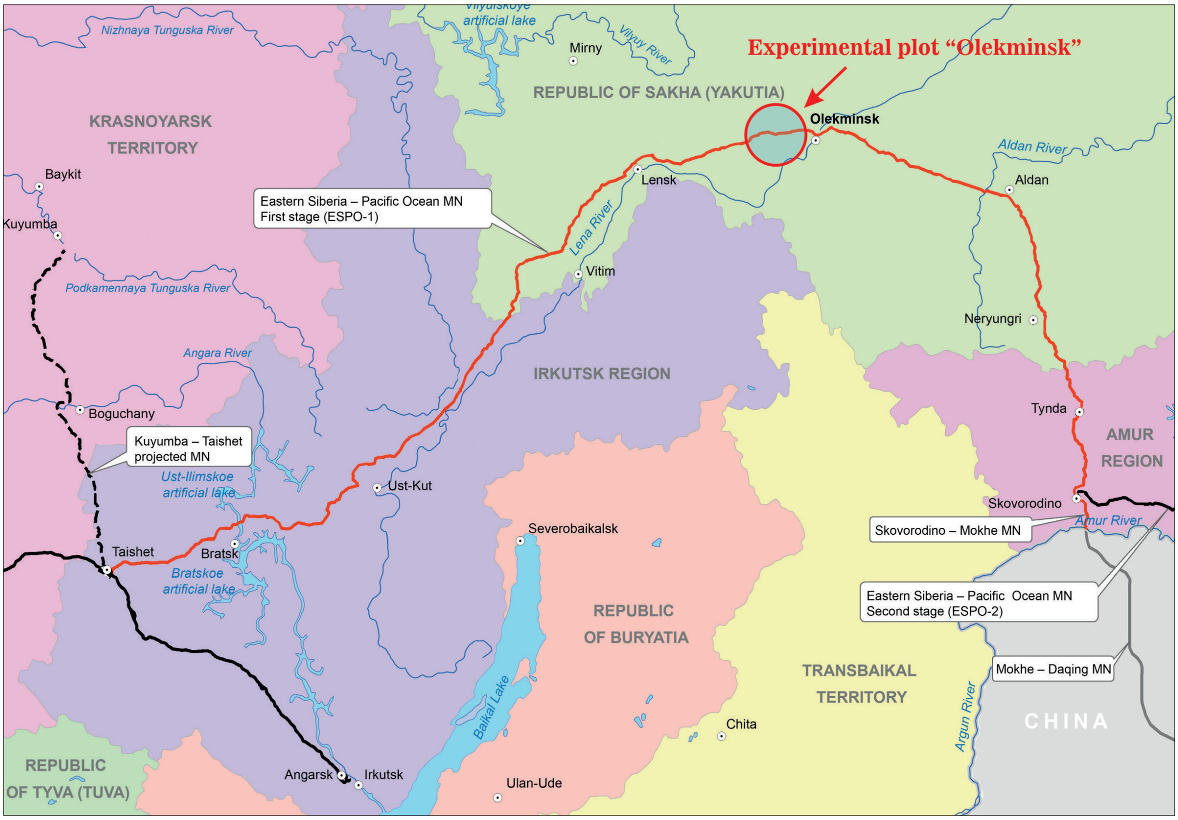

Fig.1. The Eastern Siberia - Pacific Ocean (VSTO) pipeline system (http://tn.promodev.ru/about/projects/realized/10020/).

sections, and factors including the presence of rocky and sandy soils, bogs, taiga, high seismicity, significant quantity of water obstacles, widespread permafrost soils, and high variations in air temperature.

There are only two completed oil pipelines in the western hemisphere which are similar in problems of operation and natural conditions. These are the Trans-Alaska oil pipeline in the USA, and the Norman Wells pipeline in Canada. In 2016 in Russia the Zapolyarye - Purpe oil pipeline was commissioned and is located in the eastern hemisphere.

All these oil pipelines — VSTO and Zapolyarye - Purpe in Russia, the Trans-Alaska pipeline in the USA, and the Norman Wells pipeline in Canada — have one fairly significant circumstance in common: they are all built in regions where permafrost soil is prevalent [1, 2, 3]. Although the Trans-Alaska oil pipeline and the Zapolyarye - Purpe pipeline were built on the principle of above-ground construction, while the VSTO-1 and Norman Wells pipelines are underground, the problems of the geothermal condition of the frozen soils which form the foundation bed for the pipelines remain one of the key challenges for geotechnical monitoring, as well as scientific research and pilot construction works.

In this study, the results of evaluation and analysis are presented for the temperature conditions of frozen soils in the foundation bed of underground in a linear section of the VSTO-1 pipeline1 at the Olyokminsk testing site. The primary and secondary factors which influence their thermal condition are also discussed.

- In particular, on the basis of the methodologies developed by Pipeline Transport Institute

for determining the thermal condition of soils in the foundation bed and of developed technical solutions, the following results were obtained: regarding the influence of average annual air temperatures on the change in annual temperature of frozen soils at a zero depth;
- primary and secondary factors were identified which influence the thermal condition of soils in the foundations of hangers for oil pipelines in underground sections.

The results of research data allowed us:

- as a first approximation to establish the relationship of stabilizing the soil temperatures in foundations of pipe hangers at underground sections, over time, with a combination of heat-insulating coatings and soil-temperature stabilizers;
- to suggest a range of measures to increase the efficiency of soil-temperature stabilization at the foundations of the VSTO-1 oil pipeline, as well as to increase the efficiency of monitoring operations.

Among the issues which have not yet been mentioned, it is worth noting modelling of the thermal condition of the soil-pipeline system, using soil-temperature stabilizers and heat-insulating coatings, is among a range of observations, as well as improvements to the methodology for monitoring the thermal condition of frozen soils using high-speed drilling technology.

These and other questions will be examined in subsequent studies.

2. Methods

The research methodology included studying the temperature conditions at the Olyokminsk site of the VSTO-1 pipeline system (Fig.1), in the period from 2010 to 2017, during a period of maximum frost penetration and thawing of soils, respectively, in November and June. The research methodology included several stages:

- As the first stage, reconnaissance works were carried out connected with collecting and processing information obtained over many years of research into the temperature conditions, the lithological composition of the soils, and the geomorphological zoning of results on the basis of aerial photography analysis.

- At the second stage, the baseline temperatures of the soils were evaluated and analysed, taking into account the climatic datasets, obtained from the nearest weather stations.

- The third stage included analysis and assessment of soil temperatures at the foundation bed at the Olyokminsk test site obtained from the nearest weather stations.

- The fourth stage consisted of studying soil-temperature stabilization at the foundations the pipeline hangers at the Olyokminsk test site, from June 2015 to August 2017, with a combination of heat-insulating coatings and soil-temperature stabilizers.

The aim of thermometric observations the Olyokminsk test site of the VSTO-1 pipeline system with permafrost soils was the constant monitoring of the actual soil temperature, in order to confirm the load-bearing capacity of the soils and to evaluate the efficiency of temperature-stabilization measures.

The location of thermometric boreholes was determined in two stages:

- determining the sections of the route where it was necessary to constantly monitor the

Table 1. Average annual air temperatures for the section of the Olyokminsk test site of the VSTO-1 trunk pipeline

Year											
2005	2006	2007	2008	2009	2010	2011	2012	2013	2014	2015	2016
1	2	3	4	5	6	7	8	9	10	11	12
Average annual air temperature, °C											
- 5.4	- 6.8	- 4.2	- 4.9	- 7.0	- 6.5	- 4.2	- 7.1	- 5.8	- 5.9	- 4.1	- 5.8

---

actual temperature of the permafrost soil (including sections where measures for passive soil-temperature stabilization were anticipated, in particular the use of heat-insulating screens – made from slabs of extruded polystyrene foam – between the lower surface of the oil pipeline and the frozen soil at the foundation);

- determining the location of thermometric boreholes at sections with permafrost, where constant monitoring of the actual soil temperature is necessary:

    - at sections with permafrost where, according to the results of calculation, the strength condition would not be adequate [5, 6];
    - at sections with permafrost, where measures for passive soil-temperature stabilization are anticipated;
    - at sections with permafrost where soil-temperature stabilization measures were implemented while the pipeline was laid on supports.

Baseline soil temperature was measured at a distance of 10 - 15 m from the pipe, and the soil temperature close to the underground pipeline was measured at a distance of 2.5 - 4 m from the pipe. The soil temperature for a pipeline constructed on hangers was measured inside a hanger equipped with a thermometric sensor, and outside at a distance of 0.7 - 1.0 m.

Chain of temperature sensors with an accuracy of -0.1°C (*MTsDT 0922-2-2-26-3,0- (25*x*1,0) -Y1* series) with *KTsD-1/100 - 155,156* loggers were used for temperature measurement. The length of the chains was between 10 and 15 m, while the spacing of the temperature sensors on the thermometric chain was 0.5m up to 4 m; above 4 m they were spaced at 1 m.

Data for the average annual air temperature were obtained from the weather station in the city of Olyokminsk and from the site rp5.ru, for the period 2005 - 2016 (Table 1).

3. Results

3.1. Geomorphological, climatic and engineering-geological conditions

While reconnaissance surveys were carried out, including collecting and processing information obtained over many years of research into the temperature conditions and lithological composition of the soils, and into the geomorphological zoning of results based on analysis of aerial photography, the following information was obtained and updated.

In terms of geomorphology, the Olyokminsk test site is located within the area of the Prilenskii Highland region of the Central Siberian Plateau, at 340 - 510 m above sea level. Within its area, denuded surfaces stand out with absolute elevations of 420 - 510 m, 380 - 420 m, and 300 - 380 m, which are distinguished from one another by ledges, clearly shown in the terrain. The largest area in the given section has an erosional-denuded and erosional-accumulative terrain.

The modern hydrographic network in the region has a netlike pattern, and valleys extending to the NE and NNW prevail. The distribution of the river network, as well as the morphology of the river valleys, is determined by the geological-structural conditions in the region and the fracturing of the Cambrian carbonate rocks.

For this area, a relatively harsh continental climate is characteristic, distinguished by a moderately warm summer and a harsh winter with relatively little snow. The radiation balance has negative value from October to March. Precipitation falls primarily during the summer, 4 - 5 times as much as during the winter, which is twice as long as summer. The annual total precipitation is 200 – 300 mm.

The average temperature for January varies from -25.2°C to -34°C; the average temperature for July ranges from +12°C to +16 °C. Cyclonic activity raises the quantity of precipitation sharply. Over 2 - 3 months, more than half the annual precipitation total falls, with maximum in July and the first half of August.

Based on the results of engineering-geological surveying, the section of Quaternary deposits has been studied to a depth of 10 m. Upper-Quaternary deposits are QIII, and Alluviums I and II of the above-floodland terraces with heights of 10 to 30 m along the Rivers Lena, Olyokma, and Chara are interpreted to be Upper-Quaternary deposits. The deposits are represented by loams and sands with interbedded shingles formed from pebbles of quartz, quartzite and igneous rocks. The depth of the deposits is usually not large and only occasionally reaches 15-20 m, and up to 36 m in the lower reaches of medium and small rivers.

The Olyokminsk test site of the VSTO-1 oil pipeline route is located in an area which, at a small scale, belongs to a zone of massive-insular spread of permafrost. The depth of this zone of permafrost rocks is up to 100 m [4].

Permafrost rocks at this section of the route are characterized by a distribution that is predominantly interrupted in area and continuous along the vertical (unstratified). Areas where crystalline Pre-Cambrian rocks are widespread in the permafrost account for up to 80% of the entire area. Within the limits of sedimentary-rock distribution (Lena-Aldan Plateau), permafrost formations occupy no more than 50 - 60% of the territory. One distinguishing feature of this section of the route is the variation in frozen conditions depending on zonal and non-zonal factors (the altitude of the area and its position on the terrain).

The least harsh frozen conditions belong to regions with levelled, highland, terrains and especially to their watershed areas. One important feature of these sections in engineering-geological terms is the deep seasonal frost penetration and thawing of the ground, which reaches 3 to 6 m, and the dynamic nature of their frozen condition — including the possibility of two-way transition of rocks from a frozen to a thawed state and *vice versa*. This is due to the wide development in the given territory of rocks with an average annual temperature close to zero.

The most typical soils in the layer of seasonal freezing and thawing along the entire route are pulverescent loams, from light to heavy. Less commonly, sands can be found with interlayers of sandy loam and loams, often containing elements of gruss and detritus. The depth of seasonal thawing in these soils varies from 1 to 2.5 m. The minimum depth of seasonal thawing in these soils — 0.5 to 1.5 m — is found in waterlogged sections of river valleys where peat and peaty loams are present in the cross-section.

Overall, for watershed surfaces of regions with highland terrain, the insular development of frozen earth is characteristic, while for the slopes of river valleys, unbroken development is more common.

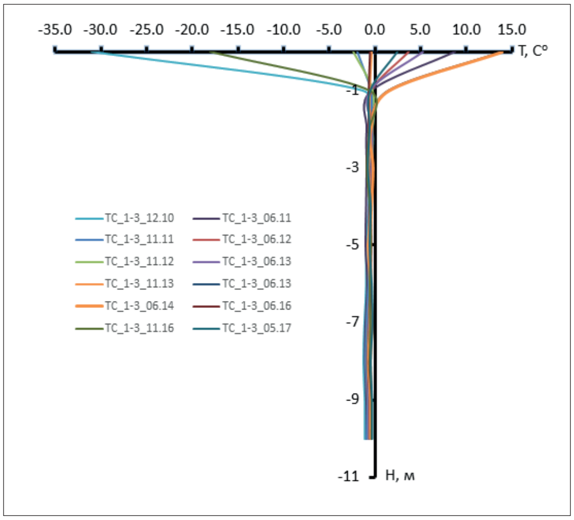

Fig.2. Results of measuring soil temperatures at the Olyokminsk test site of the VSTO-1 pipeline system, (TS 1-3, located at a distance of 10 m from the pipeline. The measuring period was from 2010 to 2017, and measurements were taken in June and November).

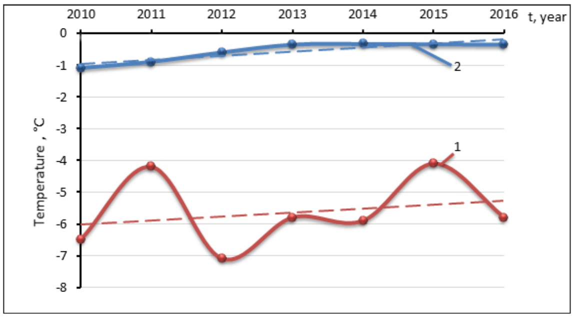

Fig.3. Trends in changes to average annual air temperatures (Olyokminsk weather station) (1), and temperatures of frozen soil at the depth of annual zero amplitudes (Olyokminsk test site, TS 1-3) (2) over the period from 2010 to 2016.

Table 2. Average annual air temperature data (from the weather station in the city of Olyokminsk) and frozen soil temperatures at a depth of annual zero amplitudes (Olyokminsk test site, TS 1-3) for the period 2010 – 2016

	Year	**Average annual air temperature, °C**	**Temperature of frozen soil at the depth of zero annual amplitude, °C**
1	2	3.0	4.0
1	2010	- 6.5	-1.1
2	2011	- 4.2	-0.9
3	2012	- 7.1	-0.6
4	2013	- 5.8	- 0.35
5	2014	- 5.9	- 0.33
6	2015	- 4.1	- 0.34
7	2016	- 5.8	- 0.35

In the period of engineering-geological surveying of the oil pipeline route, the top of frozen rock was found at a depth of 0.2 to 17.7 m. The average annual temperature of soils varied from -0.15°C to -3.8°C. The exposed depth of permafrost soils reached 20.0 m. Among the dangerous geological processes, it is worth noting thermokarst, erosion, and waterlogging.

Geomorphological, climatic and engineering-geological conditions thus distinguish this area of the test site of the VSTO-1 route by their high complexity and high contrast. The frozen conditions indicate the presence of high-temperature soils at the foundation bed (the temperature of permafrost soils is more than -1.5°C), with a depth of seasonal soil thawing, depending on the lithological composition and geomorphological conditions, from 3 to 6 m.

3.2. Thermal conditions

Research was carried out into the thermal conditions of soils at the Olyokminsk test site, with the following results.

According to data from December 2010, the baseline soil temperature in thermometric borehole TS 1-3, located at a distance of 10 m from the pipe, it was established that the depth of seasonal freezing and thawing varies from 1.5 to 2.0 m. The soil temperature at a depth of 10 m was -1.2°C, which characterizes the type of permafrost soils as high-temperature (greater than -1.5°C).

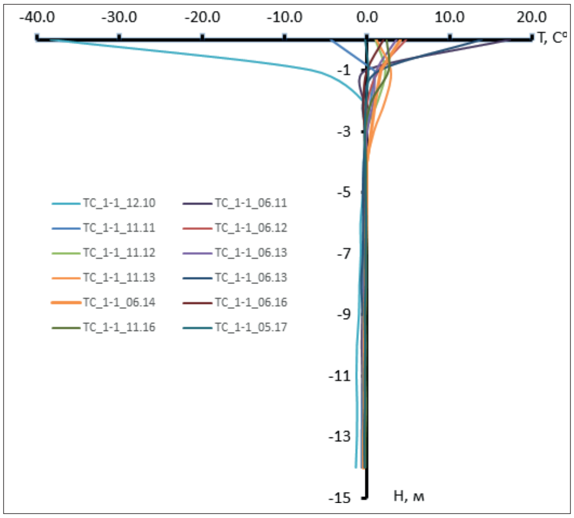

Fig.4. Results of soil-temperature measurements at the Olyokminsk test site, TS 1-3, located at a distance of 10 m from the pipeline. The measurement period was from 2012 to 2017, and measurements were taken in June and November.

In order to establish the possible influence of changes to the average annual air temperature on the long-term temperature conditions of soil at the foundation of the underground oil pipeline, a correlational analysis was carried out for the average annual air-temperature data (obtained from the Olyokminsk weather station between 2005 and 2016 – Table 1), with data from temperature measurements of frozen soil at a depth for the period from 2010 to 2016. The data from temperature measurements for the frozen soil were obtained from thermometric borehole No.3 (TS 1-3), located at a distance of 10m from the oil pipeline (Fig.2, Table 2). The following conclusions were established from analysis at the Olyokminsk test site on the route of the VSTO-1 underground oil pipeline:

- There is only an insignificant correlational link between the influence of the average annual air temperature and the change in frozen soil temperature at a depth of annual zero amplitude (Fig. 3).
- An increasing trend is characteristic both for the increase in average annual air temperature and for the increase in frozen soil temperature.
- The variation in the frozen soil temperatures with depth at a distance of 10 m from the oil pipeline, over a seven-year period, was 0.75°C (from -1.10°C to -0.35°C).
- The average air temperature, according to data from the Olekminsk weather station, over

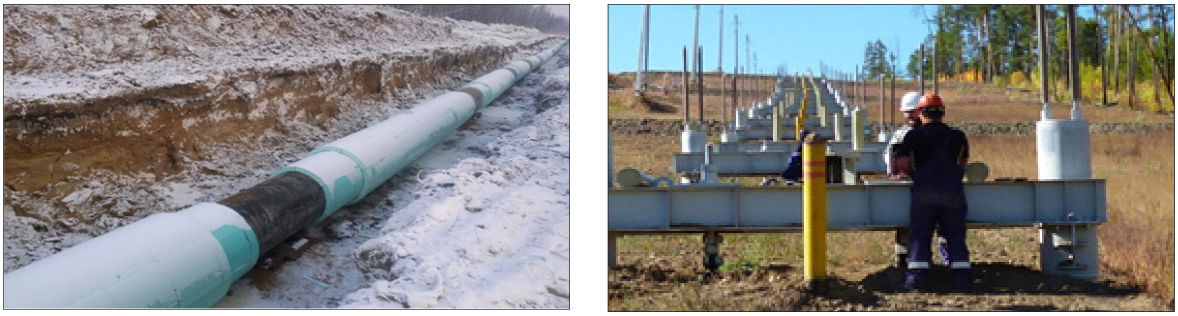

Fig.5.Process of carrying out a series of oil pipeline reconstruction works at the Olyokminsk test site on the section of route of the VSTO-1 oil pipeline.
(a - left) intstalling of double layer of thermal insulation with thickness of 200 mm;
(b - right) finishing installing of pipe hangers for the underground oil pipeline, as well as piled soil-temperature stabilizers.

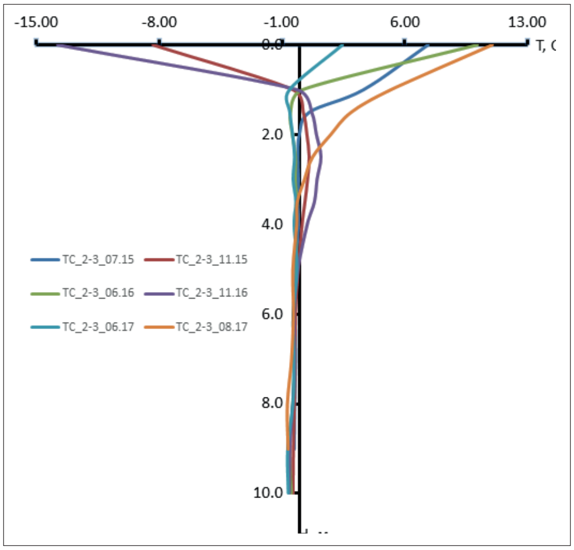

Fig.6. Results of measuring soil temperature at the Olyokminsk test site of the VSTO-1 pipeline system, TS 2-3, located at a distance of 13 m from the oil pipeline with a 200-mm thick thermal-insulation layer; measuring period from July 2015 to August 2017.

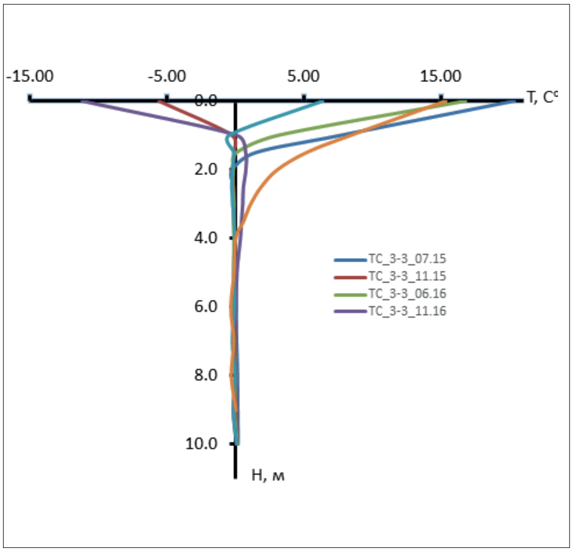

Fig.7. Results of measuring soil temperature at the Olyokminsk test site of the VSTO-1 pipeline system, TS 3-3, located at a distance of 13m from the pipe hanger; measurement period from July 2015 to August 2017.

a seven-year period was -5.6°C with maximum deviation of 1.5°C from the average annual air temperature, with temperatures increasing (-4.1°C in 2015) and decreasing (-7.1°C in 2012).

Furthermore, during pipeline operation and monitoring of the temperature condition of soil at the pipeline foundation, at a distance of 1 m from the pipeline, the following results were obtained.

At the test site over the period from January 2011 to November 2013, an increase in the depth of seasonal freezing and thawing in the soil from 2 m to 6.5 m was observed, while the temperature of the frozen soil at a depth of 10 m increased by 0.82°C and varied from -1.2 to -0.3°C (Fig.4).

The established increase in temperature and increase in depth of thawing in soil at the foundation required a geotechnical solution to stabilize and decrease the soil temperatures at the foundation at the Olyokminsk test site of the VSTO-1 pipeline system.

In March 2014, at the route test site, pilot works were carried out to stabilize the temperature condition of the soil, including installing thermal insulation with thickness of 100 mm on the oil pipeline, and with additional thermometric borehole equipment. Segments of extruded polystyrene foam were used as a heat-insulation coating for the pipeline.

Monitoring of the temperature condition of the soil at the foundation over the period from November 2014 to November 2015 after thermal insulation had been installed on the pipeline showed that there was an increase in the temperature of permafrost soil in the thermometric borehole, located 1 m from the pipeline. In particular, there was an increase in soil temperature at a depth of 10 m in thermometric borehole TS 4-1, located 1 m from the pipeline, in comparison with November 2014 and 2015, changed from -1.46 to -1.13°C. At other sections of the route, at a depth of 10 m, a change in soil temperature was noted, with a margin of error in the chain of thermometric sensors of approx. ± 0.1°C. At the same time, changes to the position of the top of

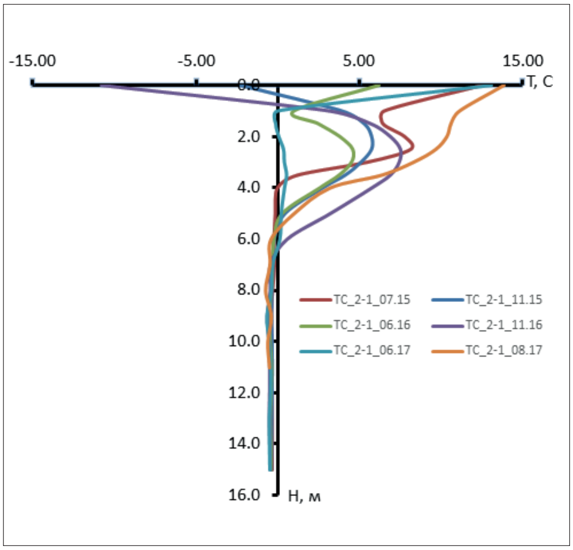

Fig.8. Results of soil-temperature measurements at the Olyokminsk test site of the VSTO-1 pipeline system, TS 2-1, located at a distance of 2.0 m from the pipeline, with a 200-mm thick thermal-insulation layer measurement period from July 2015 to August 2017.

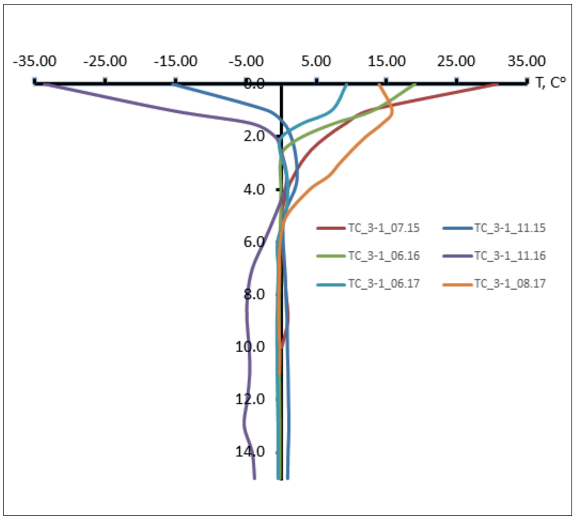

Fig.9. Results of soil-temperature measurements at the Olyokminsk test site of the VSTO-1 pipeline system, TS 3-1, located in a pipe hanger with a 200-mm thick thermal-insulation layer and soil-temperature stabilizer in the pile; measurement period from July 2015 to June 2017.

the permafrost were noted. These were 0.5 - 2.4 m, with the exception of one section, where the top of the frozen soil remained at the previous level.

In connection with this, in 2015, the decision was made to fit a second layer of thermal insulation, and to install pipe hangers for the underground oil pipeline, as well as piled soil-temperature stabilizers (Fig.5). These measures aimed to guarantee the design strength and stability of the oil pipeline, and were taken as a result of the possible soil subsidence at the foundation, and also with the oil pipeline achieving its designed carrying capacity, and with an increase in the temperature at the surface of the pipe wall from +15°C to +32 °C.

The results of geothermal monitoring of soils at the foundation at the Olyokminsk test site of the VSTO-1 pipeline system which was being reconstructed allowed the following to be established.

Measurements of baseline soil temperatures in the period from 2010 to 2017 testify to the lasting high-temperature character of the soils (> -1.5°C) in their natural state, according to the data from the thermometric borehole TC 1-3, located at a distance of 13 m from the oil pipeline.

Moreover, at a depth of 10 m, an increase in soil temperature can be observed from -1.1°C (in December 2010) to -0.63 (in August 2017 – Figs 2 and 6). The depth of seasonal freezing and thawing in the soil varied from 2.0 m (data for December 2010) to 3 - 4 m (data for November 2016), while the depth of the permafrost top was 3.5 - 5 m (Figs 2, 6, and 7).

Analysis of soil-temperature measurements at the foundations, located 2 m from the pipe hanger, indicate the development of both degradational and aggradational processes. Compensatory measures were taken as a result of this, specifically the installation of a 200-mm thick thermal-insulation layer and soil-temperature stabilizers mounted in the pipe hangers of the pipeline (Fig.8).

From the moment of installation of this thermal-insulation layer, the depth of the top of the permafrost increased from 5 to 7 m in the period from July 2015 to November 2016. This finding was based on data from the thermometric borehole TC_2-1, installed at a distance of 2 m from the pipeline. By contrast, in August 2017, the depth of the top of the permafrost decreased to 6 m. The temperature of the frozen soil at a depth of 6 m in July 2015 was -0.21°C and in 08.2017 it was -0.43°C.

The increase in the depth of permafrost soil from the moment when reconstruction work on the section of pipeline was completed testifies that there were processes which had a warming influence on the soil at the foundation. These were replacing and backfilling the soil under the pipeline foundation; backfilling the oil pipeline with soil from the side of the trench; as well as the temporal factor, including the period of construction and installation works, and especially the amount of heat from solar energy, precipitation, etc.

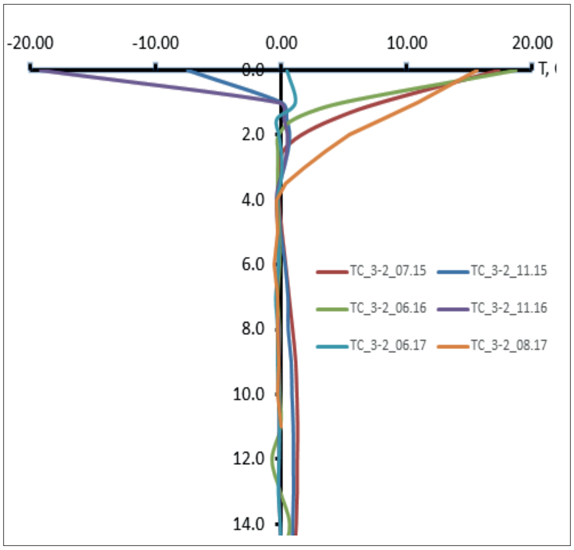

Fig.10. Results of soil-temperature measurements at the Olyokminsk test site of the VSTO-1 pipeline system, TS 3-2, located at a distance of 1 m from the pipe hanger; measurement period from July 2015 to August 2017.

As a first approximation, it can be noted that the decrease in the depth of the top of the permafrost apparently indicates the completion of degradation processes in frozen soil as a result of the pipeline's impact. This includes the avoidance of the warming effect of the pipeline surface, with pipe wall temperature +15°C, as well as carrying out construction works to apply a thermal-insulation layer on the oil pipeline.

Studying the temperature condition of the frozen soil at the thermometric boreholes TS 3-1 and TS 3-2, at the Olyokminsk test site, showed that at the moment when installation of pipe hangers was completed, in July 2015, the soil temperature at the hanger itself and at a distance of 1.0 m from it, at a depth of up to 15 m, was within the range of positive values (Figs 9 and 10).

Apparently, this is as a result of the warming impact of pipeline operations over a five-year period, as well as of construction work to reconstruct this section with overlay, and climatic factors: solar energy and precipitation.

In June 2016 the results of measuring soil temperature at this section of the route showed a positive change towards the development of aggradation processes in frozen soils. According to data from the thermometric borehole TS 3-1, the temperature in the pile showed negative values at a depth of more than 15 m; minimum and maximum temperatures for the depth of the pile were from -0.06 to -0.27°C (Fig.9). In June 2017 temperatures in the pile showed lower values from -0.38 to -0.53°C, while at the same time the depth of seasonal frost penetration in the soils was 6 m.

According to data from the thermometric borehole TS 3-2, located 1 m from the pipeline support, in June 2016 the temperature of the soil along the cross-section of the well also showed negative values up to a depth of 13 m, while at a depth from 13 to 15 m positive temperatures were recorded (Fig.10). In June 2017 the soil temperatures showed lower values at a depth up to 15m, and were from -0.05°C at a depth of 15 m to -0.35°C at a depth of 4 m, according to TW-2 data. The depth of seasonal frost penetration in the soils was 3 m.

At the present time, the data available from monitoring the temperature condition of soils

Table 3. Relative levels of impact of natural and technology-related factors on the thermal condition of permafrost soil at the foundation of an oil pipeline

	Factors	**Period of impact, years**	**Type of impact**	**Level of impact**
1	Primary			
1.1	Disturbance of the soil and vegetation cover	short-term (3-5)	technological	high
1.2	Change to the structure, composition, and properties of the frozen soil in the trench (excavation)	short-term (3-5)	technological	high
1.3	Waterlogging	short-term (3-5)	natural/technological	high
1.4	Presence of heat sources	short-term (3-5)	technological	high
2	Secondary			
2.1	Change to the terrain	mid-term (5-10)	natural/technological	medium
2.2	Climate change	long-term (more than 10)	natural	low

at the pipeline foundation the Olyokminsk test site show the positive preliminary results of the reconstruction work on the pipeline, undertaken in locations where permafrost soils are widespread.

For a full analysis and evaluation of the factors affecting the thermal condition of frozen and thawing soils, as well as for a forecast of the thermal condition of soils over time and area, it would be necessary to perform physical-mathematical modelling of the processes in the climate-pipeline-soil system with a set of results from direct methods of geotechnical monitoring of the condition of the pipeline and soils located in natural and disturbed states.

4. Discussion

The results described here from research into the thermal condition of soil at the foundation of an underground oil pipeline are one of the fundamental elements of monitoring and evaluation of the technical condition of the VSTO-1 pipeline. This is because soils at the foundation of the oil pipeline distribute in space and over time the static and dynamic loads from the engineering structures being built on them. Variation in the temperature of frozen soils leads to a change in their physical and mechanical properties, structure, and composition due to the proportion of free and unfrozen trapped water and ice in the frozen soil. This is both a reason for subsidence and development of viscoplastic deformations and, as a consequence, for lowering the load-bearing capacity of the soils. Therefore, establishing the factors which affect the thermal condition of the soils at the foundation is a high-priority task in carrying-out preventive and compensatory measures, aimed at preserving and stabilizing the temperature of soil at the pipeline foundation.

According to the results of research, the primary factors affecting the thermal condition of soils at the foundation of an underground oil pipeline include technology-related factors most relevant in the short- to mid-term periods, while the natural and climatic conditions of the area are relevant in the long-term period (Table 3). However, these natural, climatic, and technology-related factors are interlinked. A change to one of them strengthens the contribution of the other to the thermal condition of soil at the pipeline's foundation.

According to the research results, the correlation between the average annual air temperature and a change in the temperature of frozen soils at the pipeline foundation indicates that the climate does contribute to the change in the thermal condition of the frozen soil at the foundation in the given location. At the same time, the short data set of average annual air temperatures and for soil temperatures at a depth of zero annual amplitudes, located at a small distance from the oil pipeline (10-13 m), does not allow an objective evaluation to be made of the impact of the climate on the change to the present condition of the soil at the foundation. This would require further research to be carried out. However, it is worth noting that in the long-term, apparently, the impact of the climate on the thermal condition of soil at the foundation of the oil pipeline will increase.

The change in the thermal condition of the soil at the foundation the oil pipeline is most noticeable given the change in the condition of the surface of the area and the soil during construction works. Another factor is the warming impact of the oil pipeline, the temperature of which is +15^{o}C at the surface of the pipe. As can be seen from analysis of the temperature of soils which form the pipeline foundation, technological factors can lead to degradation of frozen soils over a short time, over 3 - 5 years. At the same time, the contribution of the climate increases sharply, with the change of such characteristics as: albedo (disturbance to the soil and vegetation cover, water content of the area), thermophysical properties of the soil (change to the structure and composition of backfilling soil, including due to increasing its moisture content, with the build-up of precipitation (above-permafrost waters) in the trench where the underground pipeline is laid), as well as increases to the temperature of frozen soils at the foundation bed.

The solution to this problem depends on choosing the right approach to stabilizing and restoring the temperature condition in the soil at the foundation, as well as timely detection of changes to the thermal condition of frozen soils, uncovering the causes and carrying out compensatory measures.

As shown by the present article, the methodological approach is based on principles eliminating the impact of thermal sources on the frozen soil, including the technologies aimed at diverting heat away from the soil mass. Besides this, the compensatory measures which were developed allowed to decrease the probability of soil subsidence in the underground sections of the oil pipeline route with thermokarst.

This methodology was implemented in the form of compensatory measures, including:

1. Installing a 200-mm thick thermal-insulating layer on the oil pipeline.
2. Mounting pipe hangers of the oil pipeline where it was buried.
3. Installing soil-temperature stabilizers.

Currently, it can be seen from the results of geotechnical monitoring carried out by the Centre for Monitoring and GeoInformation Systems of Pipeline Transportation Facilities of Pipeline Transport Institute st soils. This indicates that the choice to eliminate the influence of the primary factors on the thermal condition of frozen soils at the foundation of this underground oil pipeline at the Olyokminsk test site was methodologically sound.

5. Conclusion

On the basis of results from these studies, primary and secondary factors were identified that affect the thermal condition of frozen soil at the foundation of an underground oil pipeline.

The research showed that the presence of a correlation between the average annual air temperature and the temperature of frozen soil at the foundation of the oil pipeline, at a depth of zero annual amplitude, which indicates that the climate contributes to the change in thermal conditional of frozen soil at the pipeline foundation at the given location. At the same time, the small range of data for average annual air temperature and soil temperature at a depth of zero annual amplitude, located at a small distance from the oil pipeline (10-13 m), does not allow for an objective evaluation of the climate's impact on the change in the condition of soil at the foundation. This would require further studies.

It is also worth noting that apparently in the long-term the impact of the climate on the thermal condition of the soil at the pipeline foundation of an oil pipeline will increase. Climate impact on the thermal condition of the frozen soils mass is also possible in the short-term. However, this would be only part of the background of technological impacts, especially in terms of construction and installation works carried out in a programme of technical upgrades and capital repairs.

The relationships obtained between the thermal condition of soil at the foundation of the underground oil pipeline before and after reconstruction, at a first approximation, indicate the positive dynamic of aggradation in frozen soils. This allows a conclusion to be made about the methodologically correct choice of technical solutions in reconstructing sections of the underground oil pipeline route, located in permafrost soil.

Conflicts of interest

All authors have no conflicts of interest to declare.

References

[1] N. Davis, 2011.Permafrost, a guide to frozen ground in transition, University of Alaska Press.
[2] Y.V. Lisin, Y.V. Bogatenkov, V.I. Surikov, Y.B. Micheev, and A.N. Petelin, 2014. Geotechnical monitoring of base of aboveground pipeline supports in the areas of permafrost and soft soils. *Engineering Surveys* 3/2014.
[3] Y.V. Lisin, A.E. Soshchenko, V.I. Surikov, V.V. Pavlov, and M.Y. Zotov, 2014. Technical Solutions for methods sof laying oil pipeline from Zapolyarye to Purpe oil pumping station. *Science and Technologies: Oil and Oil Products Pipeline Transportation*, 1 (13).
[4] Permafrost study map of the USSR, scale 1:2500000, 1991.
[5] SP 36.13330.2012 Trunk pipelines. Revised Edition SNiP 2.05.06-85*.
[6] SP 25.13330.2012 Foundations and Foundation Beds on Permafrost Soils. Revised Edition SNiP 2.02.04-88.

To cite: S.B. Tataurov, V.I. Surikov. An evaluation of the factors affecting the thermal state of frozen soils at the foundations of a buried oil pipeline. Pipeline Science and Technology. 2018; 2(2): 83-95.DOI: 10.28999/2514-541X-2018-2-2-83-95.

TRANSNEFT
WESTERN SIBERIA

MODULAR PIPELINE

SPECIFICATIONS

- **Outer diameter**
  170 mm
- **Internal diameter**
  143 mm
- **Pipe material**
  aluminium
- **Pressure**
  6.3 MPa

REPAIR WORKS FOR

- temporary transportation of oil, petroleum products, water, oil mixtures or petroleum products and water mixtures, washing liquid;
- the supply of inert gas mixtures;
- filling and emptying of MP and MPP.

COMPETITIVE ADVANTAGES

- high speed and ease of installation of the equipment;
- the possibility to reuse;
- environmentally friendly materials;
- application at sites where welding works are prohibited;
- high strength of pipe material;
- resistance to aggressive chemicals.

THE COMPLETE SET INCLUDES

pipe, joint, insulation joint,
earthing clamp, cross-connection,
earthing cable, hardware

Branch «Central base
of production service»
of JSC «Transneft – Western Siberia»
644040, Russia, Omsk, per. Neftyanoy, 20
phone +7 (3812) 69-13-65

Vol. 2, No 2, June, 2018

A study of the cyclic damage to buried pipelines during the passage of seismic waves

by V.M. Varshitskiy*, E.N. Figarov, and O.A. Kozyrev

Pipeline Transport Institute, LLC, Moscow, Russian Federation

ARTICLE INFO

Received: 7 February, 2018
Revised: 21 May, 2018
Accepted: 22 May, 2018

ABSTRACT

THE SEISMIC STRENGTH of underground pipelines is assessed based on the axial stresses on the pipeline from the so-called particular combination of loads and impacts. When calculating the stresses from seismic impact, several standard coefficients are introduced, which assume some damage to the pipeline while ensuring the safety of people and the integrity of equipment. These coefficients also take into account anchoring, which depends on the backfill soil and the degree of pipeline criticality. Permissible stresses are accepted in accordance with regulatory documents for design (SNiP 2.05.06-85). The seismic strength of the pipeline in operation is assessed taking into account the seismic impact intensity which is actually reached during an earthquake, and the loads and impacts which affect a pipeline in an earthquake, as well as any defects present in the pipeline wall.

When a seismic wave passes through an underground pipeline, the girth welds are exposed to an alternating cyclic impact. Here, it is relevant to estimate the fatigue damages accumulated over the course of the earthquake. The magnitude of this damage depends on the intensity of the earthquake, the seismograph of the earthquake, the speed with which the longitudinal seismic wave travels along the longitudinal axis of the pipeline, the degree to which the pipeline is anchored by the soil, and the stress concentration coefficient in any defects.

This article studies the accumulation of cycle-induced damage caused by a longitudinal seismic wave. The results may be applied for evaluations of the cyclic longevity of girth welds with defects in pipelines operating in seismic zones.

Key words: pipeline, strength, stresses, cyclic recurrence, wave, seismicity

1. Introduction

When exposed to seismic impacts, pipelines are subjected to an oscillatory process together with the soil mass. The intensity of the earthquake and the specific way the oscillatory process develops in the ‘pipeline-soil’ system depends significantly on the properties of the soils. Depending on the density and homogeneity of the soil surrounding the pipeline, the presence of frozen earth, and the water and ice content of the soil, differences will be found in the intensity

---

*Corresponding author: Victor M. Varshitskiy, e-mail: VarshitskiiVM@niitnn.transneft.ru

http://doi.org/10.28999/2514-541X-2018-2-2-97-105

© 2018 Pipeline Science and Technology. Published by Pipeline Transport Institute (PTI) in association with Technical Productions Ltd. All rights reserved.

of earthquake effects, and in the composition of the seismic vibrations, and in the mechanism of interaction between the pipeline and the surrounding soil.

The requirements for ensuring seismic strength in trunk pipelines are determined by the necessity that the main structure of a pipeline system must be in operation during earthquakes and over a certain period afterwards, without any major repair works. As numerous experimental data have shown, as well as the results of inspections, underground pipelines which are laid in soils with average properties in terms of seismic characteristics are strongly bound to the soil mass. Pipeline deformations coincide with deformations in the soil mass, accurate up to a certain coefficient (as a rule, less than one).

It has been established that the degree of damage to the pipeline during an earthquake depends on a whole range of factors: the strength of the seismic impact and the directions in which the seismic waves travel, the geological and hydrological conditions, the operational loads and impacts, the construction of the pipeline and joints, the characteristics of the pipe steel, and the material of the supports, as well as the degree of 'wear and tear' in the pipeline. It is not uncommon to see old pipelines fail even after very weak earthquakes, which are barely felt otherwise.

In documents regulating the design of trunk pipelines, regulations are in place for evaluating the seismic strength when a longitudinal seismic P-wave travels along the axis of an underground pipeline. It is accepted that the soil surrounding the pipeline will involve the pipeline in its movement. The soil deformation is calculated, and pipeline deformation can then be taken as equal to the soil deformation, taking into account the coefficient of slippage. The stresses in the pipeline are calculated, given the extension and compression from the seismic wave for a defect-free pipe.

In an operational pipeline there may be defects in girth welds due to faulty fusion, inclusions, and the presence of cracks, etc. Russian researchers have found that after earthquakes the number of accidents on pipelines tends to increase [1]. Taking into account that during an earthquake the girth welds with defects are exposed to alternating loads, it becomes necessary to assess the accumulation of low-cycle damage from seismic impacts.

In order to evaluate this, it is worth examining an infinite straight-line underground pipeline which is anchored by the soil surrounding it, and which has elastic properties. As a result of an earthquake, seismic waves spread through the soil. The pipeline, connected with the soil, is subjected to the oscillatory process. The elastic interaction between the pipeline and the soil is therefore examined. A description of the interaction model is presented in this paper.

As a result of this solution, the relationship has been established between the axial stresses and time for any point on the pipeline. The low-cycle damage accumulated over the period of seismic impact was also calculated according to GOST 52857.6-2007 [2].

2. The model of interaction between the pipeline and the soil

In order to study the characteristics of the seismic impacts on the stress-strain state of the pipeline, a dynamic model has been developed showing the interaction between a linear pipeline and the soil. The longitudinal deformations of an oil pipeline due to a seismic compression-expansion wave (P-wave), which moves along the longitudinal axis of the oil pipeline, are calculated by modelling the process, and is described using differential equations:

$$at\ \left|u-u_{gr}\left(t,x\right)\right|\leq\frac{t_{pr}}{\pi\cdot D\cdot c_{x0}}$$

$$EF\frac{\partial^2u}{\partial x^2}+\pi Dc_{x0}\left(u-u_{gr}\left(t,x\right)\right)=m\frac{\partial^2u}{\partial t^2}\qquad(1)$$

$$at\ \left|u-u_{gr}\left(t,x\right)\right|>\frac{t_{pr}}{\pi Dc_{x0}}$$

$$EF\frac{\partial^2u}{\partial x^2}+sign\left(\frac{\partial u}{\partial t}-\frac{\partial u_{gr}\left(t,x\right)}{\partial t}\right)t_{pr}=m\frac{\partial^2u}{\partial t^2}\qquad(2)$$

where:

$u_{gr}(t,x)$ is the displacement of soil in the seismic compression-expansion wave (the calculated displacement is used as a function of time for the displacements of soil in the seismic wave), in metres;
t_{pr} is the ultimate resistance of the soil to longitudinal displacement of the pipeline (this can be calculated according to [3] taking into account the factor, equaling 1.6-2, which accounts for the increase in the ultimate resistance given dynamic loading), in N/m^2;
m is the mass of a unit of length of the pipeline with product, taking into account the associated mass of soil (associated mass is taken to be equal to the mass of soil replaced by the pipeline), in kg/m;
F is the area of a cross-section of the pipeline, in m^2;
E is the modulus of elasticity of the steel, in Pa;
u is the displacement of the pipeline in a longitudinal direction, in m;
D is the external diameter of the pipeline, in m;
c_{x0} is a generalized coefficient of tangential resistance of the soil, in Pa/m [4,5].

The initial conditions are taken to be zero, and the boundary conditions may be taken as different — the free ends the displacements of the ends of the section under examination coincide with the displacements of the soil.

As a result of the numerical solution of these equations (for example with the use of a three-layered difference scheme), the maximum longitudinal deformations are calculated for the pipeline from seismic impact ε_s. This formula also makes it possible to study the behaviour of the pipeline section with a gate valve when a longitudinal seismic wave passes through.

The longitudinal deformation which is transferred to the pipeline from the soil mass under the impact of a longitudinal seismic wave can also be calculated using the formula:

$$\varepsilon_s=0.16m_0\frac{a_cT_0}{c_p}\qquad(3)$$

where:

m_0 is the coefficient of pipeline jamming in the soil (taken based on Table 15 of Ref.6);
a_c is the seismic acceleration, which can be calculated according to data from seismic zoning and micro zoning, in m/s^2;

T_0 is the period of seismic vibrations of the soil mass, as determined from surveys, in secs;
c_p is the speed with which the longitudinal seismic wave propagates in the soil mass, and can be calculated from surveys, in m/sec.

It is possible to calculate the coefficient of pipeline anchoring in the soil given seismic impact using the formulas [3, 4]:

$$m_0 = \frac{1}{1+\left(\frac{2\pi}{T_0 c_p \omega}\right)^2} \tag{4}$$

$$\omega = \sqrt{\frac{\pi D c_{x0}}{EF}} \tag{5}$$

When calculating ω it is important to account for the increase in the generalized coefficient of tangential resistance of the soil given a dynamic impact, while the coefficient of the increase can be taken as equal to 1.5.

In order to assess the deformation of the pipeline under seismic impact, we can take the elastic model of interaction of the pipeline with the soil, described in Equn 1. Replacing the differential operators in Equn 1 with the ratio of the finite differences, the following are obtained:

$$\begin{aligned} \frac{\partial^2 u}{\partial x^2} &= \frac{u_{k,j-1} - 2u_{k,j} + u_{k,j+1}}{h^2} \\ \frac{\partial u}{\partial t} &= \frac{u_{k+1,j} u_{k,j}}{\tau^2} \\ \frac{\partial^2 u}{\partial t^2} &= \frac{u_{k-1,j} - 2u_{k,j} + u_{k+1,j}}{\tau^2} \end{aligned} \tag{6}$$

where:

τ is the time increment, in secs;
h is the coordinate x -axis increment, in metres;
k is the number of time increments, dimensionless;
j is the number of x-axis increments, dimensionless.

After some conversions the following is obtained:

$$u_{k+1,j} = 2u_{k,j} - u_{k-1,j} + \left[\frac{EF}{mh^2}\left(u_{k,j-1} - 2u_{k,j} + u_{k,j+1}\right) + \frac{\pi D c_{x0}}{m}\left(u_{k,j} - U_{k,j}\right)\right]\tau^2 \tag{7}$$

Deformations and stresses in the pipeline in a longitudinal direction from the seismic loads can be calculated using the following equations:

$$\begin{aligned} \varepsilon_{Nk,j} &= \frac{u_{k,j} - u_{k,j-1}}{dx} \\ \sigma_{Nk,j} &= E\varepsilon_{Nk,j} \end{aligned} \tag{8}$$

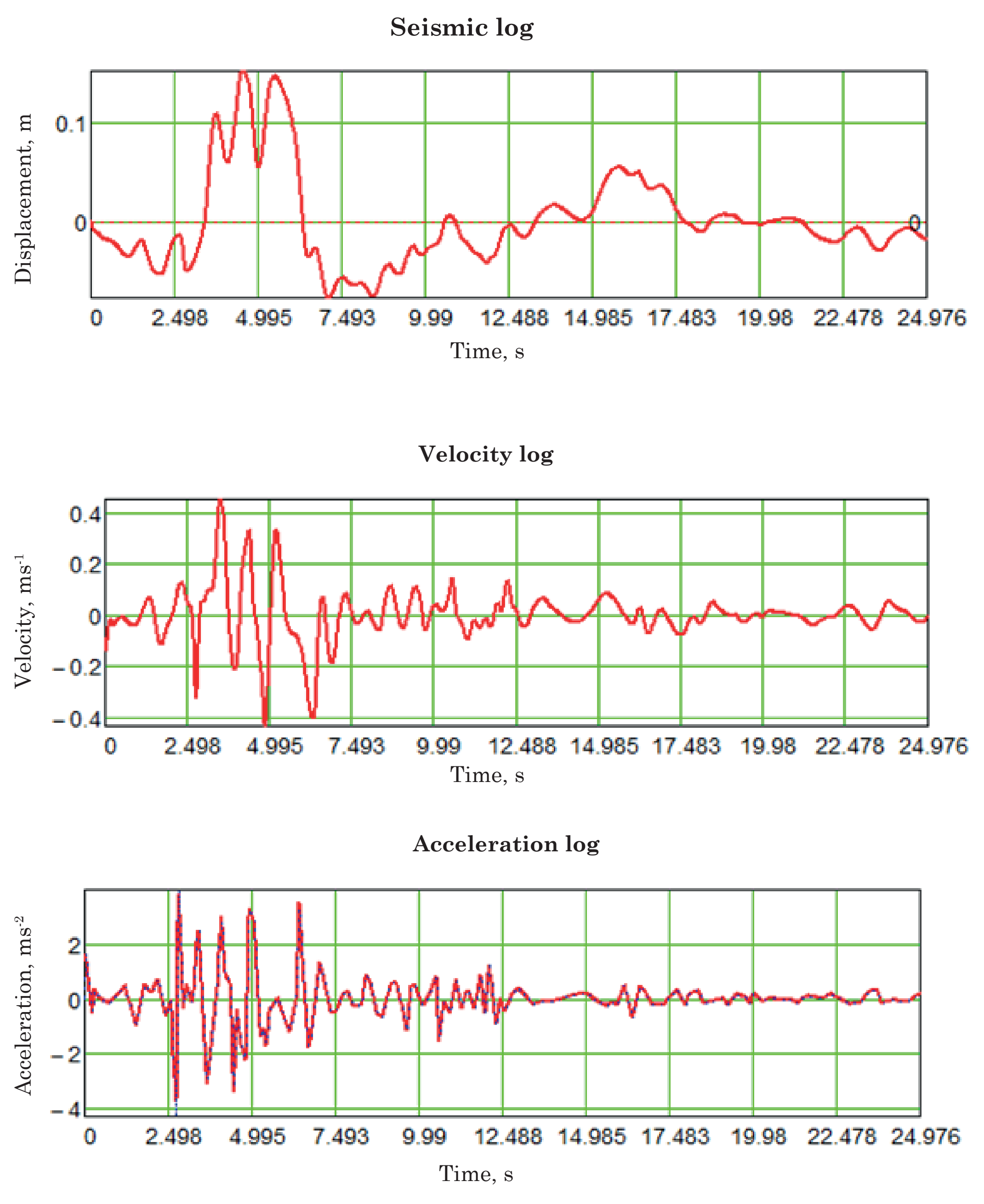

Fig.1. Seismic, velocity, and acceleration logs for the earthquake

3. The results of calculating the seismic impact on an underground pipeline

In order to assess low-cycle fatigue damage in a girth weld containing a defect, we calculate the change in longitudinal stress in a cross-section of the pipeline versus time under seismic impact. As an example, we can examine a 1220 x 16 underground pipeline, laid in free-draining sandy soil. The speed of travel of the longitudinal seismic wave c_p =150 m/s. The impact on the underground pipeline is taken for an earthquake rated at 9 points on the MSK-64 scale. The maximum acceleration of the soil is 4 ms^{-2}. The displacement of soil in the seismic wave is determined from the expression:

$$Ug(t,x) := if\left(x > vp \times t, 0, ys\left(t - \frac{x}{vp}\right)\right) \tag{9}$$

where *ys(t)* is the soil displacement versus time given in the seismic log. The seismic log was normalized for a 9-point earthquake. The seismic velocity and acceleration logs of the earthquake are presented in Fig.1.

For this solution, a three-layer difference scheme for time was used, as described above.

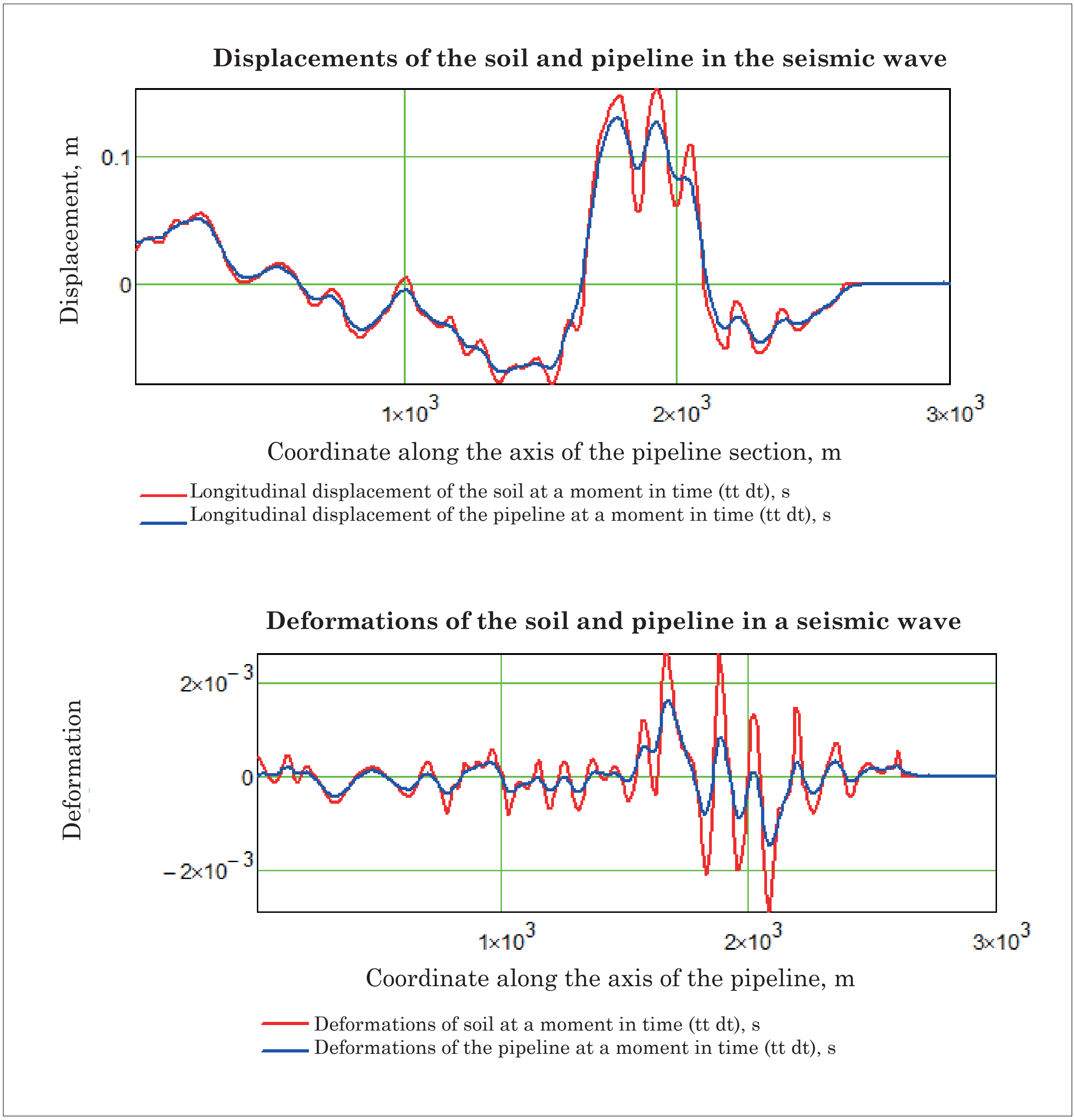

Fig.2. Displacements and deformations of the soil and pipeline in an earthquake.

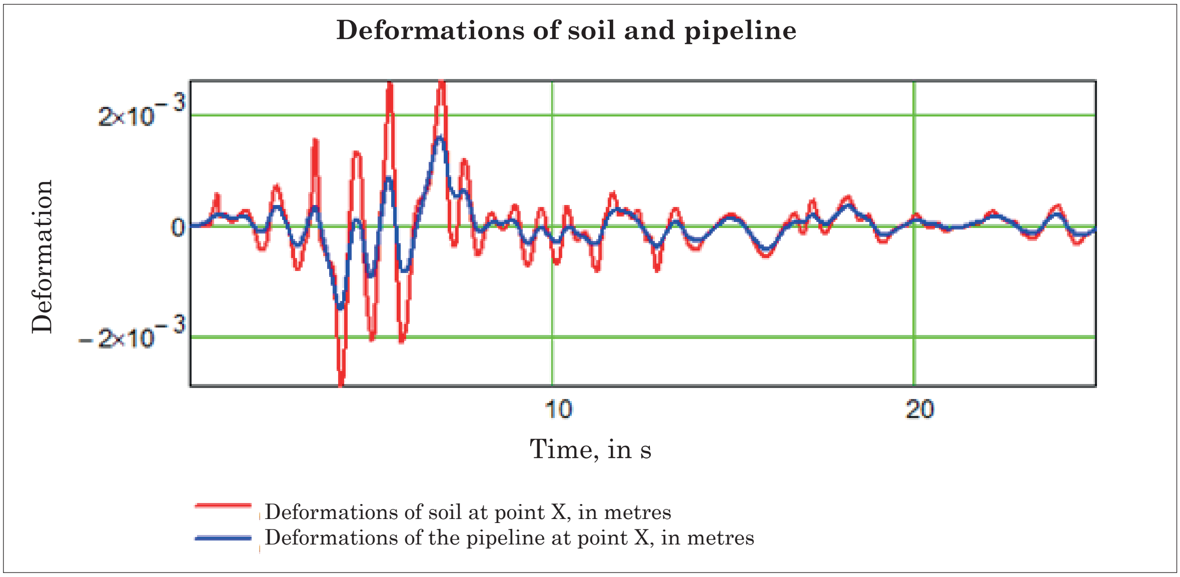

Fig.3. Soil and pipeline deformations at the section under examination.

The time increment is taken to be $\tau = 2{,}174 \times 10^{-3}$ secs, and the coordinate increment as h = 10 m. The duration of the earthquake is 25 secs and the length of the pipeline section is 3000 m.

By solving Equns 7 and 8, the displacements and deformations in the pipeline wall can be calculated. In Fig.2 the displacements and deformations of the soil and pipeline are shown in the seismic wave for the time period 17.4 secs.

Assume that the relevant section is located at the cross-section X, for which it is necessary to determine the deformations and stresses. Deformations in the soil and pipeline in relation to time in the section under examination are presented in Fig.3.

The relationship between the longitudinal stresses and time at the section of the pipeline under examination is presented in Fig.4.

For the following assessment of fatigue damage, a graph showing stress changes versus time drawn. This graph is presented in Fig.4, and was obtained by calculation.

4. An assessment of fatigue damages given seismic impact

In order to assess low-cycle fatigue damage, data for the trend of stress over the time of the earthquake (25 s) were processed using the 'rain' method in accordance with GOST 25.101-83 [7]. The low-cycle fatigue damage was assessed using GOST R 52857.6-2007 and the rule of linear addition of damage. The amplitude of stresses, taking into account concentration for the j-th block of loading, is calculated using the formula:

$$\sigma_a(j,\alpha) = 0.5\alpha\left(\sigma_{maj} - \sigma_{mij}\right) \qquad (10)$$

where:

$\sigma_{ma\,j}$ and $\sigma_{mo\,j}$ are the maximum and minimum stresses in the j-th block of loading, and α is the coefficient of stress concentration.

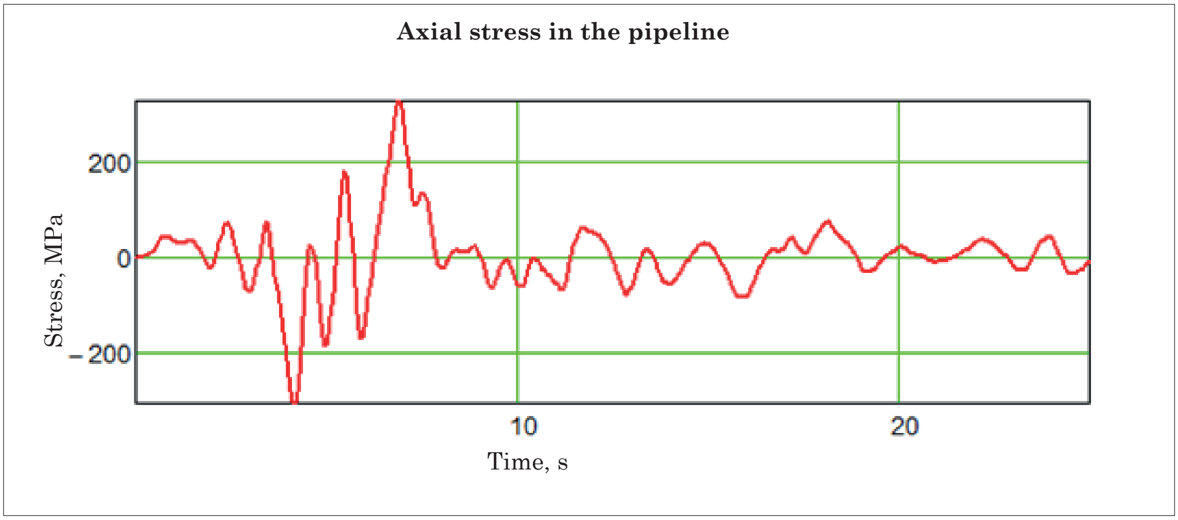

Fig.4. The relationship between longitudinal stresses in the pipeline and time.

The limit number of loading cycles for the j-th block of loading, in accordance with GOST R 52857.6-2007, can be calculated using the formula:

$$N(j,a) := \frac{1}{n_N}\left(\frac{0.99A}{\sigma_{as}(j,a) - \frac{B}{n_\sigma}}\right)^2 \tag{11}$$

where:

$$\sigma_{as}(j,a) := \max\left(\sigma_a(j,a), \frac{B}{n_\sigma}\right) \tag{12}$$

A = 0.45x10^5 MPa
B = 0.4 σ_B
σ_B = 550 MPa
n_N = 10
n_σ = 2

The relationship between the low-cycle fatigue damage and the coefficient of stress concentration in the defect can be calculated according to the formula:

$$S(\alpha) := \sum_j \frac{mn_j}{N(j,\alpha)} \tag{13}$$

where n_{nj} is the number of cycles in the j-th block of loading. The results of the calculation are shown in Fig.5.

It should be taken into account that in a general case the low-cycle fatigue damage given seismic impact will depend on the intensity of the earthquake, the seismic log of the earthquake, the speed at which the seismic wave travels along the longitudinal axis of the pipeline, the degree of pipeline anchoring in the backfill soil, the stress concentration coefficient in the defect, as well as other factors. In each specific case a separate calculation should be made according to the methodology described above.

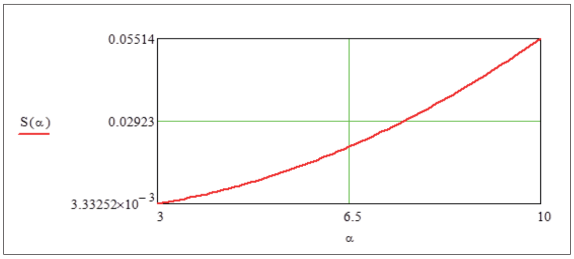

Fig.5. The low-cycle fatigue damage depending on the stress concentration coefficient given the seismic impact studied.

5. Conclusion

1. A method has been proposed for evaluating the accumulation of low-cycle fatigue damage from seismic impacts given the presence of defects in a buried pipeline.
2. An example has been presented of calculating low-cycle damage to the underground pipeline containing a defect under seismic impact.
3. Low-cycle damage following seismic impact depends on many factors (the intensity of the earthquake, the soil backfill around the pipeline, the coefficient of concentration in the defect, etc.), which must be taken into account in each situation.
4. When evaluating the safe service life of girth welds with defects in seismically hazardous zones, the damage from seismic loads in the case of an earthquake occurring should be added to the damage from differential temperatures and pressures.

Conflicts of interest

All authors have no conflicts of interest to declare.

References

[1] Sh.G. Napetvaridze, 1980. The seismic resistance of trunk pipelines and special constructions in the oil and gas industry, M., Nauka.
[2] GOST R 52857.6-2007, Vessels and apparatus. Regulations and methods for calculating their strength. Strength calculations given low-cycle loads.
[3] A.B. Aynbinder, 1991. Design of trunk and field pipelines for strength and stability, Moscow, Nedra.
[4] A.S. Gekhman, 1988. Calculation, construction and operation of pipelines in seismic zones, M.:Stroiizdat, p.180.
[5] A.S. Gekhman, Sh.G. Napetvaridze, 1980. Seismic resistance of trunk pipelines and special constructions in the oil and gas industry / O. A. Savinov. — M.:Nauka, p.172.
[6] SNiP 2.05.06-85*: Trunk pipelines.
[7] GOST 25.101-83, Methods of schematizing random processes of loading in elements of machines and constructions and a statistical presentation of the results.

To cite: V.M. Varshitskiy, E.N. Figarov, and O.A. Kozyrev. A study of the cyclic damage to buried pipelines during the passage of seismic waves. Pipeline Science and Technology. 2018; 2(2): 97-105. DOI: 10.28999/2514-541X-2018-2-2-97-105.

TRANSNEFT

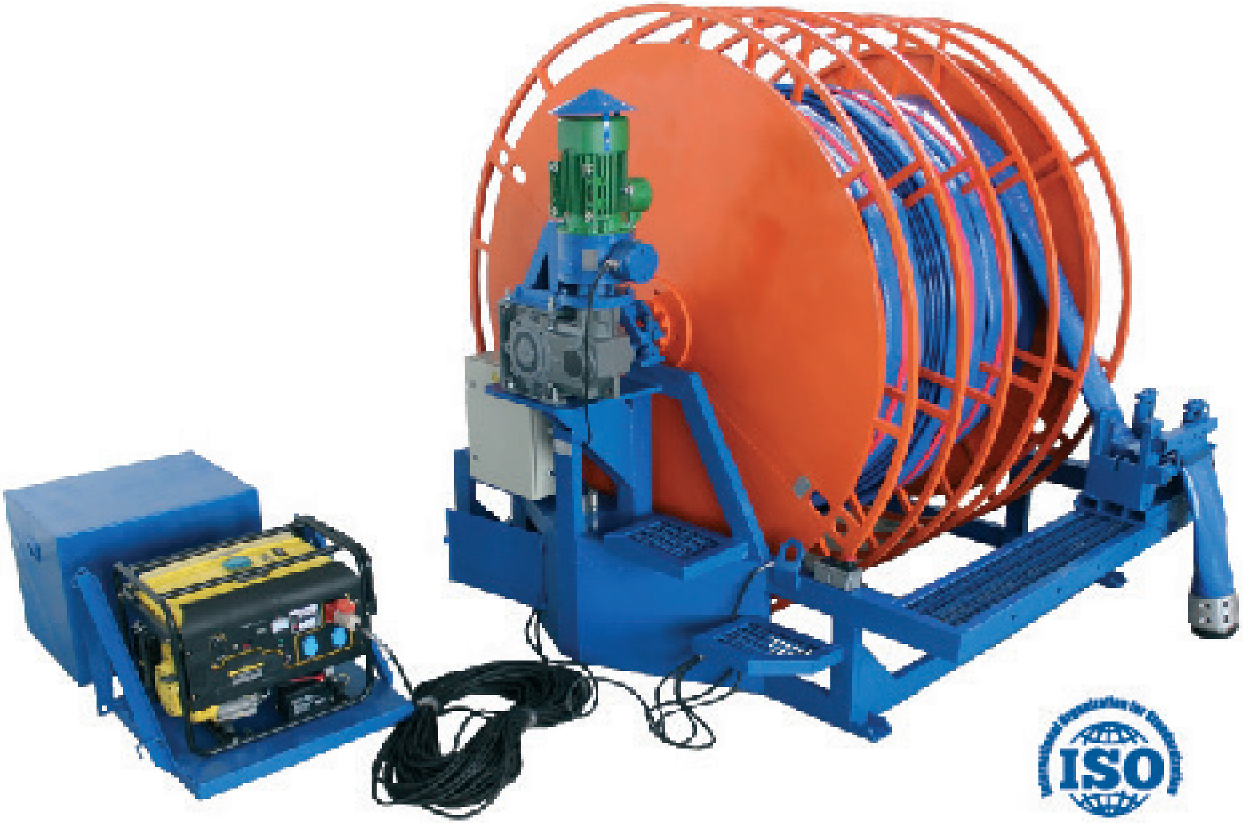

Pipelines from flexible lay-flat hoses TGPS 150-4,0

Purpose: transfer of petroleum products, oil, water during filling or emptying of main oil pipelines and oil product pipelines from -60 to + 40 ° C. The pipeline hose is a body-work basic structure of synthetic fibers with an internal sealing and protective layer of polyurethane with steel bits for CPS connection.

Product specifications: DN - 150 mm, P - 4,0 MPa, L = 100 to 500 m. Supplied with the complete installation of folding and unfolding (electric drive from the petrol station) on the transport drum.

Can be supplied separately without the installation and drum

Your goals — our solutions

Branch of JSC Transneft Volga Region, Center of Maintenance (CBPO)
8 Shosseynaya str., Novokuibyshevsk, Samara Region, Russia, 446200. Tel. +78463579288

Vol. 2, No 2, June, 2018

Statistical analysis of mechanical test results for samples of pipes from trunk oil pipelines after long-term operation

by D.A. Neganov, S.V. Skorodumov, and N.Yu. Nikitin*

Pipeline Transport Institute, LLC, Moscow, Russian Federation

ARTICLE INFO

Received: 12 March, 2018
Revised: 15 May, 2018
Accepted: 21 May, 2018

ABSTRACT

CONDUCTING ANY SCIENTIFIC RESEARCH includes the process of acquiring, processing, and analysing data which are obtained as a result of one or a series of experiments.

Over the prolonged period for which science has existed, a multitude of methods have been created for obtaining experimental data. As part of studying the properties of materials, standard methods are applied for tensile, impact toughness, and hardness tests, as well as fatigue tests. This list of tests can be taken as a base which is used to establish the level and character of loads the given material is capable to sustain during operation. This paper examines approaches to processing experiment results which are obtained using standard (basic) methods when testing pipe steels for trunk oil and oil product pipelines.

At the present time, the degree of automation in experimental equipment is fairly high. However, there is still some human participation when preparing samples and setting-up the experiments, which may lead to errors occurring when performing the tests (the human factor). This article presents some approaches which make it possible to perform initial processing and verification of experimental data for errors and reliability, and against hypotheses and distribution laws for the results obtained. Methods are also suggested for determining the minimum quantity of samples to be tested, based on evaluation of the mechanical property variations in pipe steels.

Several approaches may be applied to solve the task of identifying links and relationships between the analysed parameters. The first approach is deterministic and requires long-term study. When one takes into account the considerable number of factors being studied, it is also fairly expensive and involves rather complicated experiments. The second approach is probabilistic and statistical, which allows implicit dependences to be established between series of measurements (correlation analysis) and linear (pair regression) and non-linear dependences (multiple regression) to be revealed between the parameters being examined. This study applies the statistical approach to analysing data from mechanical tests of pipe steels in trunk oil and oil product pipelines.

---

*Corresponding author: Nikita Yu. Nikitin, e-mail: NikitinNY@niitnn.transneft.ru

http://doi.org/10.28999/2514-541X-2018-2-2-107-122
© 2018 Pipeline Science and Technology. Published by Pipeline Transport Institute (PTI)
in association with Technical Productions Ltd. All rights reserved.

Key words: Strength limit, yield strength, reduction in area, correlation, regression, statistical analysis

1. Introduction

At the present time, processing data obtained from experiments is subject to the requirements of regulatory documentation, in particular GOST R 8.736-2011 [1].

When data are processed, they are checked (verification), ordered according to certain characteristics, and searched for maximum and minimum values. Parameters are also determined for the root mean square deviation, as well as for the confidence intervals of values, and data are visualized (the process of presenting ordered data in the form of schemes, histograms and diagrams).

When it has been established that the experiment results belong to the normal distribution law, it becomes possible to apply methods of correlation and regression analysis.

Applying correlation analysis makes it possible to confirm the presence of statistically significant relationships between the values, while regression analysis establishes the type of empirical equations which link the inter-correlating parameters. This approach has been applied successfully at various metallurgical plants. Thus, at the Vyksa Steel Works it was used when developing an automatic system for steel certification [2]; around 40 parameters were examined which affect the mechanical properties of flat-rolled metal. As a result of this approach a statistical model was developed which describes the dependence of the yield strength on production parameters. This model showed that the measured value deviated from the value calculated from the equation by 5%. The economic effect is reflected in the reduction of the volume of steel sent for qualification testing checks due to failures, and in the reduced necessity of carrying out direct testing for 65% of flat-rolled steel [2]. Reference 3 presents similar statistical studies aiming to obtain regression equations which make it possible to predict the mechanical properties of cold-rolled and annealed steels of AISI 304 class (analogous to 08X18H10). The authors have obtained regression equations which connect the elongation to yield strength and the Brinell hardness to yield strength. They have also obtained a multi-factor regression equation which connects the concentration of various alloying elements, the percentage of δ-ferrite, the grain size and the yield strength. A comparison of the results of calculations based on this equation with experimental results gave a divergence of no more than 5%.

Analysing the experience of using methods of statistical analysis has shown that a fairly large quantity of results has been accumulated from applying statistical checks to the multi-parameter process, aimed at quality control for products manufactured in various technological processes [4]. Methods of statistical analysis had almost never been applied earlier with the aim of multi-factor analysis of the mechanical characteristics of steel for trunk oil and oil product pipelines after long-term operation.

2. Material and methods of testing and research

In carrying out this research, two sets of initial data were used. The first was the results of tests on steel samples where only the steel grade or the strength class was known; the second was the results of tests on samples with known values for steel grade and technical specifications of pipe manufacture [5]. The list of combinations analysed is given in Table 1.

The period of pipe operation with combinations of steel grade — technical specifications of pipe manufacture ranged from six to 40 years. The upper limit of the operating period for the samples with known steel grade values was around 50 years.

Table 1. List of the steel grades and technical specifications of pipe steel

No. in order	Initial data for the tested material
1	2
1	17G1S-U
2	17G1S-U
3	17G1S
4	К52
5	17G1S-U - TU 14-3-1698-90 (steel grade – technical specifications)
6	17G1S-U - TU 14-3-1424-86 (steel grade — technical specifications)
7	17G1S - TU 14-3-602-77 (steel grade — technical specifications)
8	K52 - TU 1381-018-00186654-2009 (steel grade — technical specifications)

The tests on the samples were carried out using standard methods [6, 7]. The mechanical characteristics and regulatory documentation (hereafter RD) are given in Table 2.

Test results were presented in the form of distribution bar graphs showing the mechanical properties. This presentation offers a range of advantages. Firstly, it allows the type of distribution to be evaluated visually (to verify the hypothesis about whether the distribution can be considered normal). Secondly, where normal distribution of results cannot be confirmed, it is possible to calculate the distribution function and switch from discrete statistical analysis to continuous.

The test results were processed according to GOST R 8.736-2011 [1] and processing included the following stages:

- eliminating known systematic errors from the measurement results;
- calculating an estimation of the measured value;
- calculating the root mean square deviation of the measurement results;
- checking for the presence of crude errors and where necessary eliminating them;
- checking the hypotheses about the normal distribution of the measurement results;
- calculating confidence limits for the accidental error when estimating the measured value.

The following statistical analysis was carried out taking into account the standard methods of

Table 2. Testing methodology and the mechanical characteristics determined

No. in order	Characteristic	Calculation method
1	2	3
1	Proof strength, σ_{02}, MPa	Tensile testing based on GOST 1497-84 [8]
2	Tensile strength (ultimate strength), $\sigma_{в}$, MPa	Tensile testing based on GOST 1497-84 [8]
3	Reduction in area in the neck after rupture, ψ, %	Tensile testing based on GOST 1497-84 [8]

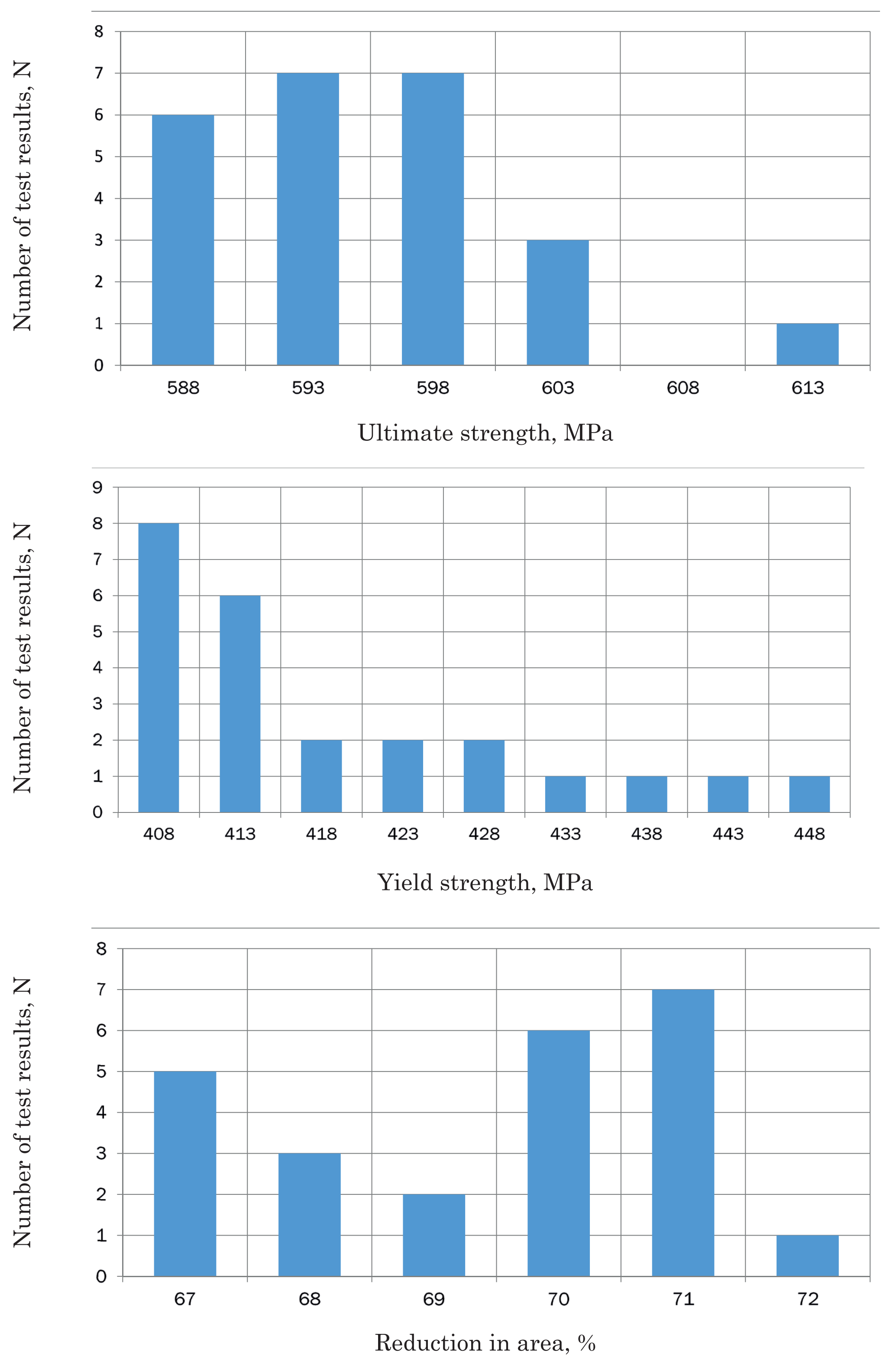

Fig.1. Distribution bar graphs for mechanical testing results for the combination steel grade — technical specifications of 17G1S per TS 14-3-602-77:
(a - top) ultimate strength; (b - centre) yield strength; (c - bottom) contraction ratio.

multi-factor correlation and single-factor regression analysis [9].

Conducting multi-factor statistical analysis of the mechanical properties of steel is conditional upon identifying the factors which affect the strength and plasticity of metal. Within the framework of this study, a systematic approach to dividing the factors which had an influence on the mechanical properties of pipe steels was applied. As a result, all factors were divided into internal and external factors.

The external factors affecting the mechanical properties of pipe steels included the number of loading cycles performed on the pipeline. This was calculated according to the accepted regulatory documentation and based on data for a pressure differential during oil and oil product pumping, in the chosen sections of the pipeline over the last three years.

The internal factors connected with the mechanical properties of pipe steel used at trunk oil and oil product pipelines included:

- the thickness of the pipe wall.
- the pipe diameter.
- the grain number (grain size).
- the structure banding.

The results of calculations using regression equations were verified using the following methods:

- the statistical ‘3- sigma’ method [4];
- the method of direct calculation and comparison of results with experimental data.

In the case of direct calculation and comparison of the calculation results with experimental data, the results of non-destructive inspection and tests may be used as experimental data. These were carried out according to the methods indicated in Table 2.

3 Statistical analysis of mechanical testing results

3.1 Visual representation of mechanical testing results

In Fig.1 distribution bar graphs are presented for the results of mechanical testing on samples of steel with combination steel grade - technical specifications of 17G1S per TS 14-3-602-77. The number of measurements for each of the mechanical properties was 24.

Qualitative analysis of distribution bar graphs for mechanical properties cannot unambiguously confirm the type of distribution of the ultimate strength, yield strength and reduction in area for the combination steel grade – technical specifications of 17G1S per TS 14-3-602-77. This behaviour of the distribution of mechanical characteristics may be linked to an insufficient quantity of accumulated data when this article was written.

Figure 2 presents an example of distribution bar graphs for the results of mechanical testing for steel grade 17G1S-U. The number of measurements for ultimate strength, yield strength and reduction in area was 160.

Visual analysis of the behaviour of a number of test results depending on the mechanical properties on distribution bar graphs of the results also does not make it possible to state a hypothesis about the normal character of the distribution of mechanical properties of pipe steels after prolonged periods of operation for steel grade 17G1S-U.

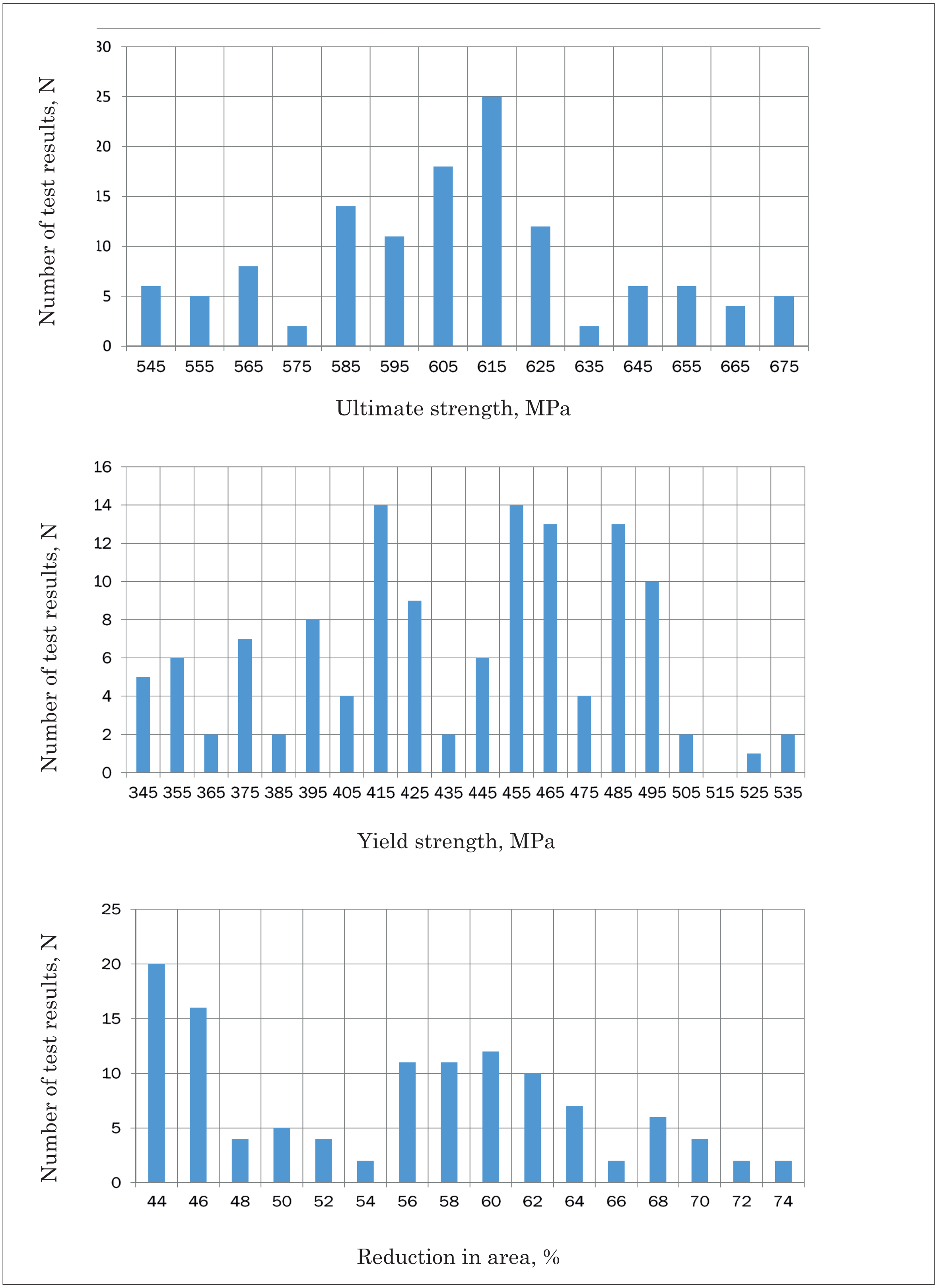

Fig.2. Distribution bar graphs for the results of mechanical testing for steel grade 17G1S-U: (a - top) ultimate strength; (b - centre) yield strength; (c - bottom) reduction in area.

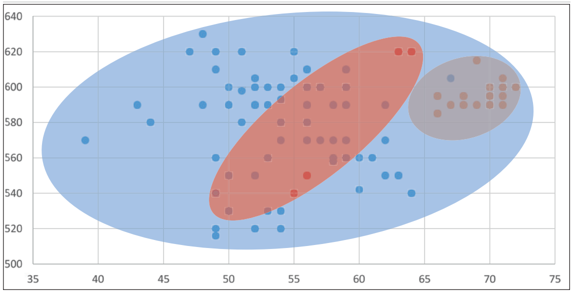

Fig.3. Diagram showing the dispersion of ultimate strength values depending on the reduction in area for the steel grade and for the combination of steel grade and technical specifications:

Blue — Steel grade 17G1S
Red — Steel grade - TS 17G1S-U TS 14-3-1698-90
Orange — Steel grade - TS 17G1S TS 14-3-602-77

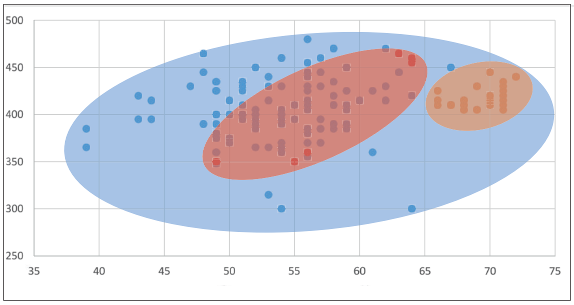

Fig.4. Diagram showing the dispersion of yield strength values vs on the reduction in area for the steel grade and for the combination of steel grade and technical specifications:

Blue — Steel grade 17G1S
Red — Steel grade - TS 17G1S-U TS 14-3-1698-90
Orange — Steel grade - TS 17G1S TS 14-3-602-77

The presented non-uniformity of the data distribution may be linked to the presence of additional factors, which affect the character of the mechanical properties' distribution for steel grade 17G1S-U. Some of these parameters are the technical specifications of pipe manufacture.

3.2 Processing test results

Figures 3 and 4 illustrate the dispersion of the results of mechanical tests of pipe steel regarding only the steel grade, and the steel grade and technical specifications of pipe manufacture. The distribution limits of tensile testing results are marked with ovals of various colours.

In Figs 3 and 4, blue ovals mark out the scatter limits for test results for steel grade 17G1S, without taking into account the technical specifications of pipe manufacture. Red and $\sigma_{0.2}/\sigma_B$ orange ovals mark out the scatter limits for the combination of steel grade and technical specification 17G1S with TS 14-3-602-77, and 17G1S-U with TS 14-3-1698-90 in the total mass of tests for steel grade 17G1S.

From the dispersion diagrams presented (Figs 3 and 4) showing mechanical characteristics, it follows that the scatter of values for ultimate strength and yield strength versus the reduction in area is reduced, when taking into account the pipe manufacture technology. When taking into account the technical specifications for pipes manufacturing, a change can be observed in the steepness of the dependence of the ultimate strength and yield strength versus the reduction in area in comparison to the observed character of the relationship for the steel grade. This conclusion is demonstrated more clearly in Figs 5, 6, and 7.

From the dependencies presented (Figs 5, 6, and 7), it is clear that the general pattern of growth in the yield strength to ultimate strength ratio, versus the reduction in area, is maintained when taking into account the technical specifications of pipe manufacture at the same steel grade.

The scatter values are calculated when evaluating the basic statistical characteristics of the mechanical properties distribution.

3.3 An evaluation of basic statistical characteristics

Based on test results, average values as well as the root-mean-square deviations (henceforth

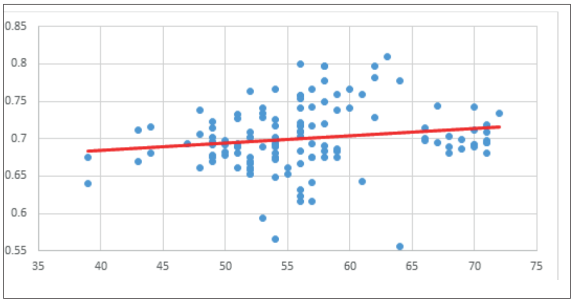

Fig.5. The dependence of the yield strength to ultimate strength ratio $\sigma_{0.2}/\sigma_B$ versus the reduction in area for steel grade 17G1S.

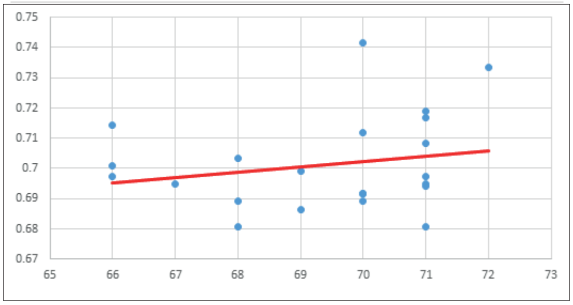

Fig 6. The dependence of the yield strength to ultimate strength ratio $\sigma_{0.2}/\sigma_B$ versus the reduction in area for steel grade – technical specifications 17G1S per TS 14-3-602-77.

RMSD) were calculated for the steel grades and for the combinations of steel grade and technical specifications (henceforth TS) presented in Table 1. In Tables 3, 4, 5 and 6 the results of these calculations are presented.

Comparative analyses of the average values of the ultimate strength, yield strength and reduction in area, calculated separately for steel grades and combinations of steel grade, technical specifications, shows that the values of the average ultimate strength and yield strength for samples of pipe with steel grade 17G1S-U are higher than for samples of pipe with combination steel grade 17G1S-U per TS 14-3-1698-90 and 17G1S-U per TS 14-3-1424-86. However, values of the average reduction in area are lower. For samples of pipe with steel grade 17G1S the values for average yield strength, ultimate strength and reduction in area are lower than for the test results of samples of steel with a combination 17G1S – TS 14-3-602-77. When examining the steel grade K52, the average values of the yield strength and reduction in area are lower than for the combination of K52 per TS 1381-018-00186654-2009, while the value of the average ultimate strength is higher.

Calculating the RMSD establishes that for all combinations of steel grade and technical specifications, the scatter of experimentally obtained values is less than for samples with known steel grade. The exception to this is the results of tests on samples of pipe with a combination of 17G1S-U per TS 14-3-1698-90 (Fig.6).

A cumulative analysis of the results of calculating the RMSD and scatter diagrams (Figs 3 and 4) makes it possible to conclude that taking into account the technical specifications for manufacturing pipes used on trunk oil and oil product pipelines allows the mechanical characteristics of pipe steels to be described more accurately at their further use, in the capacity of initial data for calculating longevity based on current regulatory documentation.

3.4 Defining the necessary and sufficient quantity of samples to be tested

Current regulatory documentation establishes the minimum number of tests which will ensure the reliability of experimental results, but criteria for the optimum number of tests are not specified.

The optimum number of tests depends on the stability and manageability of the process and the corresponding scatter of steel's mechanical characteristics (property variations). The use of statistical methods of data analysis allows the coefficient of property variation to be calculated numerically, according to the equation:

$$K_2 = \frac{S}{x} \qquad (1)$$

- where S is the RMSD of the mechanical characteristic (ultimate strength, yield strength, reduction in area etc.);
- x is the average value of the mechanical characteristic (ultimate strength, yield strength, reduction in area etc.).

Changes in the coefficient of variation, calculated on the basis of the data presented in Tables 3-6 for steel grades in the 17GS group and with various mechanical characteristics of steel, are presented in Figs 8-10.

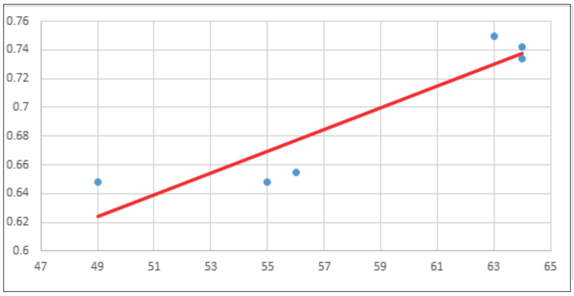

Fig.7. The dependence of the yield strength to ultimate strength ratio $\sigma_{0.2}/\sigma_B$ versus the reduction in area for steel grade and technical specifications 17G1S with TS 14-3-1698-90.

From the bar graphs shown (Figs 8-10), it can be seen that taking into account the method of pipe manufacture leads to a reduction in the variation of pipe steel properties. This indicates the high level of repeatability in the technological process. The exception to this is the behaviour of

Table 3. Average values for basic mechanical characteristics for classification per steel grade

No. in order	**Steel grade**								
	17G1S-U			17G1S			K52		
	Average $\sigma_{0.2}$, MPa	Average σ_B, MPa	Average ψ,%	Average $\sigma_{0.2}$, MPa	Average σ_B, MPa	Average ψ,%	Average $\sigma_{0.2}$, MPa	Average σ_B, MPa	Average ψ,%
1	2	3	4	5	6	7	11	12	13
1	428	598	52	408	582	57	435	564	61

Table 4. Average values for basic mechanical characteristics for classification per steel grade – TS

No. in order	**Steel grade and technical specifications**											
	17G1S-U per TS 14-3-1698-90			17G1S-U per TS 14-3-1424-86			17G1S per TS 14-3-602-77			K52 per TS 1381-018-00186654-2009		
	Av. $\sigma_{0.2}$, MPa	Av. σ_B, MPa	Av. ψ,%	Av. $\sigma_{0.2}$, MPa	Av. σ_B, MPa	Av. ψ,%	Av. $\sigma_{0.2}$, MPa	Av. σ_B, MPa	Av. ψ,%	Av. $\sigma_{0.2}$, MPa	Av. σ_B, MPa	Av. ψ,%
1	2	3	4	5	6	7	8	9	10	11	12	13
1	407	582	59	382	567	56	420	597	69	443	539	78

Table 5. RMSD for mechanical characteristics for classification according to steel grade

No. in order	**Steel grade**								
	17G1S-U			17G1S			K52		
	RMSD $\sigma_{0.2}$, MPa	RMSD $\sigma_{в}$, MPa	RMSD ψ,%	RMSD $\sigma_{0.2}$, MPa	RMSD $\sigma_{в}$, MPa	RMSD ψ,%	RMSD $\sigma_{0.2}$, MPa	RMSD $\sigma_{в}$, MPa	RMSD ψ,%
1	2	3	4	5	6	7	11	12	13
1	48	35	14	30	25	7	30	21	10

Table 6. RMSD for mechanical characteristics for classification according to steel grade and TS

No. in order	**Steel grade and technical specifications**											
	17G1S-U per TS 14-3-1698-90			17G1S-U per TS 14-3-1424-86			17G1S per TS 14-3-602-77			K52 per TS 1381-018-00186654-2009		
	RMSD $\sigma_{0.2}$, MPa	RMSD $\sigma_{\text{в}}$, MPa	RMSD ψ, %	RMSD $\sigma_{0.2}$, MPa	RMSD $\sigma_{\text{в}}$, MPa	RMSD ψ, %	RMSD $\sigma_{0.2}$, MPa	RMSD $\sigma_{\text{в}}$, MPa	RMSD ψ, %	RMSD $\sigma_{0.2}$, MPa	RMSD $\sigma_{\text{в}}$, MPa	RMSD ψ, %
1	2	3	4	5	6	7	8	9	10	11	12	13
1	59	42	6	12	6	2	13	7	2	7	6	2

the coefficient of variation for the ultimate strength and yield strength of pipe steel produced per technical specifications TS-14-3-1698-90.

It is worth noting that the conclusions made from evaluating the behaviour of the coefficient of variation of mechanical characteristics correspond to the conclusions obtained from analysing the RMSD. However, the behaviour of the RMSD characterizes only the scatter of experimental data around a certain average value. It is actually a criterion which to a greater degree describes the quality of the measurement taken, while the coefficient of variation directly describes the change to the property and does not contain hidden errors from the experiment.

The relationship between the coefficient of variation and the number of tested samples of pipe steel from the 17GS steel grade (and its analogues) is shown in Fig.11.

In the relationship shown, the maxima for each characteristic are clearly visible (for ultimate strength, yield strength and reduction in area) in the range corresponding to 20 samples. The results of a similar analyses, taking into account the technology of pipe manufacture, are shown in Fig.12.

When the manufacturing technology is accounted for, the values of the coefficient of variation for ultimate strength, yield strength and reduction in area characteristics have a maximum in the interval from 4 to 8 samples (Fig.12).

Thus, by accounting for the variation in mechanical properties makes it possible to establish criteria for choosing the pipe manufacturing technology which allows the best repeatability of mechanical properties to be assured. In its turn, this will facilitate the highest predictability in the behaviour of the pipe steel during operation.

3.5 Correlation and regression analysis

In order to establish the factors which affect strength and plasticity characteristics during pipe operation in a trunk oil or oil product pipeline, the methods of correlation and regression analysis were applied [9].

When performing correlation analysis, the following factors were considered, as they impact the mechanical characteristics:

- the grain number (grain size);
- the structure banding;
- the thickness of the pipe wall;
- the diameter of the pipe;

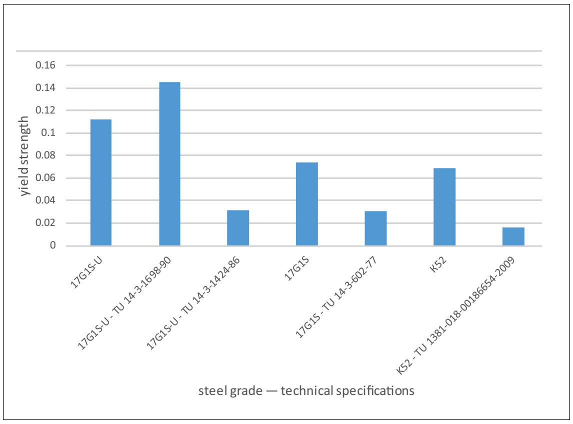

Fig.8. Coefficient of variation for yield strength in the 17GS group of steel grades.

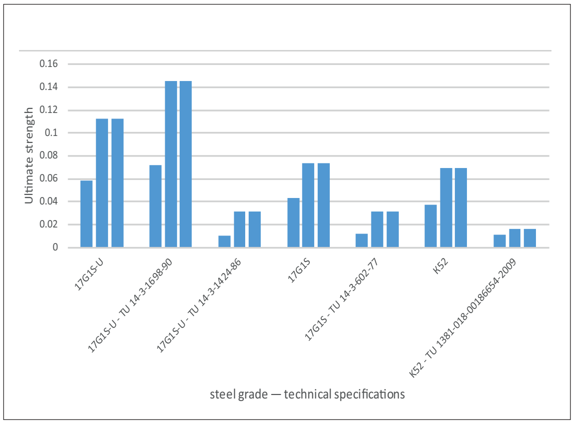

Fig.9. Coefficient of variation for ultimate strength in the 17GS group of steel grades.

- the adjusted number of pipeline loading cycles.

The results of correlation analysis are presented in the form of a correlation matrix between the basic mechanical characteristics and the adjusted cyclic loading (Table 7).

Analysis of the correlation matrix shows that the strength characteristics based on test results for the combination of steel grade (ultimate strength and yield strength) correlate closely with the adjusted number of

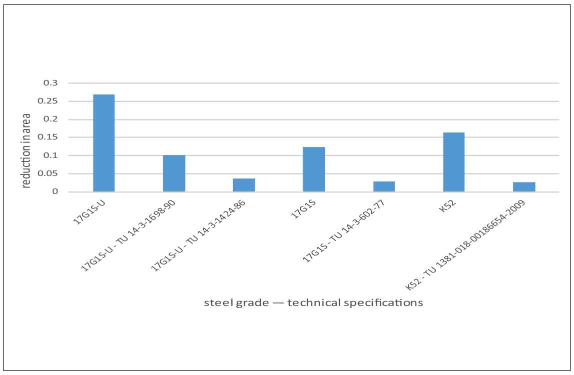

Fig.10. Coefficient of variation for reduction in area in the 17GS group of steel grades.

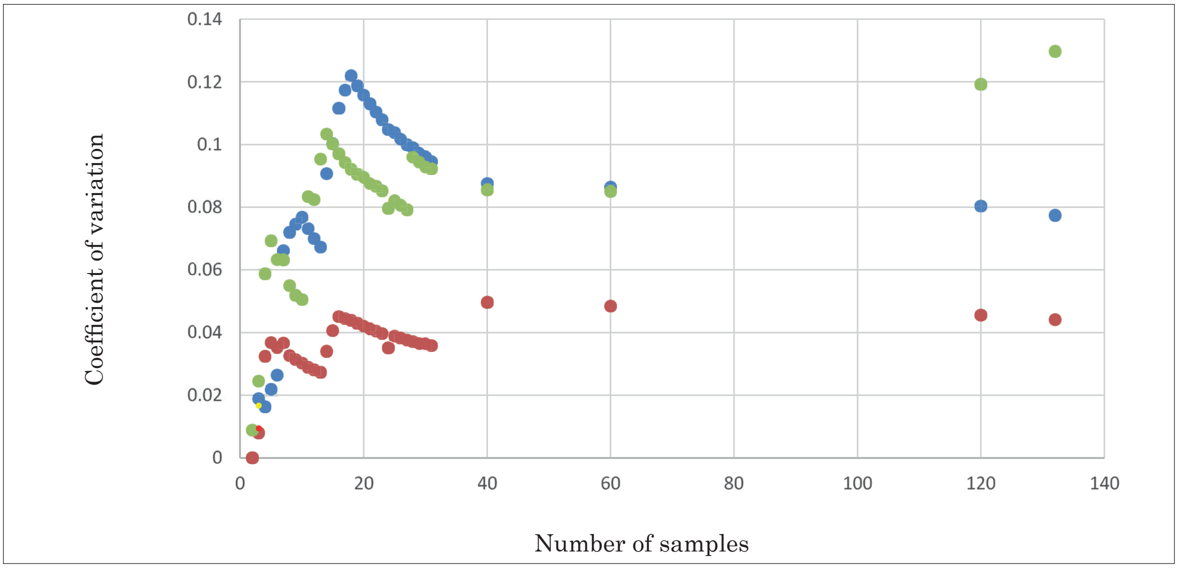

Fig.11. Change to the variation coefficient depending on the number of samples tested for steel grade 17G1S-U: Blue — Yield strength; Red — Ultimate strength; Green — Reduction in area.

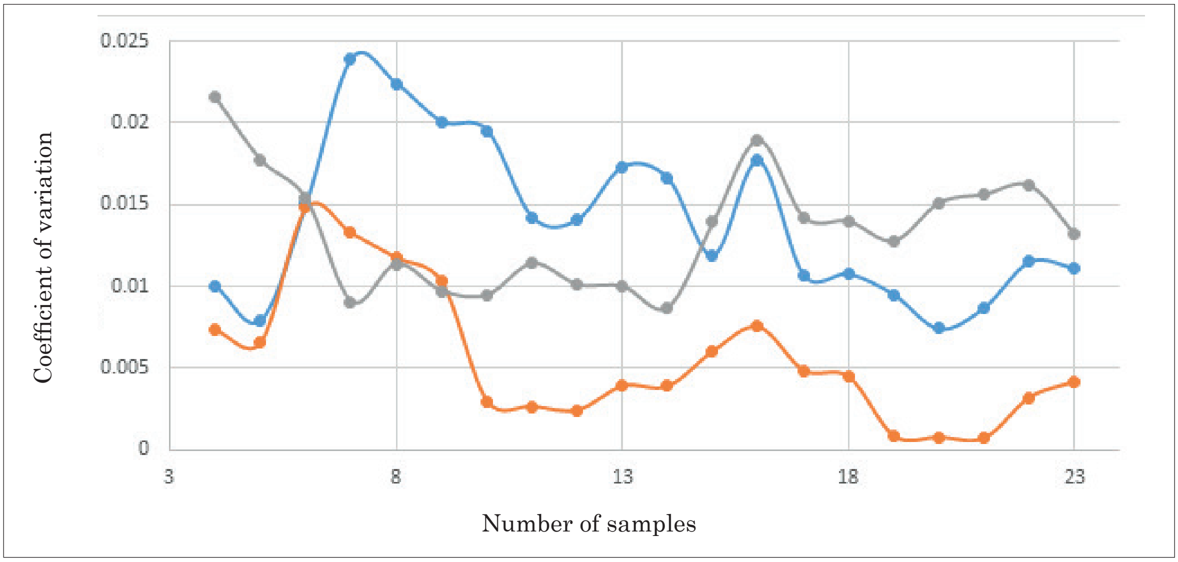

Fig.12. Change to the coefficient of variation for mechanical properties depending on the number of samples tested for the combination 17G1S per TS 14-3-602-77:
Blue — Yield strength; Brown — Ultimate strength; Gray — Reduction in area.

Table 7. Matrix of the correlation coefficients

No. in order	**Values**	**Adjusted number of loading cycles, cycles/year**	**$\sigma_{0.2}$, MPa**	**$\sigma_в$, MPa**	**ψ,%**
1	2	3	4	5	6
1	Adjusted number of loading cycles, cycles/year	1.00	0.84	0.94	0.55
2	$\sigma_{0.2}$, MPa	**0.84**	1.00	**0.95**	0.01
3	$\sigma_в$, MPa	**0.94**	**0.95**	1.00	0.24
4	ψ,%	**0.55**	0.01	0.24	1.00

loading cycles performed on the oil or oil product pipeline ($K_{corr} > 0.7$), while the reduction in area reveals an average level of correlation ($0.5 \le K_{corr} \le 0.7$). It thus follows that the ultimate strength and the yield strength have linear dependency on the number of loading cycles on the pipeline.

Table 8 presents the matrix of correlation coefficients between the mechanical properties and the structure parameters.

The results of correlation analysis between the grain size and structure banding and the mechanical properties of the pipe steel used in trunk pipelines revealed the presence of an average correlation between the microstructure banding and the strength and plasticity characteristics of the pipe steel. A linear dependency is observed only between the mechanical properties and the grain number (size).

Table 8. Matrix of the correlation coefficients for mechanical properties and structure parameters

No. in order	**Parameter**	**Structure banding**	**Grain number**	**$\sigma_{0.2}$, MPa**	**$\sigma_\text{в}$, MPa**	**ψ,%**
1	2	3	4	5	6	7
2	Structure banding	1.00	0.76	0.67	0.64	0.50
3	Grain number	**0.76**	1.00	**0.99**	**0.99**	0.94
4	$\sigma_{0.2}$, MPa	**0.67**	**0.99**	1.00	**0.95**	0.01
5	$\sigma_\text{в}$, MPa	**0.64**	**0.99**	**0.95**	1.00	0.24
6	ψ,%	**0.50**	**0.94**	0.01	0.24	1.00

Table 9. Matrix of the correlation coefficients for mechanical properties and parameters of the pipe geometry

No. in order	**Para-meter**	**$\sigma_{0.2}$, MPa**	**$\sigma_\text{в}$, MPa**	**ψ, %**	**Dn, mm**	**δ_{min}, mm**	**δ_{max}, mm**	**δ, mm**
1	2	5	6	7	8	9	10	11
2	$\sigma_{0.2}$, MPa	1.00	**0.95**	0.01	**-0.78**	**-0.99**	**0.71**	**-0.99**
3	$\sigma_\text{в}$, MPa	**0.95**	1.00	0.24	**-0.62**	**-0.99**	**0.53**	**-0.94**
4	ψ,%	0.01	0.24	1.00	**0.50**	**0.97**	-0.41	**0.88**
5	Dn, mm	**-0.78**	**-0.62**	**0.50**	1.00	**0.71**	**-0.99**	**0.85**
6	δ_{min}, mm	**-0.99**	**-0.99**	**0.97**	**0.71**	1.00	**-0.63**	**0.97**
7	¯ δ_{max}, mm	**0.71**	**0.53**	-0.41	**-0.99**	**-0.63**	1.00	**-0.80**
8	δ, mm	**-0.99**	**-0.94**	**0.88**	**0.85**	**0.97**	**-0.80**	1.00

The results of a similar analysis are presented in Table 9 for the structural parameters of pipes. The results of this analysis revealed a strong correlation (linear dependency) between the ultimate strength, the yield strength, the reduction in area and the minimum and average thicknesses of the pipe walls. The results also showed an average correlation between the mechanical properties and the diameter of the pipe, and between the maximum thickness of the pipe walls (with the exception of reduction in area).

For values which showed correlation with the mechanical properties of pipe steels, linear regression equations were obtained (see Table 10).

The relationships presented here show the growth of the ultimate strength and yield strength versus the average grain number (size) for the combinations of steel grades presented in Table 2, and the fall of the reduction in area depending on the average grain number. In the most general case, this indicates growth in strength characteristics and reduction in plasticity for the examined samples of steel from pipes in long-term operation. It is worth noting that the classic equation for describing the relationship of yield strength to grain size is the Hall-Petch equation [10, 11, 12]:

$$\sigma_{0,2} = \sigma_0 + K_y d^{-1/2} \tag{2}$$

where K_y is the Hall-Petch coefficient, σ_0 is the yield strength of a mono-crystalline sample, and d is the grain size.

Table 10. Regression equations obtained from the results of correlation analysis

No. in order	**Dependency of the values**	**Regression equation**
1	2	3
1	Proof yield strength against average adjusted number of loading cycles	$\sigma_{0.2} = 0.2311N_{perf}^{av} + 339.76$
2	Ultimate strength against adjusted number of loading cycles	$\sigma_B = 0.1834N_{perf}^{av} + 519.53$
3	Proof yield strength against grain number	$\sigma_{0.2} = 43B - 24$
4	Ultimate strength against grain number	$\sigma_B = 22.5B + 344$
5	Reduction in area against grain grade	$\psi = -0.065B + 1.12$
6	Proof yield strength against average thickness of pipe wall	$\sigma_{0.2} = -27.9\overline{\delta} + 680.75$
7	Ultimate strength against average thickness of pipe wall	$\sigma_B = -17.4\overline{\delta} + 742.84$
8	Reduction in area against average thickness of pipe wall	$\psi = 0.06\overline{\delta} - 0.12$

From Equn 2 it follows that the yield strength is inversely proportional to the square root of the grain size. The comparison of the linear relationship based on the results of regression analysis with the Hall-Petch equation indicates the significant discrepancy between the classic principle and the results of statistical analysis. However, in recent years conditions and materials have been discovered, in which the Hall-Petch law failure can be seen [13]. A detailed study of this problem has not yet been carried out for pipe steels after long-term operation, and this issue demands further studies.

The statistical method was used to verify the predictive capability of these equations at sections of trunk and technological oil pipelines with pipes manufactured using steel grades 17GS, 17G1S, 17G1S-U and the strength class K52. This method of results verification is based on the '3-sigma' rule and was used together with the method of direct comparing calculation results from regression equations with experimental data. These showed a discrepancy of less than 5%. When checking the equations at sections of trunk oil or oil products pipelines with pipes manufactured using the steel grade 13KhGS, the deviation of the calculated values from the actual measured data was 13%.

It is worth noting that, despite the small deviations between calculated results and actual measured values of mechanical properties, the results presented are not full and require further study with regard to establishing multi-factor regression equations. Future study should also carry out cluster analysis of the pipe steel grades based on their mechanical characteristics and the operating conditions at trunk oil and oil products pipelines, as well as the increase in the number of data points for corresponding groups of steel grades and technical specifications for pipes manufacture.

4. Discussion of results and conclusions

The application of methods of statistical analysis to the results of mechanical testing of pipes at trunk oil and oil products pipelines after long periods of operation made it possible to assess basic statistical characteristics, as well as to verify the confidence level of experimental results. It was also possible to establish the magnitude of scatter for the ultimate strength, the yield strength and the reduction in area, and to confirm the necessity of taking into account the technology used in pipe manufacture.

A methodology has been proposed for calculating the optimum number of testing samples and comparing the technical specifications of pipe manufacture. The methodology is based on calculating the coefficient of the mechanical properties variation.

Correlation analysis of the results of mechanical testing and data from cyclic loading of pipelines, parameters of pipe geometry, and microstructure of pipe steel made it possible to find a correlation between the parameters indicated. Regression analysis methods enabled equations to be formulated, which link the parameters studied, and to confirm the possibility of predicting the mechanical characteristics of pipe steel at sections with different levels of pipeline loading with an adequate degree of accuracy.

Further studies will be aimed at widening the list of steel grades examined, as well as technical specifications for pipe manufacture. They will also aim to divide steel grades and technical specifications for pipe manufacture into groups with close values for parameters, and to carry out multi-factor regression analysis taking into account the mutual correlation between the factors studied.

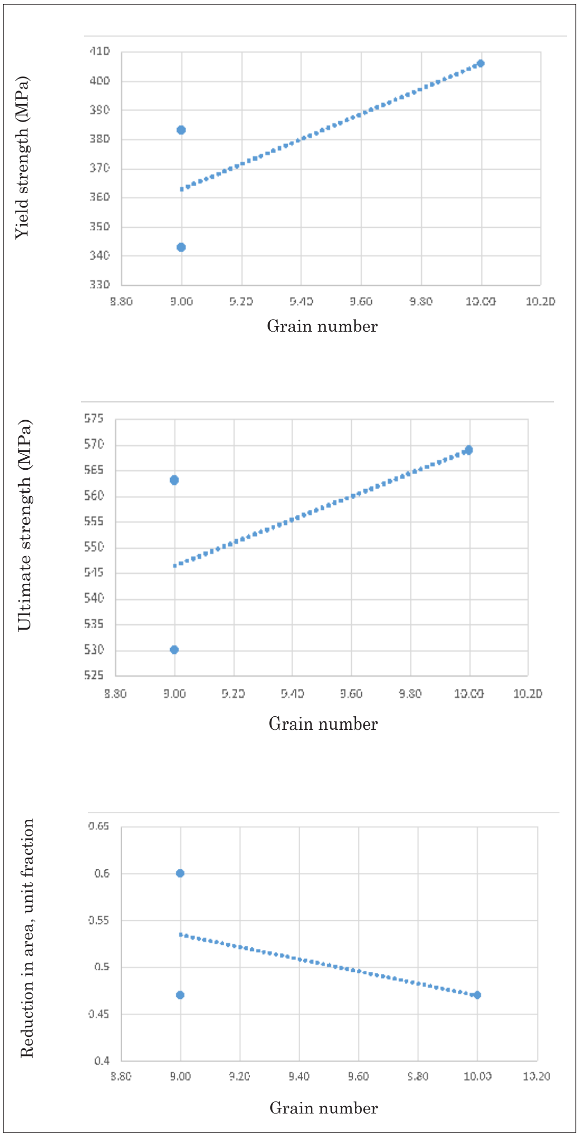

Fig. 13. Experimental values for the mechanical properties and regression equations for the relationships: (a - top) yield strength versus grain number; (b - centre) ultimate strength versus grain number; (c - bottom) reduction in area versus average grain number.

6. Acknowledgements

The authors express their deep gratitude to Dr N.A. Makhutov, Mr E.P. Studionov, and Mr P.V. Poshibaev for the professional guidance, valuable support and useful recommendations on this research work.

Conflicts of interest

All authors have no conflicts of interest to declare.

References

[1] GOST R 8.736-2011. Multiple direct measurements. Methods of processing measurement results. Main principles.

[2] O.S. Khlybov, D.V. Khrameshin, and Z.K. Kabakov, 2017. Developing and implementing an automatic system of steel attestation for mechanical properties at the Vyksa manufacturing site. Metallurg, 8, pp 14-20.

[3] A. de Schino, 2017. A quantitative evaluation of the metallurgical mechanisms which affect the strength of austenite stainless steels. Metallurg, 7, pp 42-45.

[4] V.N. Klyachkin, 2011. Models and methods of statistical control of a multi-parameter technological process. Moscow: PhysMatLit, p 196.

[5] D.A. Neganov, E.P. Studionov, S.V. Skorodumov, and V.A. Soloviev, 2017. A study of the construction of hydraulic rigs for testing pipe products. *Science and Technologies: Oil and Oil Products Pipeline Transportation*, 2, p 41.

[6] Yu.V. Lisin, N.A. Makhutov, D.A. Neganov, E.P. Studenov, and S.V. Skorodumov, 2018. Comprehensive mechanical testing in strength calculations for trunk pipelines in oil and oil products transportation. Plant laboratory. Materials assessment. *In press*.

[7] Yu.V. Lisin, 2015. A study of the physical and chemical properties of steel in long-term operating pipelines: assessing safe operation life. *Science and Technologies: Oil and Oil Products Pipeline Transportation*, 7, pp 18-28.

[8] GOST 1497-84 Metals. Methods of tensile testing.

[9] Sh.U. Nizametdinov and V.P. Rumyantsev, 2012. Data analysis. Moscow: MEPhI, p 288.

[10] N.J. Petch, 1953. Iron Steel Inst., 174, 25.

[11] R.W. Armstrong, I. Codd, R.N. Douthwaite, and N.J. Petch, 1962. *Phil. Mag.*, 7, 45.

[12] R.V. Armstrong, 1973. In: Ultrafine-grain metals. Ed. L.K. Gordienko, Metallurgia, Moscow, p 7.

[13] P.G. Sanders, J.A. Eastman, and J.R. Weertman, 1997. *Acta Mater.* 45, 4019.

To cite: D.A. Neganov, S.V. Skorodumov, N.Yu. Nikitin. Statistical analysis of mechanical test results for samples of pipes from trunk oil pipelines after long-term operation. Pipeline Science and Technology. 2018; 2(2): 107-122. DOI: 10.28999/2514-541X-2018-2-2-107-122.

Vol. 2, No 2, June, 2018

Testing of composite repairs according to ISO and ASME standards and beyond

by J. Schoene*

Henkel AG & Co, Garching, Germany

ARTICLE INFO

Received: 6 October, 2017
Revised: 9 January, 2018
Accepted: 21 March, 2018

ABSTRACT

MAINTAINING PIPELINES IS A top priority for every operator to ensure safety, efficiency and sustainability. Composite wrap repairs are an alternative repair method which is less expensive and less time-consuming, but which enables an extension in lifetime of up to 20 years. It is particularly suitable for live repairs to avoid unplanned shutdowns. Although it has been used in the field for more than two decades and is described in the standards ISO 24817 and ASME PCC-2, the technology is still not always applied, or even considered as a solution in situations where it would be of advantage.

Based on its expertise in adhesive technology, Henkel Loctite has developed a composite repair system, which meets the standards ISO 24817 and ASME PCC-2. Furthermore, in order to increase the level of confidence, the Loctite composite-repair system for pipes underwent several years of certification processes defined and fully audited by independent inspection authorities, namely DNV GL, Lloyd's Register, and TUEV Rheinland. Henkel operates with its standard repair system up to 80°C and with a newly developed high-temperature system up to 130°C. Both these systems have been approved and certified according to the standards.

In addition to the testing programme required by ISO and ASME, a range of further experimental investigations, exceeding the requirements of the repair standards, has been carried out to show the performance and robustness achievable by composite repairs. Important topics covered include tests on cyclic pressure loads, the fatigue strength of the composite, and permeation resistance vs gaseous hydrocarbons. Furthermore, a FE model has been developed that specifically enables the design of repair cases, which are not usually described in detail by the repair standards, like the repair of dents. The combination of these methods clarifies further details and improves our understanding of composite repair reliability.

1. Introduction

Maintaining pipelines is a top priority for every operator in the oil and gas industry to ensure safety, efficiency, and sustainably. By this time, there are approx. 3.5 million km of pipelines on the planet constantly exposed to the combined corrosive effects of climate factors, mechanical stress, and chemical attack [1,2], which might be added possible initial material and construction defects, consequences of ground movement, as well as third-party damage.

Estimations consider most - at least more than 60% - of existing pipelines to be older than

---

Corresponding author: Jens Schoene, e-mail: Jens.Schoene@henkel.com

http://doi.org/10.28999/2514-541X-2018-2-2-123-134
© 2018 Pipeline Science and Technology. Published by Pipeline Transport Institute (PTI)
in association with Technical Productions Ltd. All rights reserved.

45 years [3, 4]. Already in 2002 according to the large-scale two- year study *Corrosion costs and preventive strategies in the United States* the annual costs alone in the US was estimated to approx. $7 billion dollars to monitor, replace, and maintain gas and liquid transmission pipelines [5]. Subsequently operators habitually have to deal with performance losses respectively even more avoiding them.

In the past, it was common practice to remove the complete pipe or the affected sections of pipework and replace it completely [6]. Besides material and labour for the removal and welding works, this leads above all to significant costs generated by taking the pipeline out of service. Therefore, it is essential for operators to keep such downtime to a minimum.

By this time, a wide range of rehabilitation techniques is available for both onshore and offshore piping systems. Frequently used repair techniques capable of being carried out under pressure are installing a steel sleeve or a steel clamp either welded or bolted to the outside surface of the pipes [7]. These methods are suitable for straight pipe sections and generally have limited application for complex geometries like joints or bends [6].

The use of welded steel sleeves for pipeline repair was developed during work led by Kiefner *et al.* in the early 1970s [9, 10, 11]. Two general types of full- encirclement steel sleeves are distinguished between, type A and type B. Type A sleeves consist of two steel half-shells welded longitudinally to create a steel sleeve around the corroded pipe and serve as structural reinforcement only. Type B sleeves are additionally welded in circumferential direction to the carrier pipe, creating a tightly closed outer shell being also able to stop leakages.

Although in-service welding is an established, frequently carried out repair method and its risks are minimized by well-investigated process parameters those risks cannot be avoided completely. Some important concerns are named in regard to the welding process control [12]:

- HAZ: Due to the high cooling rate of the weld as a consequence of the medium flow on the pipe’s inner wall the formation of heat-affected zones (HAZ) can be promoted, leading to material properties susceptible to hydrogen cracking and, potentially, sulphide-stress cracking.

- Burnthrough: Induced by the weld arc and localized heating the remaining material strength at the inner surface might be insufficient to stand the internal pressure. The resulting wall burst, ‘burnthrough’ or ‘blowout’, typically occurs at a pinhole, allowing the content to escape.

- Unstable decomposition: When unsaturated hydrocarbon products (e.g. ethylene) are heated while under pressure, they can exothermically decompose (i.e. explode). For these cases, special precautions must be taken to prevent the inside surface of the pipe from exceeding a critical temperature.

Obviously, the second concern of a wall burst and possible leakage of the content while carrying out welding might involve consequential damages. In general every welding process involves hot work in close range to hydrocarbons and coming with it the potential risk fire and explosion scenarios [6]. Steel-clamp repairs are another alternative for repairing corroded steel pipes, which are generally assembled from two half-shelves via mechanical fastening. Besides structural reinforcement the sealing of leakages is possible. These methods are known to require heavy machinery, which can lead to a difficult process especially in limited workspace such as underground conditions [13].

Composite wrap repairs have emerged as an alternative to pipework replacement and those

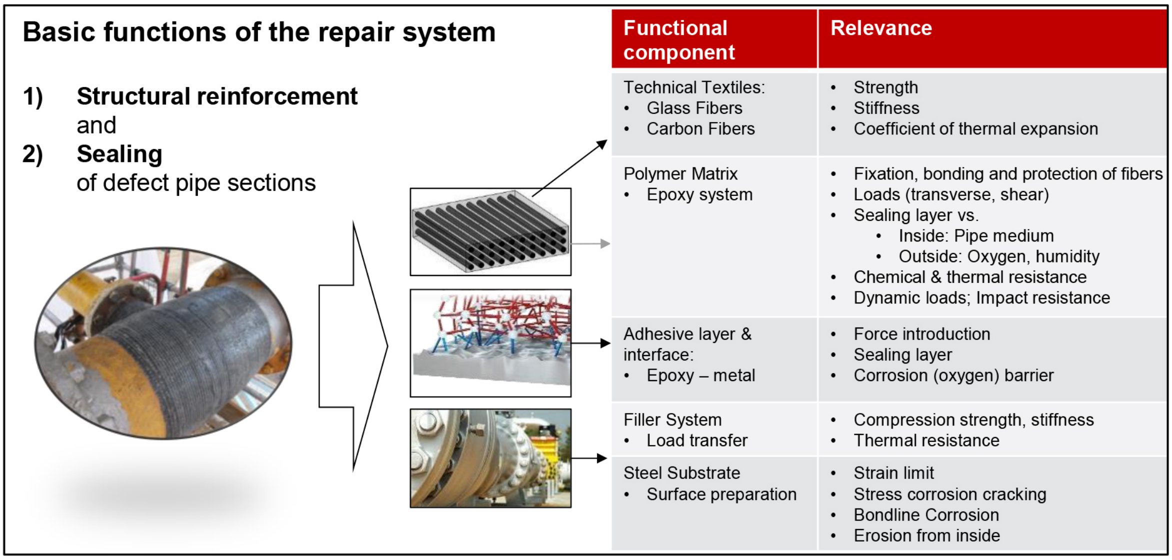

Basic functions of the repair system

1) **Structural reinforcement**
and
2) **Sealing**
of defect pipe sections

Functional component	Relevance
Technical Textiles: • Glass Fibers • Carbon Fibers	• Strength • Stiffness • Coefficient of thermal expansion

Polymer Matrix
• Epoxy system
	• Fixation, bonding and protection of fibers
	• Loads (transverse, shear)
	• Sealing layer vs.
	  • Inside: Pipe medium
	  • Outside: Oxygen, humidity
	• Chemical & thermal resistance
	• Dynamic loads; Impact resistance

Adhesive layer & interface: • Epoxy – metal	• Force introduction • Sealing layer • Corrosion (oxygen) barrier
Filler System • Load transfer	• Compression strength, stiffness • Thermal resistance
Steel Substrate • Surface preparation	• Strain limit • Stress corrosion cracking • Bondline Corrosion • Erosion from inside

Fig.1. Functional structure and components.

traditional repair practices described, without the need of welding or pre-premachined parts. According to industry analysis, composite repairs can be considered to be less expensive and less time-consuming. It was shown that repair using fibre-reinforced polymer (FRP) wraps systems are on average 24% cheaper than welded steel sleeve repairs and 73% cheaper than the complete replacement of the damaged steel pipe section [5].

One important driver for the increased use of composite repairs is the possibility to be carried out on an operating pipeline without taking it out of service – and without hot work. Since the initial industrial research project in the early 1990s by the Gas Research Institute (GRI), they are being constantly developed [13]. Although being used in the field for more than two decades by now and having its technical core described in the well-developed standards ISO 24817 and ASME PCC-2 the technology still is not always applied and often not even considered as a solution where feasible.

2. Technical background

For the assessment of repair methods and their capability by maintenance departments it is crucial to understand the overall relevant technical behaviour under the given circumstances. The term 'composite repair' refers to the rehabilitation resp. reinforcement of pressurized metal pipework by adding a hull of FRP as an additional structural component. The joining of the two components is taken out by adhesive bonding, either by bonding composite layers (impregnated and cured in advance) or by impregnating and instantly bonding the technical textiles in a 'wet-in-wet' process.

Additionally, due to the enclosed cross-section geometry of the FRP and the pipe, the mechanism of mechanical interlocking is created.

The overall design is a hybrid structure, combined of different materials on a macroscale level. The FRP itself consists - as per definition a 'composite' - of multiple components combined to an anisotropic structure on a microscale level. The given situation implies from an engineering point of view a range of technical properties and correlations, the most relevant for an epoxy-based wet-in-wet system are shown in Fig.1. For reasons of clarity not everything is shown.

2.1. Technical textile

The technical textiles like E-glass or carbon-fibres of different types are the most prominent and obvious components of the repair system. They are also the main influence for the mechanical properties of the overall FRP composite part like strength and stiffness. Furthermore, due to their mechanical dominance, they also dictate the range of the thermal expansion. As pipes are in most cases exposed to temperature cycles, the coefficient of thermal expansion, and especially its difference vs the substrate, are of interest because of the potential thermal stresses induced, often referred to as the topic of delta or CTE mismatch.

2.2. Polymer matrix

The polymer of a 'wet-in-wet' system works in two ways for the integrity of the repair. First of all, it is used as the composite matrix to keep the fibres in position, support and protect them. The main loads transmitted by the matrix are part-internally between the fibres and externally for non-fibre-directions like transverse forces, between laminate layers as well as shear and compression. Furthermore, the polymer is responsible for the long-term tightness of the overall repair - in case of leakage obviously vs the pipe content - but as well in the other direction vs humidity and oxygen penetration and permeation to protect the bondline. Often epoxy systems are used due to the high chemical and thermal resistance achievable.

2.3. Adhesive layer and interface

Another main function taken by the polymer is to create the adhesive joint, more precisely both the adhesive bulk layer and the adhesive interface vs the substrate. The joining of FRP parts, especially with metals such as steel, is one of the most challenging topics in FRP composite technologies and therefore, for some years, has been the focus international research efforts [among others, Refs 15-21].

The main reasons for the technological challenges of the joint are [22, 23]:

- dissimilar materials (e.g. thermal expansion, melt points)
- high-strength, concentrated loads within the fibres and limited (re)formability
- material-adapted load introduction (fibre joint, low strength in resin-rich layer)
- additional corrosion effects (high differences in electrochemical potential)
- surface conditions (e.g. risk of mitigating polymer contents, residues of release agents)

For the repair of pipes with a wet-in-wet system, the creation of the FRP structure and of the joint are made in one and the same process step, sometimes referred to as the technologies of 'intrinsic joining' or also 'co-curing' in the aerospace industry [24, 25]. A major advantage of this process is the homogenous material transition of matrix to adhesive zone and, thus, that only one adhesive interface exists, which is usually a hot-spot in terms of performance, quality control, and for environmental exposure.

2.4. Filler system

The purpose of the filler is in first place to fill-up the pipe wall where there is reduced wall thickness so that fibres can be positioned without performance losses in regard to the introduction of load complexes. Secondly, the loads must be transmitted from the damaged steel zone while allowing as little steel deformation as possible. Thus, the compression strength, and especially compression modulus, of the filler are most relevant properties, giving consideration also to elevated temperatures.

Table 1. Test methods in the ISO and ASME repair codes

ISO 24817 / ASME PCC-2 test methods*	**Chapter (ISO/ ASME)**
Ply / Layer thickness of laminate	Annex B/ Appendix II
Composite Elongation	Annex B/ Appendix II
Composite tensile strength	Annex B/ Appendix II
Young's modulus (axial and circumferential direction)	Annex B/ Appendix II
Poisson's ratio (load direction circumferential)	Annex B/ Appendix II
Thermal expansion coefficient (axial and circumferential direction)	Annex B/ Appendix II
Shear modulus, shear strength	Annex B/ Appendix II
Glass transition temperature Tg or HDT of matrix	Annex B/ Appendix II
Barcol or Shore hardness	Annex B/ Appendix II
Lap shear (laminate to substrate)	Annex B/ Appendix II
Environmental compatibility	Annex B/ Appendix II
Short-term pipe spool survival test	Annex C/ Appendix III
Energy release rate	Annex D/ Appendix IV
Long-term strain / strength of composite	Annex E/ Appendix V
Measurement of impact performance	Annex F + D / Appendix VI+ IV
Fire performance	7.5.9.4 / 3.4.10.3
Cathodic disbondment	7.5.9.5 / 3.4.10.6
Electrical conductivity	3.4.10.4
Environmental compatibility	7.5.2 / 3.4.10.5
Cyclic loading	ASME Table 1
Compressive Modulus of Filler material	ASME Table 1

2.5. Steel substrate

Both major repair codes for composite repairs, the ASME PCC-2 (Scope, 1.1) and the ISO 24817 (Definitions, 3.39) define the term 'repair system' to comprise among others the substrate [26, 27]. The steel substrate is to be considered a part of the repair system because of the interconnection and interference on the overall mechanical behaviour of the hybrid cross section and the importance of the chemical and topographic condition of the surface for the development of intermolecular covalent forces within the adhesive interface.

3. Testing and engineering

The assessment of the overall technical performance and design guidelines has been driven during the last decades, and the successive editions of ISO 24817 and the chapter 4.1 (and 4.2) of the ASME PCC-2 are significant milestones of the development of engineering models and design rules, as well as the setting-up of testing procedures for composite repairs. The fundamental targets of the design are to ensure that strains in the repaired steel section, on the one hand, and in the composite reinforcement, on the other hand, do not reach unacceptable levels, under all given circumstances and during the designated repair lifetime. In Table 1 an overview is given regarding the explicit test methods of the two repair standards.

Based on its expertise in both general polymer and specifically adhesive and sealing technology, Henkel Loctite developed a composite repair system qualified according to ISO 24817 and ASME PCC-2 codes. Furthermore, in order to increase the level of confidence and reliability the Loctite composite-repair system had to undergo several years of qualification and certification process. The testing programme covered both the ISO and the ASME standards and all required tests were audited by inspection authorities, namely DNV GL (former Det Norske Veritas and Germanischer Lloyd), Lloyd's Register, and TUEV Rheinland.

On the one hand, the level of confidence and trust towards third parties is enhanced by auditing and approval of inspection authorities. On the other hand, the extensive co-operation and the ongoing input of independent expert groups during the years of development and qualification led to a range of insights in regard to the details of the codes and the requirements for testing procedures. Based on the discussion, some requirements and comments were added for the test programme and a range of additional tests was carried out.

3.1. Composite material properties

A basic, nevertheless essential, requirement refers in first place, but not exclusively, to the coupon tests dictated by the two codes to evaluate the material properties of the composite. Fibre-reinforced components - their quality, performance, the ratio of fibres and polymer resin - are strongly influenced by the way they are manufactured. For laboratory analysis it is in general preferred and common practice to achieve a reproducible outcome, for example by using a hot press or autoclave, etc., and set the final thickness of the specimen via the machine control.

In general all properties of the composite strongly depend on the fibre-volume ratio, especially the stiffness, strength, thermal expansion, humidity absorption, and the long-term behaviour. Consequently the fibre- volume ratio (also known as the fibre-volume fraction, sometime also given in mass ratios) is a major parameter to describe a composite and is generally in FRP technology strongly advised to be documented for every experiment carried out [22].

To give an example for clarification of the impact of different processing methods: this value can be increased for a given textile-matrix-combination between approx. 20% -30% for a hand-laminated composite up to 80% by adding the process step of vacuum bagging afterwards [25, 26].

The large part of loads is taken by the fibres and properties like strength and stiffness moduli are always standardized, i.e. referenced to the full cross-section area including the polymer part. Thus at the same time the structural material properties increase by a comparable factor as the fibre-volume-ratio changes, see also Fig.2:

- in first place because of less 'waste matrix material' in regard to the overall strength and stiffness and by reaching similar force levels with less cross- sectional area;
- secondly because of the increasing uniformity of fibre distribution and orientation coming along with higher fibre-volume fractions [22].

Both standards require generally the repair laminate to be 'the same' within the qualification tests, but neither refer to the impregnation and consolidation process despite its strong importance for the results. Nor do they refer to the fibre-volume fraction as a significant material parameter in terms of documentation and also quality control - although the thickness measured might help to reconstruct and compare in general [25, 26].

Thus, one focus point set jointly with the inspection authorities for the certification process of the Loctite composite-repair system was the method to manufacture the specimens to be kept absolutely the same as in a field process. The fibre-volume ratio was measured and documented accompanying the tests and is furthermore given as a reference for quality control in field applications.

It is a suggestion for future revisions of the codes to add stronger guidelines in regard to the manufacturing method of all specimens, and to control and document the outcome in terms of the fibre-volume fraction.

3.2. Gas permeation

The repair of pipework containing gaseous hydrocarbons is part of the scope of both repair codes and through-wall, leaking defects. For liquid media in general it might be sufficient to measure the burst-pressure performance and conclude, up to a certain confidence level, ideal leak-tightness.

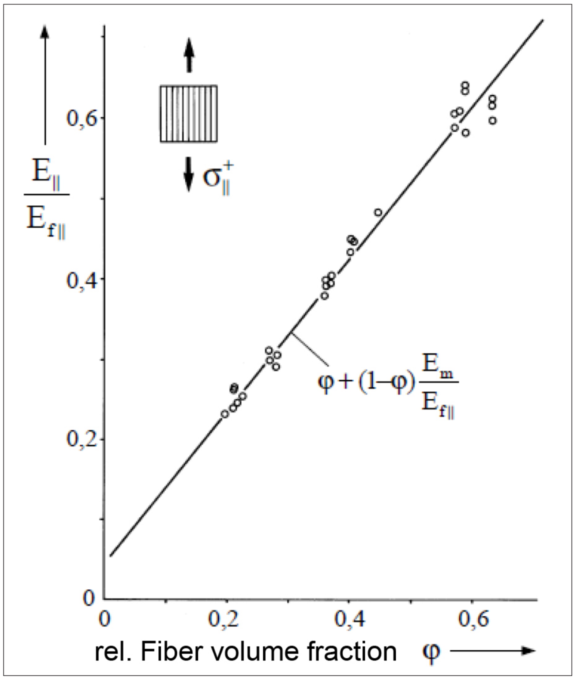

Fig.2. Young's modulus of composite Ell vs fibre Efll in relation to fibre-volume fraction, comparison between modelled and empirical data [Reference: Deutsches Kunststoff Institut, Darmstadt, 1966].

In regard to contents in gaseous condition, though, the gas traverse through the layers of a polymer-based composite should be considered. Especially for gases of small molecule weight, the diffusion rate might be at a significant level either for material losses or for risks because of uncontained hazardous substances.

Thus, the permeation resistance of the Loctite composite-repair system vs relevant small molecule weight gas was determined in a series of tests in addition to the codes' requirements. The results had to meet a range of limits from the field of gas pipe works, and were found to deliver satisfying results for the according codes of practice and regulations to prove the applicability for gas piping systems.

3.3. Cyclic loading

The topic of cyclic loading is covered by both standards via sophisticated design rules, which take into account standardized de-rating factors for the allowable strain of the composite, independent of the number of cycles and the ratio of upper and lower pressure [25, 26]. In regard to the assessment of the specific performance of a certain repair system there is no explicit testing programme included in ISO 24817, while ASME PCC-2 gives two reference for testing: in first place it is refers to ISO 24817 (where the reason is not clear), and secondly ISO 14692 for glass-reinforced plastic (GRP) piping.

The design factors of ISO 24817 are largely based on the design rules of ISO 14692 in regard to cyclic loading, i.e. on de-rating factors for the fatigue behaviour of GRP pipes. ASME gives different formulas, but as well for the de-rating the allowable strain of the composite.

Thus, both standards base the assessment of fatigue degradation solely on the composite behaviour in a standardized way - without a material-specific test base. As the adhesive bond

Table 2. Dynamic three-point bending test series

	Specimen property	Value
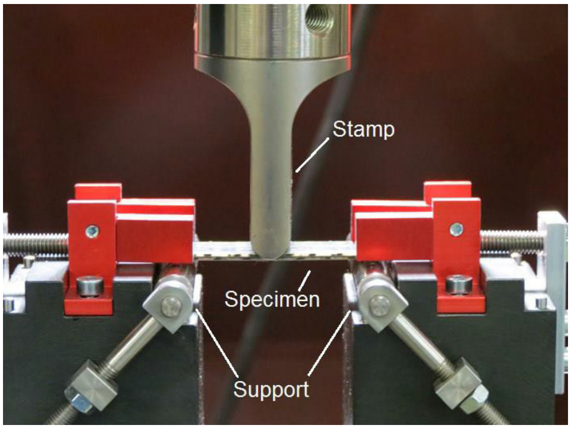	Specimen Length	60 ± 0,1) mm
	Specimen Width	15,0 (± 0.5) mm
	Specimen Thickness	2,0 (± 0.2) mm
	Distance between supports	40 mm
	Radius of supports	5 mm
	Radius of stamp	5 mm
	Load frequency	10 Hz, stress ratio R=0.1
	Maximum deflection	2,5 mm
	Maximum number of load cycles	2 million

is a crucial, functional, element of the repair system, it seems critical to completely keep it out of sight. Especially for repairs of leaking components, the adhesive bond is clearly of major importance and directly exposed to any cycles loading via internal pressure variations.

In one conclusion it was decided to carry out fatigue tests in regard to the fatigue behaviour of the specific composite of the Loctite system - manufactured according to the field-hand lamination process (see also the section on composite material properties). The test was carried out according to ISO 14125, see Table 2.

The result of 2,000,000 cycles passed at a very conservative maximum deformation of 2.5 mm showed a high fatigue performance for the composite - as property of the material alone.

In regard to the overall performance of the repair system under inclusion of the adhesive bond, it was decided also to carry out cyclic pressure-fatigue tests on the complete Loctite repair system under real conditions. Besides other tests, including the structural reinforcement of type A repairs, tests were carried out on type B leakage defects. The test parameters and results are given in Table 3.

In regard to the fatigue behaviour - and essentially the adhesive bond in this case - a decent robustness and reliability of the Loctite repair system could be shown and also proven to certification authority.

3.4. Temperature performance

As a major point the performance of repair systems and the assessment of the same, especially at elevated temperature, will now be discussed, as the dependency of polymer's behaviour on temperature is a complex topic.

3.4.1. Glass-transition temperature measurement

Both codes require the measurement of the glass-transition temperature (Tg), or the 'heat-deflection temperature' (HDT), in order to define the maximum application temperature of the repair system. The values are reduced in dependency on the kind of defect and service parameters.

The HDT is in generally accepted to be related to mechanical properties, and the glass-transition

Table 3. Cyclic fatigue-pressure test series, type B

Pipe diameter	150 mm
Pipe wall thickness	3 mm
Defect type	Through wall defect (“Type B”), hole diameter 10 mm
Cycling load	**Full load cycles** (w. medium water) Upper pressure limit 113 bar Lower pressure limit 0 bar (0 - 10 bar due to system regulation)
Pressure Frequency	Approx. 10 min^{-1}
Repair design	Specimens were designed **only for static pressure** Repair was calculated for **no cyclic load at all**
Approval Requirement	7,000 cycles
All type B specimens passed **minimum**	> 70,000 cycles

temperature may be a quite close value [28]. The Tg is allowed to be measured by the most common methods via differential scanning calorimetry (DSC) or thermomechanical analysis (TMA). While all these methods are accepted to characterize the temperature behaviour of polymers, values might differ as much as by more than 30°C [29].

From the methods named above to determine the Tg, the DMA is typically accepted as the most sensitive way to measure subtle transitions in polymer’s characteristics [30]. In regard to the background of composite-pipe repairs, it is described that the Tg of highly cross-linked thermoset resins are often only measurable by DMA, because DSC and TMA may not be sensitive enough [31]. Furthermore, it has to be said that a DSC won’t give any empirical insight in regard to the mechanical performance of a certain system. Goertzen and Kessler have already discussed the use of DMA for the assessment of composite repair systems for pipes and have shown the feasibility [32].

Considering this background, the DMA method was chosen for the certification of the Loctite composite-repair system. It should be pointed out that even with the measurement method fixed, a range of parameters can be chosen. The test parameters, such as heating rate and frequency, will

Table 4. DMA measurement: Tg vs frequency and heating rate

Tg (°C)	**Heating rate (°C/min)**							
	0.5		1		2		3	
Freq. (Hz)	Tan δ	E”	Tan δ	E”	Tan δ	E”	Tan δ	E”
0.316	62.0	58.2	60.3	57.1	60.6	58.4	61.5	59.2
1.00	65.2	61.0	63.2	59.9	63.3	60.1	63.3	60.2
3.160	68.9	64.5	66.5	62.8	66.5	62.9	66.3	62.5
10.00	73.0	68.0	70.5	66.0	70.0	66.0	69.5	64.5
31.60	77.7	72.3	74.4	69.9	74.0	69.6	73.5	69.0

change the Tg measurement within the same DMA set-up: increasing frequencies and heating rates will shift the measured value of Tg upwards [30, 33-35]. Therefore, it is recommended to keep these parameters in a rather conservative range not to overestimate the Tg. Table 1 shows as an example an overview of comparison tests carried out [32].

3.4.2. System testing at elevated temperatures

While the ASME PCC-2 requires qualification tests to be carried out at the "maximum temperature at which the repair system is to be used in service", ISO defines a "qualification test temperature" and dictated how to calculate two de-rating factors in regard to higher temperatures. An example is the ISO's Annex E and ASME's Appendix V for the optional measurement of "performance test data" to determine the design values of allowable the long-term strain and the long-term strength of the composite [26, 27]. The performance of the repair system is de-rated per design rules according to the design temperature (the service temperature of the application) in comparison to the maximum temperature of the repair system.

This opens-up the possibility of testing and qualifying composite repair systems at lower temperatures than the real application temperature.

At this point it has to be highlighted that polymers exhibit a complex mechanical behaviour dominated by their viscoelasticity in regard to further influences like the deformation condition and deformation rates, relaxation as well as other time-related parameters. The overall mechanical response of polymeric structure during loading is temperature- and time-dependent in close relationship to the real load complex [36].

It is therefore strongly advised to also consider the temperature-related characteristics of those other polymeric materials crucible for the functionality of the repair system. While still having an indication for the matrix resin in regard to the polymer´s resistance vs heat, there is no link for the adhesive (if different from matrix) nor for the filler system, which might also be of polymeric nature, as well.

The filler has to exhibit high compression performance at the same temperature as the matrix resin, and mostly under a constant long-term load. Static loads on polymers always involve the topic of creep; the combination of static loads and elevated temperatures the viscoelastic nature might lead to higher deformation than expected. While ASME requires the filler's modulus to be tested without a reference to temperature, ISO does not require the determination of filler properties at all.

As a consequence, it was decided to carry out all tests related to the qualification test temperature of ISO 24817 at the overall maximum application temperature of the Loctite repair system. In regard to the example of the long-term performance tests (Annex E resp. the Appendix V) pipe specimens were pressurized and kept at elevated temperatures for 1000 hours:

- at 80°C for the Loctite standard repair system; and
- at 130°C for the recently introduced Loctite high-temperature repair system.

4. Conclusion

The composite-wrap repair technology merged from two 'novel' (or at least considered to be novel) technological fields at once: fibre-reinforced polymers and adhesive technology. While, traditionally, metals are used in construction and the design paths are well-known and accepted, new approaches first have to overcome doubts. In order to increase the confidence in reliability and long-term durability, it is crucial to assess the technical behaviour.

As the topic of composite repair involves multiple sub-topics, each f some complexity, the overall technical assessment of the multi-material system under a range of load scenarios is highly challenging. Therefore it is a required further to develop the testing and design methodology as described in ASME PCC-2 and ISO 24817 permanently, and to extend them iteratively.

Additionally to the testing procedure according to the both repair standards, the certification process of the Loctite composite-repair system was defined by the inspection authorities to include a range of further experimental investigations. These are not covered by the codes at this time, but are worth considering.

Conflicts of interest

The author has no conflicts of interest to declare.

References

[1] The world factbook – Central Intelligence Agency" field listing: pipelines, Retrieved September 6, 2016: https://www.cia.gov/library/publications/the-world- factbook/fields/2117.html.

[2] H.A. Kishawy, and H.A. Gabbar, 2010.Review of pipeline integrity management practices," International *Journal of Pressure Vessels and Piping*, vol. 87, pp. 373-380.

[3] "Evaluating different rehabilitation approaches", *Pipelines International*, January 5th, 2010; Retreived Feburary 23rd, 2017: www.pipelinesinternational.com/2010/01/05/evaluating-different-rehabilitation approaches/.

[4] "More Than Half of U.S. Pipelines Are at Least 46 Years Old", *The Wall Street Journal*.

[5] G.H. Koch, M.P. Brongers, N.G. Tompson, Y.P. Virmani, J.H. Payer. Corrosion cost and preventative strategies in the United States. Federal Highway Administration, Office of Infrastructure Research, and Development. pp 260–311, 2002.

[6] K.S. Lim, S.N.A. Azraai, N.M. Noor, N. Yahaya. An Overview of Corroded Pipe Repair Techniques Using Composite Materials, World Academy of Science, Engineering and Technology, *International Journal of Chemical, Molecular, Nuclear, Materials and Metallurgical Engineering* Vol:10, No:1, pp.19-25, 2016.

[7] M. Mohitpour, H. Golshan, A. Murray, 2003. Pipeline design and construction: a practical approach. Second ed. New York, United States, New York, American Society of Mechanical Engineers.

[8] J.F. Kiefner, A.R. Duffy, J.S. Bunn, L.E. Hanna. Feasibility and Methods of Repairing Corroded Line Pipe", *Materials Protection and Performance*, Vol. III, No.10, 1972.

[9] J.F. Kiefner, A.R. Duffy: A study of two methods for repairing defects in line pipe. Final Report to the Pipeline Research Committee of the American Gas Association, Catalog No. L22275, October 1974.

[10] J.F. Kiefner, G.R. Whitacre, R.J. Eiber: Further Studies of Two Methods for Repairing Defects in Line Pipe, Final Report to the Pipeline Research Committee of the American Gas Association, NG-18 ReportNo. 112, March 2, 1978.

[11] I.-W. Bang, Y.-P. Son, K.H. Oh, W.-S. Kim, Y.-P. Kim. Numerical simulation of sleeve repair welding of in-service gas pipelines. *Welding Journal* 2002; 81; pp. 273-282.

[12] J. Kou, and W. Yang. Application progress of oil and gas pipeline rehabilitation technology. In the Proceeding of the International Conference on Pipelines and Trenchless Technology (ICPTT), Beijing, China, 26–29 October 2011, pp. 1285–1292.

[13] N.C. Fawley. Development of Fibreglass Composite Systems for Natural Gas Pipeline Service. Final Report to the Gas Research Institute, GRI-95/0072, March 1994.

[14] A. Gross, H. Schäfer: Fügen von Faserverbund-Kunststoffen, Technica, Zürich * Band 39, (1990) Heft 21, S. 44-49, 51.

[15] G. Kelly. Joining of Carbon Fibre Plastics for Automotive Applications. Dissertation, Royal Institute of Technology, Schweden, 2004.

[16] F. Balle, G. Wagner, D. Eifler. Ultraschallmetallschweißen von Aluminiumblechen an einen kohlenstofffaserverstärkten Thermoplastmatrix-Verbundwerkstoff, Advanced Engineering Materials * Band 11 (2009) Heft ½, Seite S. 35-39, 2009.

[17] Surface modification for increased material joint strength between aluminium and infiltrated titanium structure elements, Materials Science and Engineering 2012, Darmstadt, 25.-27.09, 2012.

[18] J. Schoene, A. Schiebahn, U. Reisgen. Smart Multi Material Joint. Hybrider Verbund zwischen. Stahl und FVK, 4. Doktorandenseminar Klebtechnik.Vorträge der gleichnamigen Veranstaltung inBremen,S.64-71, 2013.
[19] H. Lohse: Kleben von Composite-Bauteilen in der Automobilfertigung,DVS-Jahrbuch, 2013.
[20] K.-W. Jung, Y. Kawahito, M. Takahashi, et al. Laser direct joining of carbon fibre reinforced plastic to aluminum alloy. Journal of Laser Applications, Volume 25, Issue 3, ISSN 1042-346X.
[21] H. Schürmann: Konstruieren mit Faser-Kunststoff-Verbunden. Berlin; Heidelberg: Springer, ISBN 978-3-540-72189-5, 2005.
[22] S. Süllentrop, G. Meschut, O. Hahn: Fügen von Leichtbaustrukturen in der FVK/Metall-Mischbauweise, In:www.kunststofflandnrw.de/fileadmin/user_upload/Bilder/News/LWF_Praesentation_Kunststoffland.pdf, Retreived: 09.10.2013.
[23] R. Matsuzaki, M. Shibata, A. Todoroki. Reinforcing an aluminum/GFRP co-cured single lap joint using inter-adherend fibre. *Journal Composites*: Part A 39 (2008), S. 786–795, 2008.
[24] DFG Schwerpunktprogramm SPP1712 Ausschreibung: Intrinsische Hybridverbunde – Grundlagen der Fertigung, Charakterisierung und Auslegung, DFG, 2013.
[25] American National Standard ASME PCC-2-2015 Repair of Pressure Equipment and Piping. The American Society of Mechanical Engineers 2015.
[26] International Standard ISO 24817:2015. Petroleum, petrochemical and natural gas industries — Composite repairs for pipework — Qualification and design, installation, testing and inspection. ISO 2015.
[27] M. Flemming, G. Ziegmann, S. Roth: Faserverbundbauweisen – Fertigungsverfahren mit duroplastischer Matrix, Springer Berlin Heidelberg. ISBN: 978-3-642-63557-1, 1999.
[28] N.N.: Handbuch der Faserverbundwerkstoffe. R&G GmbH, Waldenbuch, 2. Auflage, 2001/2002.
[29] G.D. Sims, S.J.P. Gnaniah: Improved procedures for the determination of Tg by Dynamic Mechanica Analysis, Proceedings of 17th International Conference on Composite Materials (2009).
[30] J-P. Pascault, H. Sautereau, J. Verdu, R. Williams. Thermosetting polymers. New York: Marcel Dekker, Inc.; 2002.
[31] J. Wolfrum, G. Ehrenstein, M. Avondet. Dynamic mechanical thermoanalysis of high performance reinforced materials. J Therm *Anal Calorim* 1999; 56(3):1147–54.
[32] W.K. Goertzen, M.R. Kessler. Dynamic mechanical analysis of carbon/epoxy composites for structural pipeline repair. Composites: Part B 38 (2007) 1–9.
[33] T. Hatakeyama, F. Quinn. Thermal analysis: fundamentals and applications to polymer science. 2nd ed. Chichester, UK: John Wiley & Sons; 1999.
[34] K. Menard. Dynamic mechanical analysis: a practical introduction. Boca Raton, FL, USA: CRC Press; 1999.
[35] G. Li, P. Lee-Sullivan, R. Thring. Determination of activation energy for glass transition of an epoxy adhesive using dynamic mechanical analysis. *J Therm Anal Calorim* 2000;60(2): 377–90.
[36] T. Osswald. Understanding Polymer Processing, Carl-Hanser-Verlag, 2010. ISBN: 978-3-446-42404-3.

To cite: J. Schoene.Testing of composite repairs according to ISO and ASME standards and beyond. Pipeline Science and Technology. 2018; 2(2): 123-134. DOI: 10.28999/2514-541X-2018-2-2-123-134.

Vol. 2, No 2, June, 2018

Assessment of a cracked pipe subject to transient flow by the Monte Carlo method

by M. Hassani*[1], O. Bouledroua[2], M. Hadj Meliani[2,3], L. Sadou[2], and G. Pluvinage[3]

[1] *LR3MI,Mechanical Engineering Department,University of Badji Mokhtar, Annaba, Algeria*
[2] *LPTPM, Hassiba Benbouali University of Chlef, Chlef, Algeria*
[3] *ENIM-LaBPS, Metz, France*

ARTICLE INFO

Received: 14 November, 2017
Revised: 19 January, 2018
Accepted: 30 March, 2018

ABSTRACT

THE PURPOSE OF THIS WORK is to assess the risk of failure of cracked pipe due to fluid transient. A mathematical model has been established based on the mass and momentum conservation laws, the system of hyperbolic partial differential equations has been solved by the method of characteristics and a finite difference method to calculate the maximum pressure in the pipe. Afterwards, a finite element method have been used to perform a reliable assessment analysis of a cracked pipe used in water distribution by using Monte Carlo method and failure assessment diagram (FAD) tools to evaluate the safety factor from deterministic and probabilistic view points.

Key words: Monte Carlo method, failure assessment diagram, water hammer, method of characteristics

1. Introduction

The increasing demand of water to meet the needs of different water uses requires an increase in the water distribution networks, which requires implantation of adequate maintenance strategy to avoid the additional costs of maintenance, and an increase the pressure of the service, and this begs the question about the safe operating of the system. Despite the security measures and standardized design methods, there are other inevitable factors that can affect the structure integrity and leads to the failure of water pipelines. This failure may manifested by two cases, either by rupture or leak, and in both cases the consequences are very disastrous, compounded by compromising the health of the population due to water contamination.

The water pipeline failure [1] reason can be assumed to be corrosion pitting, scratches, gouges, and also service loading conditions depend on soil movement, e.g. ground slip, earthquakes or repeated loading due to road traffic.

The presence of cracks in water pipelines is related to many causes e.g. micro-void, inclusion, manufacturing defects. Theses defects grow under mechanical and environment condition and failure occurs when defect has reached the critical size under service condition or under unusual loading condition such as water hammer.

---

*Corresponding author: Mohamed Hassani, email: moha82.hassani@hotmail.fr

http://doi.org/10.28999/2514-541X-2018-2-2-135-145
© 2018 Pipeline Science and Technology. Published by Pipeline Transport Institute (PTI) in association with Technical Productions Ltd. All rights reserved.

Water hammer is produced by a rapid change of flow velocity in the pipe line that may be caused by sudden valve opening or closure, failure of a pump, mechanical failure of device, rapid change in demand condition, etc. It could result in violent change of the pressure head, which is then propagated in the water pipeline in the form of a fast pressure wave leading to severe damage [2].

In this present work the water hammer effect on pipe failure is described in order to provide a reliable structure integrity and safety method, using Monte Carlo method and failure assessment diagram.

1.1. Theory/calculation methodology

A defect can be detected by non-destructive test [3], and the question is the defect is acceptable or not. In order to answer to this question there are various methods of assessment of defect assessment e.g. R6 Method, BSI PD6493, SINTAP. In this study a failure assessment diagram is used according to the SINTAP procedure with level 1, in order to be able to make decision about the failure risk of the water pipeline, when a water hammer occurs. The random characteristics of the governing parameters in real pipelines have motivated many researchers to develop probabilistic approaches to assess the probability of failure of pipelines. The Monte Carlo simulation method is used to assess the uncertainty to estimates the safety factor of cracked pipe.

The high instantaneous pressure due to water hammer is calculated from the mathematical model of fluid transient, and then the value of maximum pressure is incorporated into finite element code to calculate the stress intensity factor at the vicinity of crack tip. Once the value of stress intensity factor is calculated, it is used to plot the defect assessment point coordinates.

The value of maximum stress can be calculated via thin-walled hollow cylinder assumption $\sigma = PD/2t$ where P = pressure, D = diameter, t =t hickness.

2. Failure assessment diagram

2.1. SINTAP procedure

This procedure [4, 5] is a unitary European Community approved programme to assess structure integrity of a have defect, against the level of failure risk. This procedure is based on the failure mechanics principles. The relationship between applied stress sig defect size a and toughness is replaced by two parameters corresponding to brittle fracture K ($K_r = 1$, $L_r = 0$) and plastic collapse L ($K_r = 0$, $L_r = L_{max}$). These parameters can be defined as follows:

$$K_r = \frac{K_I}{K_{IC}} \tag{1}$$

$$L_r = \frac{\sigma_n}{R_c} \tag{2}$$

where: $R_c = \frac{1}{2}\left(\sigma_y + \sigma_u\right)$

These two variables represent the ratio between the applied value of either stress or stress intensity factor and the resistance parameter of the corresponding magnitude (yield stress or fracture toughness).

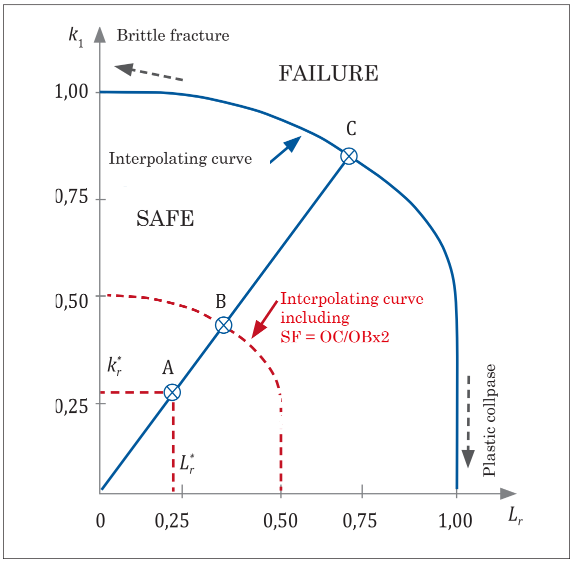

Fig.1. Typical failure assessment diagram (FAD).

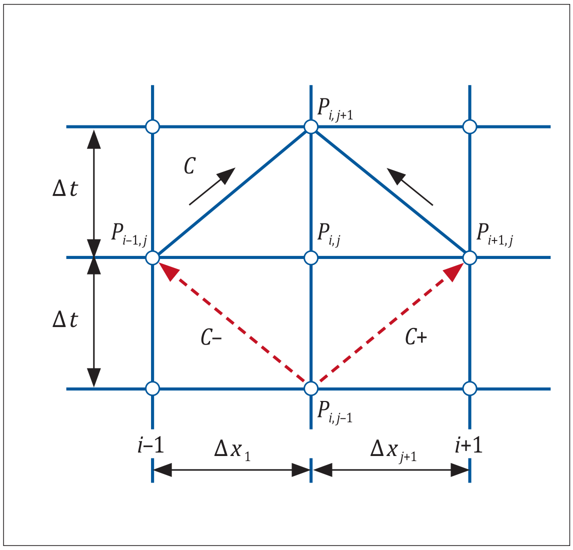

Fig.2. Staggered grid for internal points.

2.2. Level 1 investigation

The failure assessment diagram is limited by the failure assessment curve defined by a relation $K_r = f(L_r)$, the level of analysis allow us to choose the parameters necessary to establish the risk analysis. The level 1 analysis is the minimum recommended level. This level requires the yield strength, the ultimate stress, and the value of fracture toughness of the material. The FAD curve is defined as follows:

For $0 \leq L_r \leq 1$

$$f\left(L_r\right)=\left[1+\frac{L_r^2}{2}\right]^{-1/2}\left[0.3+0.7e^{-1/4 L_r^6}\right] \tag{3}$$

where: $L_r^{max} = 1 + \left(\frac{150}{\sigma_y}\right)^{2.5}$

2.3. Assessment diagram

The assessment diagram is plotted in coordinates K_r and L_r [6]. Two particular points of this diagram represent successively brittle fracture conditions ($K_r = 1$, $L_r = 0$) and plastic collapse ($K_r = 0$, $L_r = 1$). The curve which defined the assessment diagram encloses between the coordinates a safe domain.

The loading conditions of a structure are represented by a point A of coordinates (K_r*, L_r*). If this point is inside of this domain, this ensures the structure's integrity. If this point C is on the curve, failure occurs (Fig.1).

3. Water hammer equation

The mathematical formulation of the transient is developed based on the equation of conservation of mass, the conservation equation of momentum, and the equation of thermodynamic behaviour [7], for unsteady pipe flow. The classical theory of water hammer takes into account the effect of skin (fluid-wall) friction, approximated by Trikha model. The pipe is straight, thin-walled, linearly elastic and of circular cross-section. The two equations, governing velocity V and pressure P are:

$$\frac{\partial V}{\partial x}+\frac{1}{\rho a^2}\frac{\partial P}{\partial t}=0 \tag{4}$$

$$\frac{\partial V}{\partial t}+\frac{1}{\rho}\frac{\partial P}{\partial x}+\frac{4T_f}{\rho D}+g\sin\theta=0 \tag{5}$$

in which:

x = axial distance
ρ = mass density of liquid
a = liquid (elastic) wave speed
t = time
T_f = friction term
D = internal pipe diameter
g = gravitational acceleration, and
θ = pipe slope.

Equations 4 and 5 make a system of partial hyperbolic differential equations which connect the pressure *P* and the fluid velocity *V*.

3.1 Determination of the shear stress

To model the friction term, we used the Trikha model [8], which relates wall shear stress in transient laminar pipe flow to the instantaneous mean velocity and weighted past velocity changes.

$$T_f(x,t)=-\frac{8\rho\nu}{D}\left\{V(x,t)+\frac{1}{2}\int_0^t\frac{\partial V}{\partial t}W(t-s)\,ds\right\} \tag{6}$$

in which n_c = fluid kinematic viscosity, *W* = a weighting function, and *s* = variable of integration.

3.2 Method of resolution

The method used to solve mathematical systems that govern the phenomenon is the method of characteristics (MOC) [9]. This is used to transform the equations of partial derivative equations to total derivatives which are integrated along the characteristic direction of lines. The MOC transformation of Equns 4 and 5 yields the water hammer compatibility equations which are valid along the characteristic lines. The physical meaning of the characteristics lines is propagation path of pressure wave. The compatibility equations, written in a finite-difference form within the staggered grid are shown in Fig.2.

Along the C^+ characteristic line (Δx/Δt = +a):

$$H_i^{j+1}-H_{i-1}^{j}+B\left(Q_i^{j+1}-Q_{i-1}^{j}\right)+RQ_{i-1}^{j}\left|Q_{i-1}^{j}\right|\Delta x=0 \tag{7}$$

Along the C^- characteristic line (Δx/Δt = -a):

$$H_i^{j+1} - H_{i+1}^{j} + B\left(Q_{i+1}^{j} - Q_i^{j+1}\right) - RQ_{i+1}^{j}\left|Q_{i+1}^{j}\right|\Delta x = 0 \quad (8)$$

where: $B = {}^{a}\!/_{(gA)}$ and $R = {}^{f}\!/_{\left(2gDA^2\right)}$

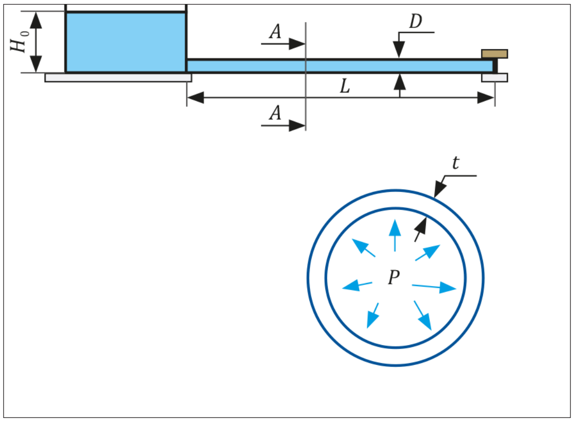

Fig.3. Pipe with external surface crack.

4. Case study

In this study a tank pipe valve system is considered Fig.3. The pipe has an axial edge defect of length *a* subjected to an internal source pressure *P* = 1.688 MPa. The cast iron pipe is used with diameter *D* = 450 mm and thickness *t* = 8.6 mm with Poisson's ratio ν = 0.28. The mechanical properties are defined in Table 1.

5. Finite element modelling

A finite element code called Ansys APDL has been used to modelling the pipe geometry (Fig.4), considered as a plan strain state. According to the symmetry, only on half of the pipe has been considered. 8-node quadrilateral elements has been adapted to meshing the pipe; we have refined the mesh near the crack tip which represents the critical zone of the pipe.

6. Results and discussion

Different *a/t* ratios have been computed to find stress intensity factor. The value of K_I has been calculated for service pressure *P* =1.688 MPa and for maximum pressure resulting from water hammer, and for a thickness of *t* = 8.6 mm.

According to Fig.5 we note that the stress intensity factor increases with increase in service pressure, and more the ratio a/t of the defect size increase the more the pressure is important. The arise of stress intensity factor value is due to pipe well section reduction by the crack, which lead to stress concentration effect at the vicinity of the crack tip.
Figures 6 and 7 show the calculus of the pair (K_r , L_r) for various ratios a/t (0.1, 0.2, 0.3, 0.4, and 0.5) using the SINTAP code for cracked pipe. The assessment points are given on the figures for different ratios crack sizes. The interpolating curve defined for safety factor Fs = 2, established the limit zone between safety zone and the security zone.

The failure prediction of the pipe due to water hammer may be considered from the safety factor calculation. Conventionally, it is considered the failure is possible to occur if the safety factor is less than two.

Whenever the ratio a/t increases, the safety factor also increases, which means that the risk of failure of water pipeline increases. According to Fig.8 the structure is reliable if the value of

Table 1. Mechanical properties of cast iron

σ_y (MPa)	σ_u (MPa)	ρ (kg/m³)	K_{Ic} (MPa.m$^{1/2}$)
300	420	7050	14.90

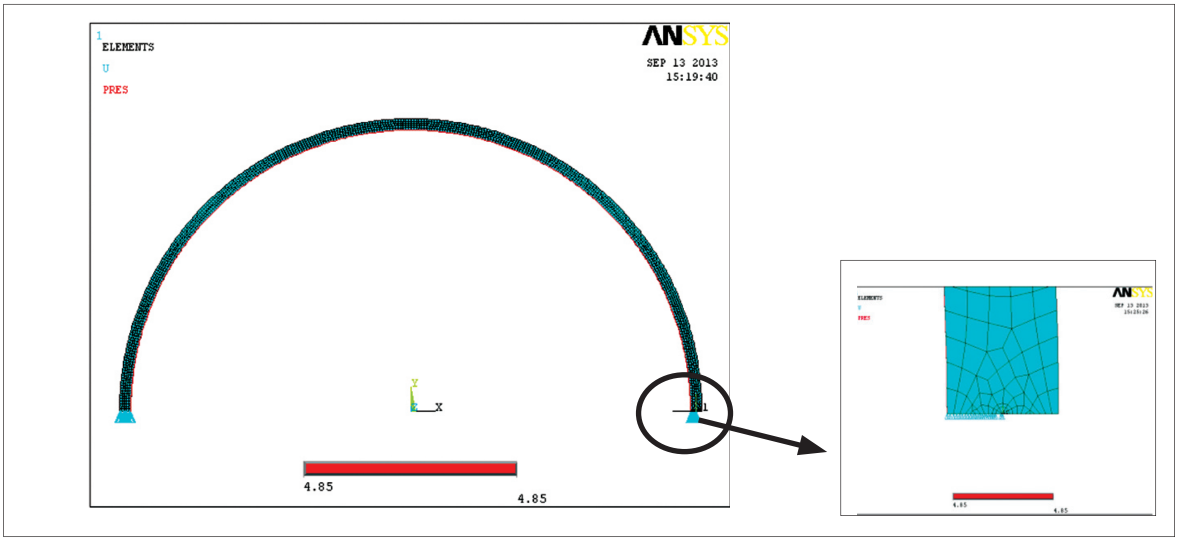

Fig.4. Pipe modelling and mesh around the crack tip.

safety factor is greater than two. Also has been found that the more the pressure increases, the more the safety factor decreases.

According to Fig.8 it has been shown that the pressure is more influential on the safety factor than the ratio a/t of crack size.

It has been found that the safety factor is reduced from the value of safety factor Fs= 4.9 at a pressure of 1.688 MPa to Fs = 1.7 at a pressure of 4.85 MPa water hammer for the ratio a/t = 0.2, which proves that the phenomenon of water hammer is dangerous for the integrity of the structure, which can lead to failure.

7. Probabilistic safety factor

From the probabilistic point of view, the failure assessment diagram can take in account the uncertainty of random variable to calculate the safety factor. The material failure curve is a particular case for which the failure probability is equal to unity, because failure is then a certainty. When using a probabilistic approach, each variable is viewed as a probability distribution. Monte Carlo (MC) method that uses to calculate the failure probability integral, the calculated value be interpreted as a mean value in a stochastic experiment. An estimate is therefore given by averaging a suitably large number of independent outcomes of this simulation. The samples parameters are generated by random numbers from a uniform distribution between 0 and 1. This random number can be used to generate a value of the desired random variable with a given distribution. The advantage with MC simulation is that it is robust and easy to implement into a computer program, and, for a sample size when N tenda to infinity, the estimated probability converges to the exact result. Another advantage is that MC simulation works with any distribution of the random variables. There is no restriction on the limit state functions.

Table 2 Safety factors for two different pressures.

a/t	P = 1.688 MPa	P = 4.85 MPa
0.1	6.4	2.2
0.2	4.9	1.7
0.3	3.26	1.13
0.4	2.16	0.75
0.5	1.06	0.37

In order to allow determination of safety factor

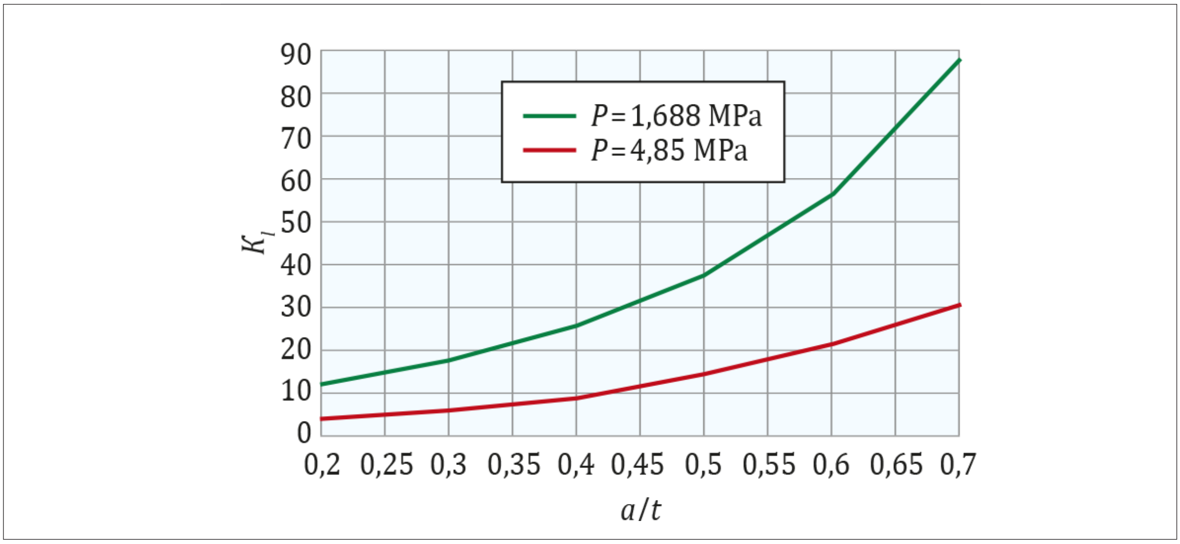

Fig.5. Variation of stress intensity factor with a/t for P = 1.688 MPa and P = 4.85 MPa.

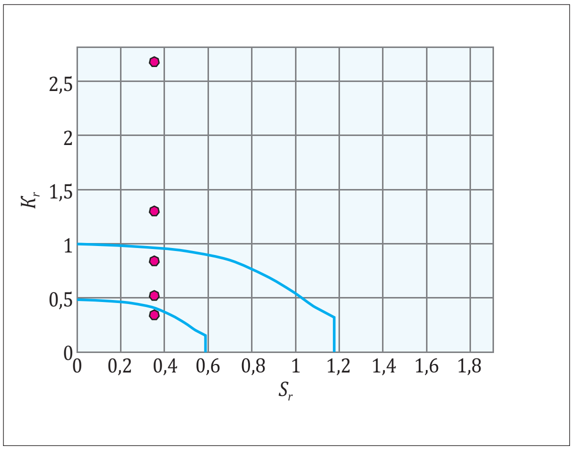

Fig.6. FAD for pressure = 1.688 MPa.

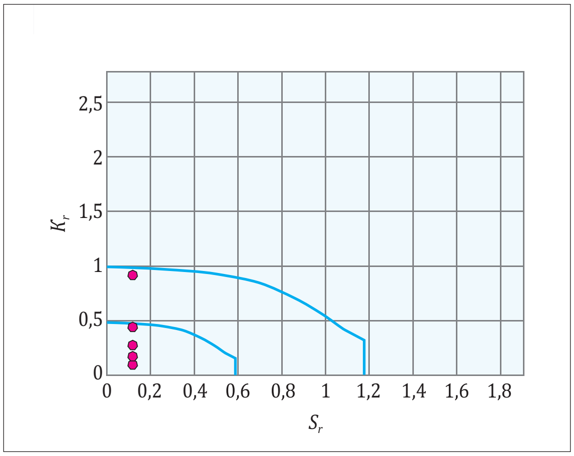

Fig.7. FAD for pressure = 4.85 MPa.

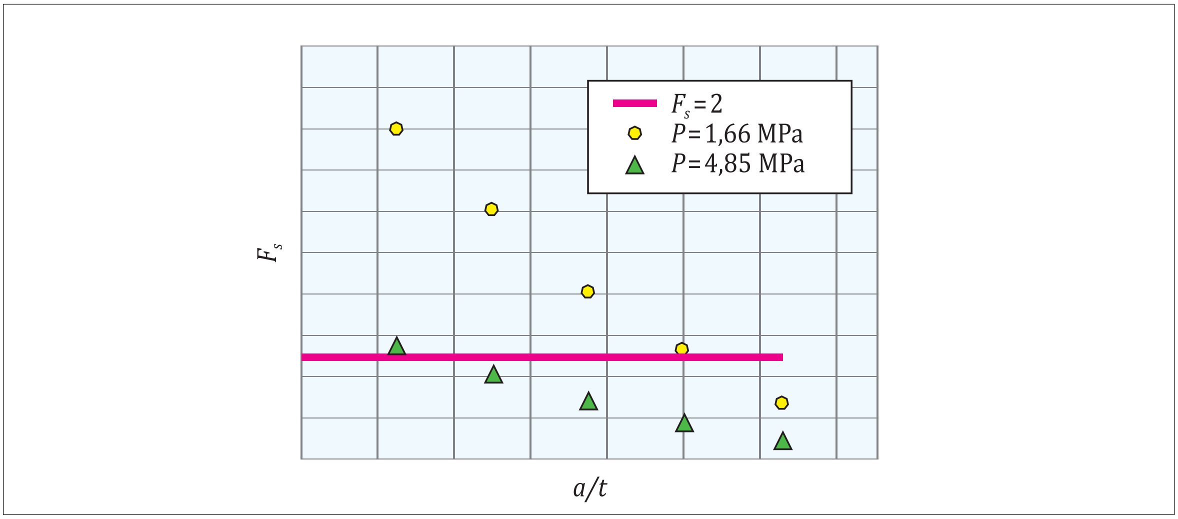

Fig.8. Safety factor evolution for P = 1.688 MPa and 4.85 MPa.

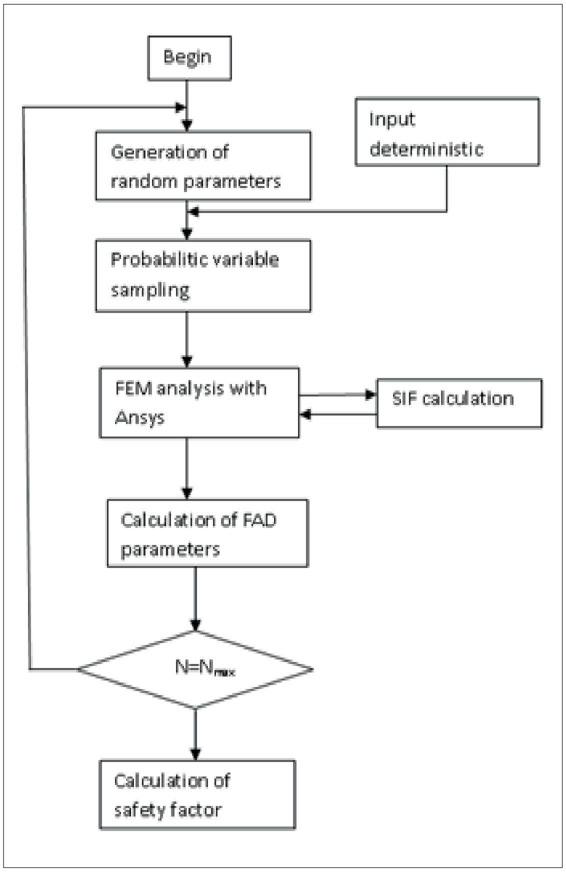
Begin
Input deterministic
Generation of random parameters
Probabilitic variable sampling
FEM analysis with Ansys
SIF calculation
Calculation of FAD parameters
N=N_max
Calculation of safety factor

Fig.9. Analysis flow chart.

by Monte Carlo method within the chosen procedure of Fig.9, the following parameters are treated as random parameters and introduce into the failure assessment diagram:

- fracture toughness
- yield strength
- ultimate tensile strength
- defect depth
- maximum pressure

These random parameters are treated as not being correlated with one another. For each parameter, the distribution is chosen according to the usual distributions described Table 3.

Fracture toughness is assumed to have a Weibull distribution. The probability density function has the following form:

$$f\left(x\right)=\left(\frac{k}{c}\right)\left(\frac{x}{c}\right)^{k-1}\exp\left(-\frac{x}{c}\right)^{k}$$

where k is the shape parameter and c is the scale parameter. The mean and variance of the distribution are given by:

$$\lambda\text{“}\left(1+\frac{1}{k}\right)$$

$$\sigma=\lambda^{2}\left[\text{“}\left(1+\frac{2}{k}\right)-\text{“}^{2}\left(1+\frac{1}{k}\right)\right]$$

Yield strength, ultimate tensile strength, and internal pressure can be assumed mainly to have a normal distributions. An exponential distribution generally prevails for defect size analysis. Consequently the probability density function has the following form:

$$f\left(x\right)=\lambda\exp\left(-\lambda x\right)$$

Using Monte Carlo method, several assessment, 50 points were generated using the characteristic

Table 3. Mechanical properties of cast iron and used distribution

Mechanical property	Yield strength (Re)	Ultimate strength	Circum-ferential stress	Fracture Toughness	Defect
Mean	300	420	44.16	14.9	0.86 mm
CV	0.1	0.1	0.44	0.1	
σ	30	42	19.47	1.4	
Distribution	Normal	Normal	Normal	Weibull	Exponential

Table 4. Failure domain represented by domain angle

Pure brittle fracture	**Brittle fracture**	**Elastic-plastic fracture**	**Plastic collapse**	**Instability**
$\theta = 90°$	$0 > \theta \geq q_1$	$q_1 > \theta \geq q_2$	$q_2 > \theta > 90$	$\theta = 0°$

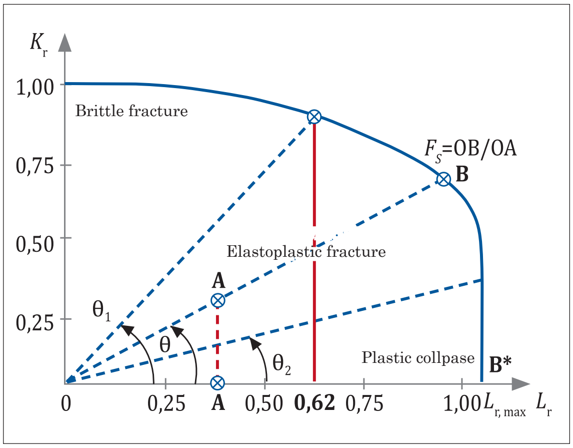

Fig.10. Definition of domain angle in FAD.

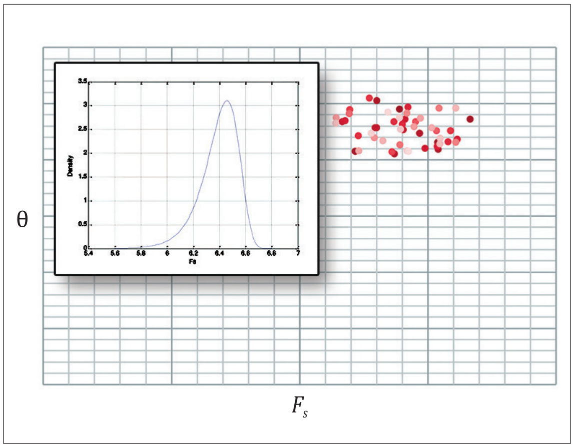

Fig.11. Safety factor analysis.

parameters of the distribution. Any assessment point in a failure assessment diagram is localized by polar coordinates *r* and θ. The angle θ is a parameter which represents the belonging of the assessment point to a failure domain and, for this reason, it is called the angle domain. According to the following Table 4, the angle domain indicates the failure type.

Domain angles θ_1 and θ_2 are presented in Fig.10. In the case of a failure curve given by the SINTAP procedure, values of θ_1 and θ_2 are respectively $\theta_1 = 55°$ and $\theta_2 = 22°$. It has been shown that general trend is that the margin of safety on the FAD is minimum in the middle (elastic-plastic) region, slightly higher in the plastic collapse region and maximum in the brittle fracture region. However, this overall trend is complicated by varying degree of scatter in the different regions. For this reason, we have examined the evolution of the safety factor with θ from a statistical point of view [10].

Using Monte Carlo method, the K_r and L_r coordinates of the assessment points have been computed and reported in domain failure assessment diagram and the associated safety factor is computed Fig.11. It has been shown that the θ angle is in range of brittle fracture. Note that the value of the safety factor is relatively high because the internal pressure is relatively low

All data are scattered band of range in the [μ - 3σ, μ + 3σ] region of brittle failure. The safety factor distribution is represented with a Weibull distribution. The goodness of fit was tested with Kolmogorov-Smirnov test, the results indicates that the Weibull distribution is significant at 55 %. In the domain failure assessment diagrams, a particular assessment point can be is calculated from mean values of all the variable parameters.

The safety factor and the domain angle are computed for a/t = 0.1 and *P* = 1.668 MPa. The results are reported in Table 5. It has been found that the deterministic value of safety factor is close to probabilistic value calculated by Monte carlo Method.

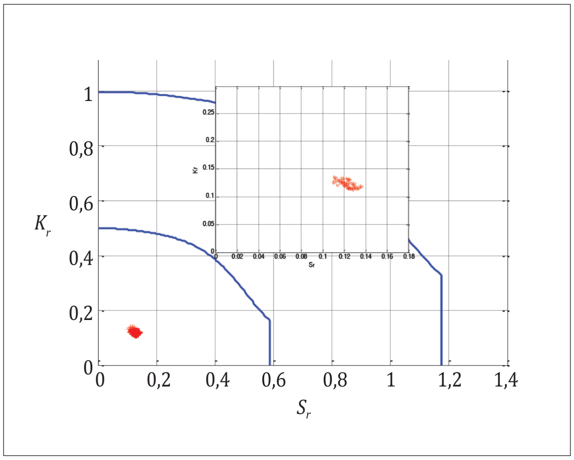

Fig.12. Distribution of the safety factor with angle.

8. Conclusion

A numerical model based on mass, momentum conservation laws is developed to simulate the transient flow and predict the maximum pressure value in the pipe. By using the SINTAP failure diagram assessment code we are able to decide rapidly about the acceptability of the crack defect size. Under transient service pressure, the safety factor is distributed randomly according to a Weibull distribution We can use this diagram as a tool combined with the Monte Carlo method to assess the uncertainty of parameters in order to estimate the safety of the structure, and to minimize the water risk of failure and the associated costs of maintenance.

Table 5. Deterministic and probabilistic values of safety factor and domain angle

P = 1.66	**Fs D**	**Fs P**	**θ D**	**θ P**
0.1	6.4	6.39	45.29	45.44
0.2	4.9	4.31	56.31	56.3
0.3	3.26	3.3	67.37	67.09
0.4	2.16	2.18	74.88	74.84
0.5	1.06	1.13	82.5	82.11

Conflicts of interest

All authors have no conflicts of interest to declare.

References

[1] C. Schmitt, G. Pluvinage, E. Hadj-Taieb, and R. Akid, 2006. Pipeline failure due to hammer effects water. *Fatigue Fracture Engng Mater. Struct.,* 29 (12), 1075–1082.

[2] R. Wichowski, 2006. Hydraulic transients analysis in pipe networks by the method of characteristics. *Archives of Hydro-Engineering and Environmental Mechanic*s. 53 3, 267–291.

[3] N. Abdelbaki, E. Bouali, M. Gaceb, and M. Bettayeb, 2009. Study of defect admissibility in gas pipelines based on fracture mechanics. Journal of Engineering Science and Technology, 4, 1, 111 - 121.

[4] SINTAP: Structural Integrity Assessment Procedure, Final report, EU project BE95-1462, BRITE/EURAM Programme, Brussels, Belgium, 1999.

[5] M. Hadj Meliani, Z. Azari, G. Pluvinage, and J. Capelle, 2010. Gouge assessment for pipes and associated transferability problem. *Engng Failure Analysis*, 17, 1117-1126.

[6] K. Rouabeh, C. Schmitt, S. Elaoud, E. Hadj-Taïeb, and G. Pluvinage, 2012. Failure of grey cast iron water pipe due to resonance phenomenon. *Engineering Failure Analysis*, 26, 120–128.

[7] E.B . Wylie, V.L. Streeter, and L. Suo, 1993. Fluid transients in system. Prentice Hall, New Jersey.

[8] A.K. Trikha, 1975. An efficient method for simulating frequency-dependent friction in transient liquid flow. *ASME Journal of Fluids Engineering,* 97, 97-105.

[9] M.H. Afshar and M. Rohani, 2008. Water hammer simulation by implicit method of characteristic. I*nternational Journal of Pressure Vessels and Piping*, 85, 12, December, 851-859.

[10] S. Jallouf, C. Schmitt, G. Pluvinage, E. Hadj-Taieb, and M. Lebienvenu, 2011. A probabilistic safety factor for defect assessment of water pipes subjected to water hammer. *Journal of Strain Analysis for Engineering Design*, 46, 14.

To cite: M. Hassani, O. Bouledroua, M. Hadj Meliani, L. Sadou, and G. Pluvinage. Assessment of a cracked pipe subject to transient flow by the Monte Carlo method. Pipeline Science and Technology. 2018; 2(2): 135-145. DOI: 10.28999/2514-541X-2018-2-2-135-145.

Forthcoming international events

15th Moscow International Oil and Gas Exhibition / MIOGE
18-21 June
Moscow, Russian Federation
http://www.mioge.ru/en-GB
MIOGE is Russia’s largest international exhibition of oil and gas equipment and technologies.

Oil & Gas Africa
6-8 July
CTICC, Cape Town
http://oilgasafrica.com/
Oil & Gas Africa is dedicated to developing the mid-stream and downstream sectors across the continent and features leading industry experts sharing a platform to discuss the latest challenges, market developments and opportunities.

The International Fair INNOPROM
9-12 July
Ekaterinburg, Russian Federation
http://www.innoprom.com/en/

ussian’s leading metalworking and welding trade fair. It unites the key sectors of industry – industry automation, power engineering technologies, machine building and components for mechanical engineering, metalworking.

52nd ASME Pressure Vessels & Piping Conference
15-20 July
Prague, Czech Republic
https://www.asme.org/events/pvp
The ASME 2018 PVP Conference is an international technical forum for participants to further their knowledge-base by being exposed to diverse topics, and exchange opinions and ideas both from industry and academia in a variety of topics related to Pressure Vessel and Piping technologies for the Power and Process Industries.

ASCE Pipelines Conference
15-18 July
Toronto, Canada
http://www.pipelinesconference.org/
Premier industry event covering the most current state-of-the-art engineering technologies for pipeline and utilities infrastructure.

Pacific Oil Conference
4-6 September
Los Angeles, California
http://www.petroshow.com/
The POC is an engaging event offering multiple ways to network with others in the industry, attend valuable education sessions from business professionals and meet with vendors offering the products and services you need.

continued on p 159

Vol. 2, No 2, June, 2018

Design aspects for connections, supports, and expansion loops in pipelines made from composite materials

by D.G. Pavlou*

Department of Mechanical and Structural Engineering and Materials Science, University of Stavanger, Norway

ARTICLE INFO

Received: 19 February, 2018
Revised: 15 May, 2018
Accepted: 22 May, 2018

A B S T R A C T

IT IS WELL KNOWN THAT sufficient methods and design codes exist for the design of connections and supports, as well as expansion loops, for pipelines made by carbon steel. However, since the fibre-reinforced composite materials are not widely used for pipelines fabrication, there is still a lack of design rules. The aim of the present work is to provide theoretical tools for dimensioning of joints, supports and expansion loops for pipelines made by composite materials. The derived formulae are based on the classical lamination theory. In order to avoid complex equations that are non-convenient for practical use, reasonable assumptions are adopted. Numerical results and practical design suggestions are provided.

Key words: pipelines, composite materials, connections, supports, expansion loops

1. Introduction

The use of fibre-reinforced composite materials is very promising due to their superior strength, low weight, excellent corrosion resistance and fatigue behaviour [1]. Nowadays, composite materials are mainly used for pipeline repair [2]. Implementation of composite materials in demanding technologies, e.g. deep-sea mining [3], is advantageous as well. Systematic studies on the dynamic response of multi-layered fibre-reinforced plastic (FRP) pipelines under transient flow conditions can be found in [4-7]. Even though the material cost is still higher than the steel, their high strength and low density yield considerable material saving, resulting thus in comparable cost with the use of carbon steel. However, there is still a lack of design tools for design of connections, supports, and expansion loops for pipelines made by composite materials. A useful collection of methods for composite materials in piping applications is provided by the author in the monography [8]. This monograph is the main source for the present paper. Since the symbols, the mechanical properties, and the terms of provided formulae are based in the classical lamination theory, a brief introduction of the mechanics of composite materials is necessary:

1.1. Generalized Hooke's law

Since the composite materials are fibre-reinforced (Fig.1) their mechanical properties are different in the three principal detections, i.e. in the axis x_1 which is aligned with the fibre

---

*Corresponding author: Dimitrios Pavlou, e-mail: dimitrios.g.pavlou@uis.no

http://doi.org/10.28999/2514-541X-2018-2-2-147-158
© 2018 Pipeline Science and Technology. Published by Pipeline Transport Institute (PTI)
in association with Technical Productions Ltd. All rights reserved.

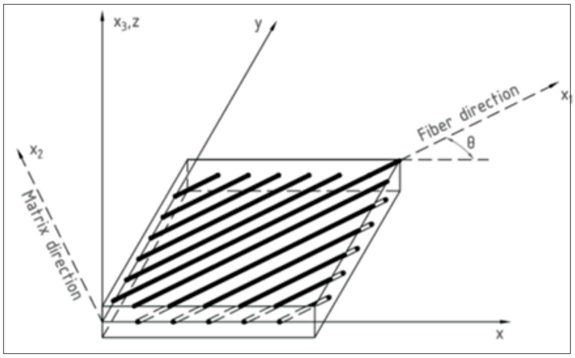

Fig.1. Material element of a fibre-reinforced composite material.

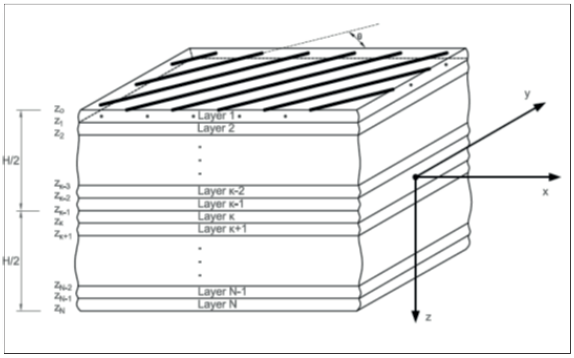

Fig.2. A laminated material element.

direction, and in the axes x_2 lying in the plane of the layer) and x_3 perpendicular to the plane of the layer). Pipelines made using composite materials are utilized in thin–walled laminae. The main characteristic of the above components is that the value of at least one of their characteristic geometric dimensions is much smaller than the two other dimensions. Taking into account this assumption, the Hooke's law in terms of the mechanical properties along the principal directions is given by the following formula:

$$\begin{Bmatrix} \sigma_1 \\ \sigma_2 \\ \tau_{12} \end{Bmatrix} = \begin{bmatrix} Q_{11} & Q_{12} & 0 \\ Q_{12} & Q_{22} & 0 \\ 0 & 0 & Q_{66} \end{bmatrix} \begin{Bmatrix} \varepsilon_1 \\ \varepsilon_2 \\ \gamma_{12} \end{Bmatrix} \tag{1}$$

where the parameters Q_{ij} are called reduced stiffnesses. The above parameters can be calculated by the principal materials properties in the x_1, x_2, x_3 directions which are provided by the composite material manufacturers:

$$Q_{11} = \frac{E_1}{1 - v_{12} v_{21}} \tag{2}$$

$$Q_{12} = \frac{v_{12} E_2}{1 - v_{12} v_{21}} = \frac{v_{21} E_1}{1 - v_{12} v_{21}} \tag{3}$$

$$Q_{22} = \frac{E_2}{1 - v_{12} v_{21}} \tag{4}$$

$$Q_{66} = G_{12} \tag{5}$$

Since the loads acting on a multi-layered laminate have common direction for all layers composing the laminate, the stresses and strains to with respect to the global coordinate system $x – y$ - z (Fig.1) is given by the following formula:

$$\begin{Bmatrix} \sigma_x \\ \sigma_y \\ \tau_{xy} \end{Bmatrix} = \begin{bmatrix} \overline{Q}_{11} & \overline{Q}_{12} & \overline{Q}_{16} \\ \overline{Q}_{12} & \overline{Q}_{22} & \overline{Q}_{26} \\ \overline{Q}_{16} & \overline{Q}_{26} & \overline{Q}_{66} \end{bmatrix} \begin{Bmatrix} \varepsilon_x \\ \varepsilon_y \\ \gamma_{xy} \end{Bmatrix} \tag{6}$$

where:

$$\overline{Q}_{11} = Q_{11}m^4 + 2\left(Q_{12} + 2Q_{66}\right)n^2m^2 + Q_{22}n^4 \tag{7}$$

$$\overline{Q}_{12} = \left(Q_{11} + Q_{22} - 4Q_{66}\right)n^2m^2 + Q_{12}\left(n^4 + m^4\right) \tag{8}$$

$$\overline{Q}_{16} = \left(Q_{11} - Q_{12} - 2Q_{66}\right)nm^3 + \left(Q_{12} - Q_{22} + 2Q_{66}\right)n^3m \tag{9}$$

$$\overline{Q}_{22} = Q_{11}n^4 + 2\left(Q_{12} + 2Q_{66}\right)n^2m^2 + Q_{22}m^4 \tag{10}$$

$$\overline{Q}_{26} = \left(Q_{11} - Q_{12} - 2Q_{66}\right)n^3m + \left(Q_{12} - Q_{22} + 2Q_{66}\right)nm^3 \tag{11}$$

$$\overline{Q}_{66} = \left(Q_{11} + Q_{22} - 2Q_{12} - 2Q_{66}\right)n^2m^2 + Q_{66}\left(n^4 + m^4\right) \tag{12}$$

The parameters $\overline{Q}_{ij}$ correlating the stress with respect to the strains in the global coordinate system are called transformed reduced stiffnesses and vary with the fiber orientation θ.

In above equations the parameters Qij are given by the Equns 2-5, and the parameters m and n are:

$$m = \cos\theta \text{ and } n = \sin\theta \tag{13}$$

1.2. Classical lamination theory

A laminated material element consisting of *N* layers (Fig.2) is considered for describing the relation of the force and moment resultants to the strains and curvatures:

$$\begin{Bmatrix} \varepsilon_x^0 \\ \varepsilon_y^0 \\ \gamma_{xy}^0 \\ k_x^0 \\ k_y^0 \\ k_{xy}^0 \end{Bmatrix} = \begin{bmatrix} a_{11} & a_{12} & a_{16} & b_{11} & b_{12} & b_{16} \\ a_{12} & a_{22} & a_{26} & b_{21} & b_{22} & b_{26} \\ a_{16} & a_{26} & \alpha_{66} & b_{61} & b_{62} & b_{66} \\ b_{11} & b_{12} & b_{61} & d_{11} & d_{12} & d_{16} \\ b_{12} & b_{22} & b_{62} & d_{12} & d_{22} & d_{26} \\ b_{16} & b_{26} & b_{66} & d_{16} & d_{26} & d_{66} \end{bmatrix} \begin{Bmatrix} N_x \\ N_y \\ N_{xy} \\ M_x \\ M_y \\ M_{xy} \end{Bmatrix} \tag{14}$$

In the above Equn 14 the 6 x 6 matrix consisting of the components A_{ij}, B_{ij}, D_{ij}, is called laminate stiffness matrix or *ABD* matrix. Inversion of the above equation provides the relation of the strains and curvatures with the force and moment resultants:

$$\begin{Bmatrix} \varepsilon_x^0 \\ \varepsilon_y^0 \\ \gamma_{xy}^0 \\ k_x^0 \\ k_y^0 \\ k_{xy}^0 \end{Bmatrix} = \begin{bmatrix} a_{11} & a_{12} & a_{16} & b_{11} & b_{12} & b_{16} \\ a_{12} & a_{22} & a_{26} & b_{21} & b_{22} & b_{26} \\ a_{16} & a_{26} & \alpha_{66} & b_{61} & b_{62} & b_{66} \\ b_{11} & b_{12} & b_{61} & d_{11} & d_{12} & d_{16} \\ b_{12} & b_{22} & b_{62} & d_{12} & d_{22} & d_{26} \\ b_{16} & b_{26} & b_{66} & d_{16} & d_{26} & d_{66} \end{bmatrix} \begin{Bmatrix} N_x \\ N_y \\ N_{xy} \\ M_x \\ M_y \\ M_{xy} \end{Bmatrix} \tag{15}$$

In above equations the strains $\varepsilon_x^0, \varepsilon_y^0, \gamma_{xy}^0$ are called reference surface extensional strain in the x direction, reference surface extensional strain in the y direction and reference surface in–plane shear strain respectively. The quantities $k_x^0 \; and \, k_y^0$ are the curvatures of the reference surface in the x and y directions respectively, while the quantity k_{xy}^0 is the reference twisting curvature.

The nomenclature of the force and moment resultants is shown in Fig.3. The unit of the force resultants is force per unit length while the unit of the moment resultants is moment per unit length. For example, the resultants N_x, M_{χ}, are:

$$N_x = \frac{\hat{N}_x}{\overline{AB}} \tag{16}$$

$$M_x = \frac{\hat{M}_x}{\overline{AB}} \tag{17}$$

where $\hat{N}_x$ and $\hat{M}_x$ are the force and moment acting on the segment AB (Fig.3), and $\overline{AB}$ is the length of the segment AB.

The elements of the *ABD* matrix are given by the following formulae:

$$A_{ij} = \sum_{k=1}^{N} \overline{Q}_{ijk} (z_k - z_{k-1}) \tag{18}$$

$$B_{ij} = \frac{1}{2} \sum_{k=1}^{N} \overline{Q}_{ijk} (z_k^2 - z_{k-1}^2) \tag{19}$$

$$D_{ij} = \frac{1}{3} \sum_{k=1}^{N} \overline{Q_{ijk}} (z_k^3 - z_{k-1}^3) \tag{20}$$

1.3. The Tsai–Wu failure criterion

Based on a concept similar to that followed for the derivation of the von Mises criterion for isotropic materials, the Tsai–Wu criterion for composites, assuming the plane–stresses assumption is given by the following formula:

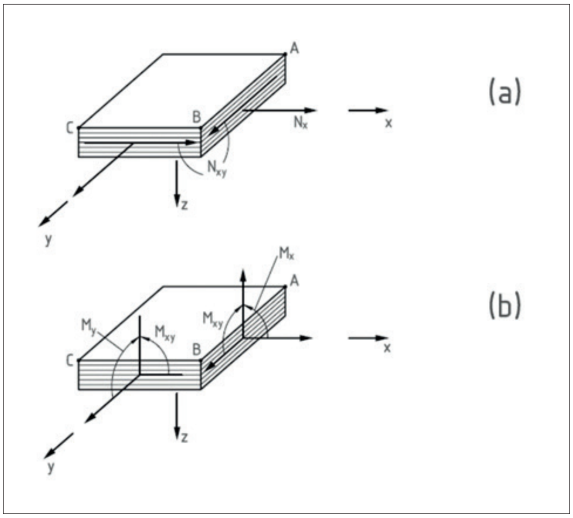

Fig.3. Nomenclature of the force and moment resultants.

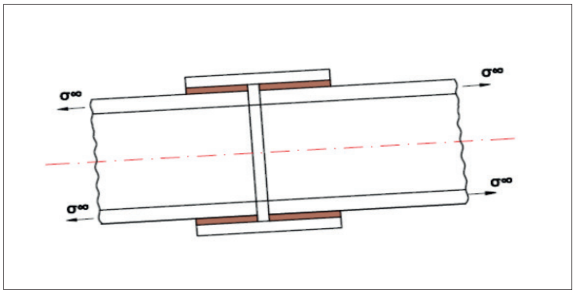

Fig.4. Butt joint.

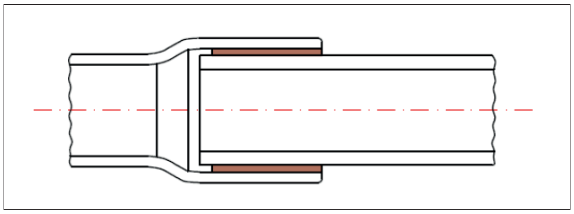

Fig.5. Socket adhesive joint.

$$F_1\sigma_1 + F_2\sigma_2 + F_{11}\sigma_1^2 + F_{22}\sigma_2^2 + F_{66}\tau_{12}^2 - \sqrt{F_{11}F_{22}}\,\sigma_1\sigma_2 \le 1 \qquad (21)$$

where :

$$F_1 = \left(\frac{1}{\sigma_1^{\mathrm{T}}} + \frac{1}{\sigma_1^{\mathrm{C}}}\right) \qquad (22)$$

$$F_2 = \left(\frac{1}{\sigma_2^{\mathrm{T}}} + \frac{1}{\sigma_2^{\mathrm{C}}}\right) \qquad (23)$$

$$F_{66} = \left(\frac{1}{\tau_{12}^{F}}\right)^2 \qquad (24)$$

$$F_{11} = -\frac{1}{\sigma_1^{\mathrm{T}}\sigma_1^{\mathrm{C}}} \qquad (25)$$

$$F_{22} = -\frac{1}{\sigma_2^{\mathrm{T}}\sigma_2^{\mathrm{C}}} \qquad (26)$$

The material properties in Equns 22–26 are symbolized by the following notations:
`

σ_1^{C} = compression failure stress in the x_1 direction
σ_1^{T} = tensile failure stresses in the x_1 direction
σ_2^{C} = compressive failure stresses in the x_2 direction
σ_2^{T} = tensile failure stresses in the x_2 direction
τ_{12}^{F} = shear failure stresses in the x_1-x_2 plane

Table 1. Allowable axial tension

Number of Layers = 50									
L/D = 0.05		**L/D = 0.10**		**L/D = 0.15**		**L/D = 0.20**		**L/D = 0.25**	
D (m)	N (N)	D (m)	N (N)	D (m)	N (N)	**D (m)**	N (N)	D (m)	N (N)
0.1	65951.2	**0.1**	130841	**0.1**	193674	**0.1**	253581	**0.1**	309863
0.2	261681	**0.2**	507162	**0.2**	724021	**0.2**	905662	**0.2**	1051140
0.3	581021	**0.3**	1086030	**0.3**	1474200	**0.3**	1745290	**0.3**	1922210
0.4	1014320	**0.4**	1811320	**0.4**	2327060	**0.4**	2620150	**0.4**	2774560
0.5	1549320	**0.5**	2627850	**0.5**	3203680	**0.5**	3468200	**0.5**	3581280
0.6	2172060	**0.6**	3490590	**0.6**	4065190	**0.6**	4278980	**0.6**	4353760
0.7	2867970	**0.7**	4367880	**0.7**	4898970	**0.7**	5059850	**0.7**	5106210
0.8	3622650	**0.8**	5240310	**0.8**	5705310	**0.8**	5820620	**0.8**	5848140
0.9	4422590	**0.9**	6097780	**0.9**	6489170	**0.9**	6569020	**0.9**	6584840
1.0	5255690	**1.0**	6936390	**1.0**	7256200	**1.0**	7310170	**1.0**	7319060
1.1	6111470	**1.1**	7755900	**1.1**	8011520	**1.1**	8047200	**1.1**	8052110
1.2	6981180	**1.2**	8557960	**1.2**	8758690	**1.2**	8781960	**1.2**	8784620

2. Joints of pipelines made by reinforced multilayered composite materials

The usual joints for composite pipelines connections are the butt joints [9], and the socket adhesive joints (Figs 4 and 5). The first one (Fig.4) is usually made by wrapping layers of fibre impregnated with a catalyst resin over the butted joint and is cheap, permanent and very satisfactory [10]. The second one is based on joining pipe pieces by adhesive layer (Fig.5). In order the joint to be successful, the adhesive layer should be able to carry the developed shear stresses.

The axial force and bending moment capacity of the above joints is given [8] by the following approximate formulae:

$$\overset{\wedge}{\mathrm{N}}^{a} = \frac{\tau_\alpha}{\mathrm{G}_a}\, t_a\, \pi\, D\, t\, E_x\, NP\, \lambda \tanh(\lambda L / 2) \tag{27}$$

$$\widehat{\mathrm{M}_a} = \left(\frac{D}{4} + \frac{a_{11}}{d_{11} D}\right)\frac{\tau_\alpha}{\mathrm{G}_a}\, t_a\, t\, E_x\, NP\, \lambda \tanh\left(\lambda L/2\right) \tag{28}$$

In above equations the following notations are used:

t_α = thickness of the adhesive layer
t = thickness of the pipe wall
L = length of the adhesive layer along the pipeline axis
D = mean diameter of the joint
G_α = shear modulus of the solidified adhesive material
T_α = shear strength of the solidified adhesive material
NP = number of layers of the pipeline wall laminate

Table 2 Allowable bending moment.

Number of Layers = 50									
L/D = 0.05		**L/D = 0.10**		**L/D = 0.15**		**L/D = 0.20**		**L/D = 0.25**	
D (m)	M (N * m)	D (m)	M (N * m)	D (m)	M (N * m)	D (m)	M (N * m)	D (m)	M (N *m)
0.1	5287.59	**0.1**	10490.1	**0.1**	15527.6	**0.1**	24843.1	**0.1**	24843.1
0.2	20863	**0.2**	40434.4	**0.2**	57723.8	**0.2**	83803.8	**0.2**	83803.8
0.3	46274.7	**0.3**	86495.7	**0.3**	117411	**0.3**	153092	**0.3**	153092
0.4	80755.2	**0.4**	144208	**0.4**	185268	**0.4**	220896	**0.4**	220896
0.5	123328	**0.5**	209180	**0.5**	255017	**0.5**	285075	**0.5**	285075
0.6	172883	**0.6**	277830	**0.6**	323565	**0.6**	346533	**0.6**	346533
0.7	228261	**0.7**	347638	**0.7**	389907	**0.7**	406401	**0.7**	406401
0.8	288315	**0.8**	417059	**0.8**	454067	**0.8**	465434	**0.8**	465434
0.9	351972	**0.9**	485291	**0.9**	516439	**0.9**	524054	**0.9**	524054
1.0	418266	**1.0**	552022	**1.0**	577479	**1.0**	582476	**1.0**	582476
1.1	486365	**1.1**	617233	**1.1**	637576	**1.1**	640806	**1.1**	640806
1.2	555573	**1.2**	681056	**1.2**	697031	**1.2**	699094	**1.2**	699094

E_x = extensional modulus of elasticity in the longitudinal direction given by the formula:

$$E_x = \frac{E_1}{\cos^4\theta + \left(\frac{E_1}{G_{12}} - 2\nu_{12}\right)\sin^2\theta\cos^2\theta + \frac{E_1}{E_2}\sin^4\theta} \qquad (29)$$

where θ is the fiber orientation and E_1, E_2, G_{12}, ν_{12} are the elasticity properties of the pipe material in the principal axes, and

$$\lambda^2 = \frac{2G_a}{E_x NP\, t t_a} \qquad (30)$$

With the aid of Equns 27 and 28, the numerical results [8] are listed in Tables 1 and 2 for S-Glass/Epoxy material, pipeline laminate consisting of 50 layers of 0.15-mm thickness, pipe of diameters 100-120 mm, and L/D ratios 0.05-0.25.

3. Supports of pipelines made by reinforced multilayered composite materials

Typical supporting methods of pipelines are shown in Figs 6 - 8.

Important parameters to be derived for pinned supported pipes are: (a) the maximum spacing *L* (Fig.9) between supports, (b) the minimum hanger widths, and (c) the allowable deflection of expansion loops for anchored pipelines.

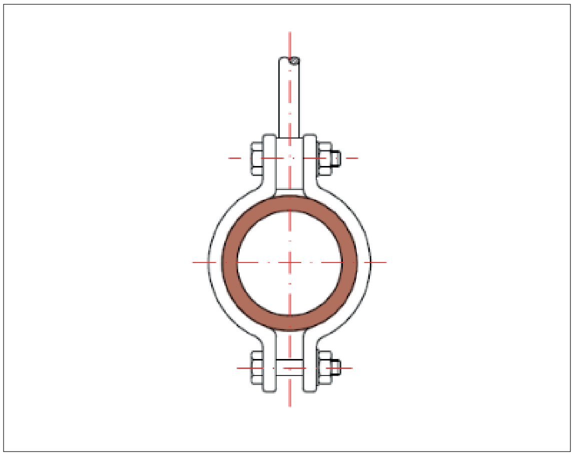

Fig.6. Support for a suspended pipe.

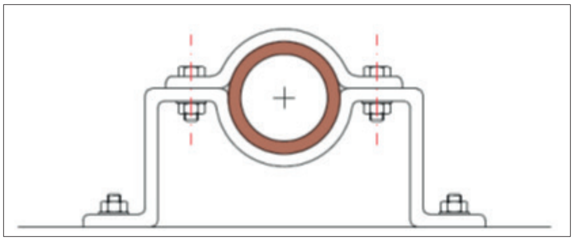

Fig.7. Pipeline clamped on the ground.

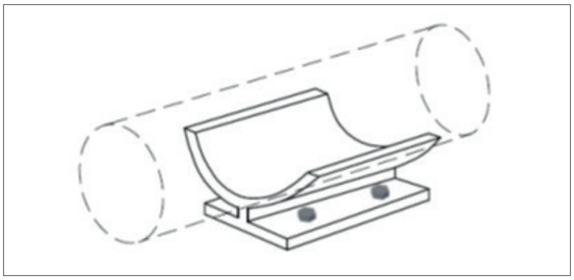

Fig.8. Pipeline supported by a shoe.

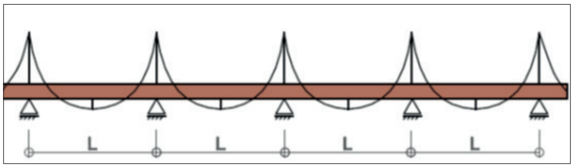

Fig.9. Pinned supported pipeline (bending moment distribution).

3.1.Maximum spacing between supports

According to the Ref.8 the maximum length between successive equi-spaced supports (Fig.9) is given by the following equation:

$$L \le \sqrt{\frac{\mathrm{M}_{\max}}{\lambda^* \pi D\left(t\gamma_p + 0.25D\gamma_f\right)}} \qquad (31)$$

where M_{max} is the minimum value between the allowable bending moment M^a (for avoiding failure) and the critical one M_{cr} (for avoiding buckling):

$$\mathrm{M}_{\max} = \min\left\{\mathrm{M}^a, \mathrm{M}_{cr}\right\} \qquad (32)$$

Analytic methodology for the calculation of the moments M^a and M_{cr} is given in Ref. 8. The parameters γ_p, γ_f are the specific gravities of the pipe material and the fluid respectively. The parameter λ^* depends onto the number of supports tending to be stable for more than six supports. The value $\lambda^* = 0.125$ can be used in the engineering practice.

Taking into account the Equn 31, numerical values for the maximum length L between supports for pipelines made by S-Glass/Epoxy materials can be found in Fig.10 for fibre orientation $\varphi = 30^{\circ}$.

3.2. Minimum hanger width

The lower part of the pipe segment which is in contact with the support is subjected to bending moment and compression due to the shear stress distribution along the perimeter of the cross section (Fig.11).

Apart from the above loads, the bending stresses are acting on the cross section, yielding the loading conditions in the point C shown in Fig.12.

According to the Ref.8 the loading components on the point C can be calculated by the following formulae:

$$\mathrm{M}_c = \frac{0.145wLD}{2B} \qquad (33)$$

$$\mathrm{N}_c = \frac{0.145wL}{B} \qquad (34)$$

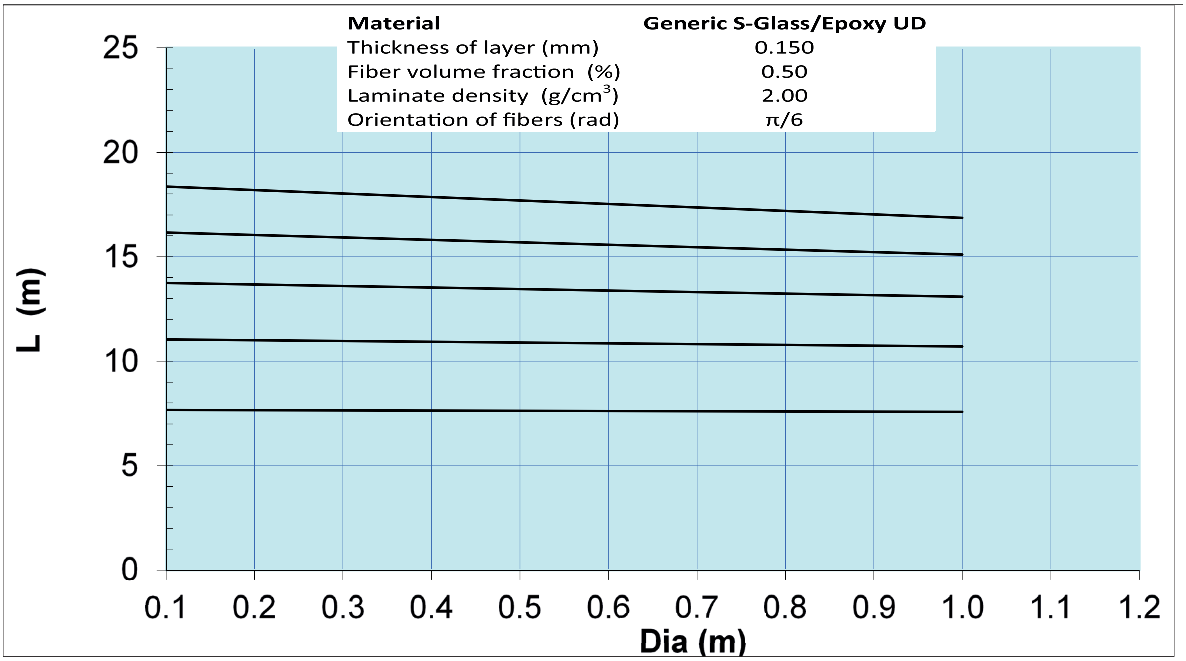

Fig.10. Maximum length L between supports for pipelines made by S-Glass/Epoxy material.

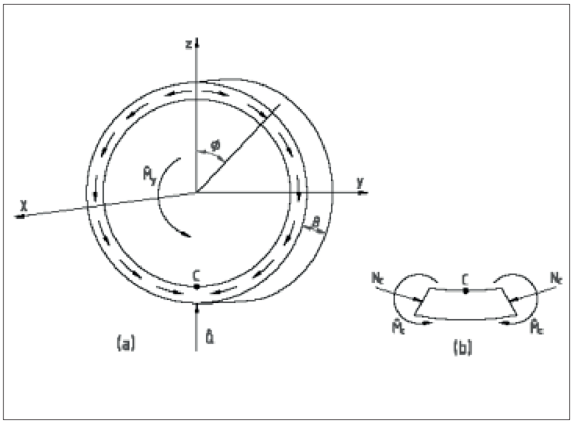

Fig.11. Loading of the pipe segment in contact with the support.

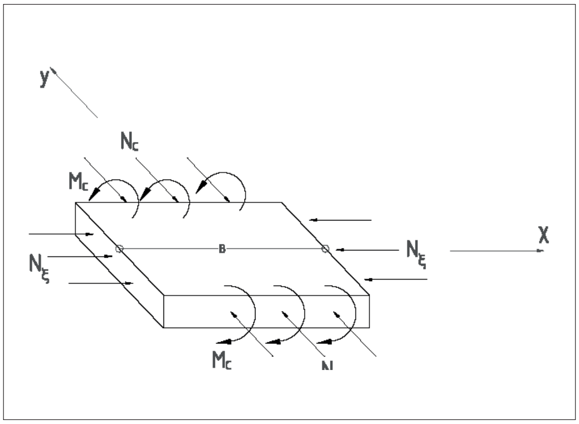

Fig.12. Loading conditions in the point C.

$$N_\xi = \frac{0.5 D d_{11} w L^2}{\left(d_{11} D^2 + 4 a_{11}\right) B} \qquad (35)$$

where w is the distributed load per unit length of the pipeline, and B is the hanger width.

Taking into account the above loads, the principal stress can be calculated, and the Tsai-Wu failure criterion can be applied. Numerical results [8] for the hanger width B of a pipeline made by S-Glass/Epoxy material, fiber orientation $\phi = 15^\circ$ and length between supports L = 10 m are demonstrated in Fig.13.

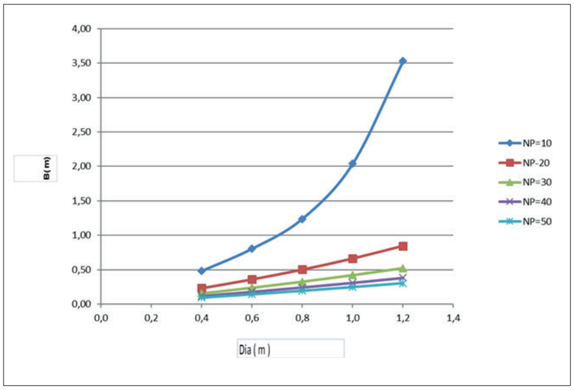

Fig.13. Hanger width versus pipeline diameter for a pipeline made by S-Glass/Epoxy material, fiber orientation ϕ =15° and length between supports L = 10 m.

4. Expansion loops of pipelines made by reinforced multilayered composite materials

Temperature changes yield significant axial forces in pipeline segments with anchored ends, and these forces may have catastrophic consequences in the pipeline structural integrity due to buckling. Therefore, the installation of expansion loops (Fig.14) is the suitable technique, especially for long runs [8]. The basic problem of analysis of the temperature change consequences in the configuration of Fig.14 is to estimate the magnitude of these stresses and check whether or not they are tolerable.

According to Ref.8, the maximum axial force and bending moment on an expansion loop due to a temperature ΔT is given be the following formulae:

$$F = k\frac{\mathrm{EA}\alpha_x L\Delta\mathrm{T}}{EA + kL} \tag{36}$$

$$\mathrm{M_B} = k\frac{E\ A\ \ a_x\ L\ \Delta\mathrm{T}}{E\,A + k\,L}\ \frac{\mathrm{C}_{MH}\mathrm{C}_{VV} - \mathrm{C}_{VH}\mathrm{C}_{VM}}{\mathrm{C}_{VV}\mathrm{C}_{MM} - \mathrm{C}_{VM}^2} \tag{37}$$

In the above equations the following parameters [11] should be used:

$$\mathrm{C}_{VH} = \frac{ab^2}{2EI} \tag{38}$$

$$\mathrm{C}_{MH} = \frac{a^2}{2EI} + \frac{ab}{EI} \tag{39}$$

$$\mathrm{C}_{MM} = \frac{a+b}{EI} \tag{40}$$

$$\mathrm{C}_{VM} = \frac{b^2}{2EI} \tag{41}$$

$$\mathrm{C}_{VV} = \frac{b^3}{3EI} \tag{42}$$

$$\mathrm{C}_{HH} = \frac{a^3}{3EI} + \frac{a^2 b}{EI} \tag{43}$$

and [8]

$$k = [\mathrm{C}_{HV}\frac{\mathrm{C}_{VH}\mathrm{C}_{MM} - \mathrm{C}_{MH}\mathrm{C}_{VM}}{\mathrm{C}_{VV}\mathrm{C}_{MM} - \mathrm{C}_{VM}^2} + \mathrm{C}_{HM}\frac{\mathrm{C}_{MH}\mathrm{C}_{VV} - \mathrm{C}_{VH}\mathrm{C}_{VM}}{\mathrm{C}_{VV}\mathrm{C}_{MM} - \mathrm{C}_{VM}^2} - \mathrm{C}_{HH}]^{-1} \tag{44}$$

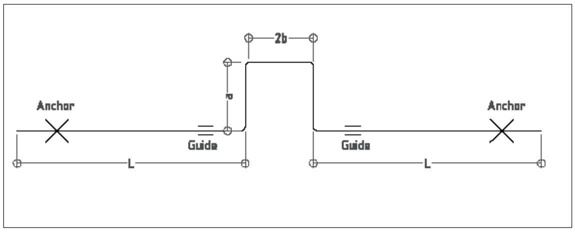

Fig.14. Schematic representation of an expansion loop.

The parameter α_x is the longitudinal (i.e. along the pipe's axis) coefficient of thermal deformation that can be approximately given by the following formula:

$$\alpha_x = \alpha_1 \cos^2 \theta + a_2 \sin^2 \theta \tag{45}$$

In the above formula α_1 and α_2 are the thermal deformation coefficients in principal coordinates 1 and 2, and φ the fiber orientation in a filament wound pipe with stacking sequence [± θ].

Using the values F, MB, the following conditions should be satisfied in order an extension loop to be accepted:

$$F < N^a \tag{46}$$

$$F < \lambda_{cr} \tag{47}$$

$$M_B < M^a \tag{48}$$

$$M_B < M_{cr} \tag{49}$$

In the above equations N^a is the allowable axial force to avoid failure, λ_{cr} is the minimum eigenvalue in order to avoid buckling, M_a is the allowable bending moment to avoid failure and M_{cr} is the critical value of bending moment to avoid buckling. More details for these parameters can be found in the Ref.8.

Conflicts of interest

The author has no conflicts of interest to declare.

References

[1] D.G Pavlou, 2017. Vibration of pipelines under flexural dynamic loads. *Science and Technologies: Oil and Oil Products Pipeline Transportation*, 7, 5 pp 51-55.

[2] N.A. Egorova, D.S. Zmienko, and I.V. Kozin, 2017. Overseas trends in application of composite materials in pipeline repair, *Science and Technologies: Oil and Oil Products Pipeline Transportation*, 7, 7, pp 88-97.

[3] D.G. Pavlou, 2017. Anisotropic pipelines in deep-sea mining: an approximate model for stability analysis. *Science and Technologies: Oil and Oil Products Pipeline Transportation*, 7, 6.

[4] D.G. Pavlou, 2016. Dynamic response of a multi-layered FRP cylindrical shell under unsteady loading conditions. *Engineering Structures*, 112, pp 256-264.

[5] D.G. Pavlou, 2016. Transfer matrices analysis of FRP pipelines stability. *International Review of Mechanical Engineering* (IREME), 10, 3, pp 165-172.

[6] D.G. Pavlou, 2016. Flow-induced instability of multi-layered anisotropic pipelines. *International Journa of Computational Methods & Experimental Measurements*, 4, 4, pp 543-553.

[7] D.G. Pavlou, 2015. Undamped vibration of laminated FRP pipes in water hammer conditions. *Journal of Offshore Mechanics and Arctic Engineering-Transactions of ASME*, 137, 6.

[8] D.G. Pavlou, 2013. Composite materials in piping applications, Destech Publications.

[9] D.G. Pavlou, 2017. An approximate method for stress analysis in butt joints of FRP pipelines. I*nternational Review of Mechanical Engineering* (IREME), 11, 2, pp 108-113.

[10] C.H. Wang and L.R.F. Rose, 2010, Stress analysis and failure assessment of lap joints, in: Recent Advances in Structural Joints and Repairs for Composite Materials, edited by L.Tong and C.Soutis. Kluwer Academic Publishers.
[11] W.C. Young, 1989. ROARK'S Formulas for Stress & Strain, McGraw-Hill.

To cite: D.G. Pavlou. Design aspects for connections, supports, and expansion loops in pipelines made from composite materials. Pipeline Science and Technology. 2018; 2(2): 147-158. DOI: 10.28999/2514-541X-2018-2-2-147-158.

Forthcoming international events

(continued from p 146)

Oil Sands Trade Show & Conference
12-13 September
Fort McMurray, AB, Canada
https://oilsandstradeshow.com/
The Oil Sands Trade Show and Conference focuses on promoting the latest technologies, innovations and business efficiencies in the areas of facility operations, maintenance, shutdown/turnarounds, mining, upgrading, health & safety, and environmental strategies.

IoT in Oil and Gas
18-19 September
Houston, TX, USA
https://iotinoilandgas.com/
Exploring the latest developments of IoT in oil and gas.

Rio Oil & Gas
24-27 September
Rio de Janeiro, Brazil
http://www.riooilgas.com.br/
The leading oil and gas event in Latin America is organized every two years by the Brazilian Petroleum, Gas and Biofuels Institute (IBP).

PetroChem Canada
25-26 September
Edmonton, AB, Canada
https://petrochemcanada.com/
Petrochem Canada brings together senior leaders in the petrochemical industry along with government officials, investors, regional development representatives and more. The industry experts will gather to discuss how to attract global capital investment to the region, current incentives to build, and the need for government policies to support diversification in the market.

Tube China - International Tube & Pipe Industry Trade Fair
29 September
Shanghai, China
http://www.tubechina.net/
Given the strong demand in tube & pipe, and great opportunities along with the fast growing tube & pipe industry in East China, Tube China will continue to lead the latest trend in China's tube and pipe industry and establish the best trade and exchange platform in China and even in Asia.

continued on p 160

Forthcoming international events

(continued from p 159)

Future Oil & Gas Agenda
27 September
UK
http://www.futureoilgas.com
The business conference that brings together oil majors and technology innovators with financiers and investors at a high-level conference with formal meetings and network sessions.

Energy Efficiency and Energy Development International Forum - 'Russian Energy Week' (REW)
2-6 October
Moscow, Russian Federation
http://rusenergyweek.com/en/
REW is to become a unified world-class industry-based business communication platform in Russia with a focus on energy issues. The Forum will discuss prospects for the development of such core sectors of the economy as the oil, gas, coal, and petrochemical industries.

Offshore Marintec Russia
2-5 October
St Petersburg, Russian Federation
http://offshoremarintec-russia.com/
Offshore Marintec Russia showcases the capacity of the Russian and global shipbuilding industry and the advanced technology for marine and transport construction as an important sector for development of offshore infrastructure.

Geofluid
3-6 October
Piacenza, Italy
http://www.geofluid.it/
Geofluid is focusing on the specialized target of drilling and underground working sectors, including subsoil fluid prospecting and extraction, soil investigation, special foundations and geotechnical works and other geological and geophysical applications.

European Autumn Gas Conference
7-9 November
Milan, Italy
http://www.theeagc.com/
EAGC is Europe's commercial and strategic gas conference, used by the most senior executives from the world's largest gas companies to network with peers and customers, review trends, question policy and agree future strategy.

PIPELINE TRANSPORT INSTITUTE

Pipeline Transport Institute is a research and development center of the Transneft, PJSC, for carrying out of research-and-development and design-and-experimental operations, as well as development of new technologies, equipment, materials, and regulatory documentation in the field of design, construction, operation, and repair of the pipelines for transportation of oil and petroleum products.

Areas of activities:

- carrying out of research-and-development, design-and-experimental, and technological operations, as well as development of technical solutions, ensuring safe and reliable operation of main and technological pipelines, buildings, and structures (facilities) of Transneft, PJSC, and Transneft system organizations (TSO);
- development of interstate, national, and industry standards, as well as other normative documents, in the field of construction and operation of main and technological pipelines, as well as pipeline transportation facilities;
- formation and maintenance of an information system for assessing the conformity of equipment and materials; carrying out of technical documentation examination and laboratory tests for compliance with the requirements of national, interstate, and foreign standards, as well as with the requirements of normative documents of Transneft, PJSC; development of standard programs, organization and/or participation in the activities for addition (extension of certification) of the products into the Core products register;
- provision of expert-consulting and engineering services in the field of design, construction, and operation of main, field, distribution, technological pipelines, and other facilities of the fuel and energy complex;
- scientific and technological support for construction of the facilities of Transneft, PJSC;
- assessment of the technical state of pipelines, development of the methods for increasing the transmission capacity of main pipelines;
- control, coordination, and provision of implementation of the activities on realization of the innovative development program of Transneft, PJSC, including search, development, approbation and introduction of innovative products and technologies;
- development of the documents in the field of industrial and fire safety, as well as the documents for prevention and elimination of emergencies in the field of environmental protection;
- assurance of the status of Pipeline Transport Institute, in the external market as a national research center, carrying out a wide range of operations in the field of hydrocarbons pipeline transportation.

Pipeline Transport Institute
47a, Sevastopolskiy prospekt St.,Moscow, 117186
Tel.: (495) 950-8295, Records Management: (499) 799-8285, fax: (495) 950-8297
www.niitnn.transneft.ru, e-mail: niitnn@niitnn.transneft.ru

minerva